2011

Late-Pleistocene Glacial and Climate Fluctuations in the Torres del Paine Region (51°S), Southern South America

Juan Luis Garcia

LATE-PLEISTOCENE GLACIAL AND CLIMATE FLUCTUATIONS IN THE TORRES DEL PAINE REGION (51°S), SOUTHERN SOUTH AMERICA

By

Juan Luis García

B.S. Pontificia Universidad Católica de Chile, Santiago-Chile, 2000

M.S Universidad Austral de Chile, Valdivia-Chile, 2007

A THESIS

Submitted in Partial Fulfillment of the

Requirements for the Degree of

Doctor of Philosophy

(in Earth Sciences)

The Graduate School

The University of Maine

May, 2011

Advisory Committee:

Brenda L. Hall, Associate Professor, Earth Sciences and Climate Change Institute, Advisor

Michael R. Kaplan, LDEO Associate Research Scientist, the EarthInstitute at Columbia University

Jorge Strelin, Professor, Geología Básica, Universidad Nacional de Córdoba

George H. Denton, Professor, Earth Sciences and Climate Change Institute

Peter O. Koons, Professor, Earth Sciences and Climate Change Institute

Terence J. Hughes, Emeritus Professor, Earth Sciences and Climate Change Institute

DISSERTATION

ACCEPTANCE STATEMENT

On behalf of the Graduate Committee for Juan Luis García I affirm that this manuscript is the final and accepted dissertation. Signatures of all committee members are on file with the Graduate School at the University of Maine, 42 Stodder Hall, Orono, Maine.

Brenda L. Hall, Associate Professor, Earth Sciences and Climate Change Institute — Date

LIBRARY RIGHTS STATEMENT

In presenting this thesis in partial fulfillment of the requirements for an advanced degree at the University of Maine, I agree that the Library shall make it freely available for inspection. I further agree that permission for “fair use” copying of this thesis for scholarly purposes may be granted by the Librarian. It is understood that any copying or publication of this thesis for financial gain shall not be allowed without my written permission.

Signature:

Date:

LATE-PLEISTOCENE GLACIAL AND CLIMATE FLUCTUATIONS IN THE TORRES DEL PAINE REGION (51°S), SOUTHERN SOUTH AMERICA

By Juan Luis García

Thesis Advisor: Dr. Brenda L. Hall

An Abstract of the Dissertation Presented
in Partial Fulfillment of the Requirements for the
Degree of Doctor of Philosophy
(in Earth Sciences)
May, 2011

Variations in Earth's orbital parameters affect insolation and are thought to drive ice-age cycles (Milankovitch Theory). Northern and southern mid-latitudes show opposing insolation signals, because of the effect of precession. Despite this difference, paleoclimate records from both hemispheres display broadly synchronous glacial-interglacial climate changes tied to northern hemisphere insolation. This would imply that southern hemisphere glaciers advanced in the face of increasing local summer insolation during the last glacial maximum and thus raises questions about the orbital theory of ice ages.

Well-dated paleoclimate records are important for testing hypotheses concerning the origin of ice ages, particularly in the southern hemisphere. Glaciers are sensitive recorders of past climate. In this thesis, I used precise mapping of moraines deposited by outlet glaciers, together with ^{10}Be exposure and radiocarbon ages, to establish the timing

of ice fluctuations throughout the last glacial period in Torres del Paine, Patagonia (51°S). I also determined the relationship of ice fluctuations to potential forcing factors, such as insolation and CO_2.

My data show that the Patagonian ice sheet deposited seven moraine belts in the Torres del Paine region during the last ice age, with advances to the outer moraines at ~49,000, 41,000, ~16,500 and 14,200 years ago. Glacial fluctuations were accompanied by the formation of paleolake Tehuelche. Maximum ice extent occurred during MIS 3, a finding that has been documented so far only rarely in South America. The chronology also shows that the Patagonian ice sheet expanded between 14,200 and 12,600 ka, providing conclusive evidence for the full duration of the Antarctic Cold Reversal in the southern mid-latitudes, as recorded by glaciers. I conclude that southern mid-latitude glacier expansions occurred irrespective of the insolation phase and seem to have coincided with stadials in Antarctica and northern shifts of the southern westerly wind belt, which likely played a key role driving near simultaneous changes throughout the southern hemisphere.

DEDICATION

"Hay paisajes, como instantes de la vida,

que no se borran jamás de la mente; vuelven siempre a traspasarnos desde adentro, cada vez con mayor intensidad."

("There are landscapes, as moments of life,

that always remain in the mind; they come back from inside, each time with stronger intensity")

Francisco Coloane (Tierra del Fuego)

To Berni, a source of life and love, and

To Francisco Coloane, a source of Patagonian inspiration.

ACKNOWLEDGEMENTS

The National Geographic Society, the Churchill Exploration Fund, and the Graduate Student Government at the University of Maine supported this research. I'm are very grateful to park rangers (Ricardo Cid) and people at the Corporación Nacional Forestal (CONAF) XII Región de Magallanes and Torres del Paine National Park (CHILE). Many thanks to Rodrigo Vega (Coy), Víctor García, Carmen Daggett, Marcelo Arévalo, Trauco, VERTICE, Stefan Krauss, Ursula Widmann and Charles Porter for support and assistance during field campaigns. Special thanks to the LDEO Cosmogenic Lab: Joerg Schaefer, Roseanne Schwartz, Jeremy Frisch and Brent Goehring. I thank Daniel Belknap, Marcelo Solari, Esteban Sagredo, Aaron Putnam, Sean Birkel, Katherine Pingree, Ann Dieffenbacher-Krall and Christopher Marden for rich discussions that improved this thesis.

TABLE OF CONTENTS

LIST OF FIGURES

LIST OF TABLES

CHAPTER

1. INTRODUCTION

The origin and termination of ice ages remains one of the greatest unresolved problems in earth sciences. Understanding the ice ages and their impact on climate, as well as the abrupt climate variations that characterized the last glacial-interglacial cycle, is prerequisite for addressing potential future climate scenarios. The Milankovitch theory, the most widely accepted model for the origin of ice ages, proposes that changes in latitudinal and seasonal insolation from variations in Earth's orbital parameters give rise to climate changes (e.g., glacial-interglacial cycles) (Milankovitch, 1941). The theory is centered in the northern hemisphere (NH) and affirms that ice ages begin as a linear response (e.g., Raymo and Nisancioglu, 2003) to minimum insolation intensity occurring at 65ºN during summer, allowing ice to survive the ablation season and begin a positive feedback growing process.

There has been a good amount of support for Milankovitch astronomical theory (Mesolella *et al*. 1969; Kukla, 1975; Weertman, 1976; Suarez, and Held, 1976; Johnson and McClure, 1976; Hays *et al*., 1976; Imbrie *et al*., 1992; Roe, 2006). Mesolella *et al*. (1969) matched the construction of coral terraces with high insolation periods at 125 ka, 105 ka and 80 ka. Then, Hays *et al*. (1976) produced a proxy climate record of ice volume, subantartic sea-surface temperature (SST) and Antarctic surface-water structure and noted that it contained variance at the same periodicities as precession, obliquity and eccentricity cycles. Although the presence of the orbital frequencies in the geological record (e.g., benthic foraminifera $\delta^{18}O$, ice volume record) is unequivocal, the

mechanisms by which these orbital variations pace global ice ages, as well as their abrupt terminations, remain unsolved. For example, Shaw and Donn (1968) argued that mean temperature depressions (2.7ºC in high latitudes) obtained from absolute minimum insolation in the NH were not enough to trigger glaciations. Wunsch (2004) examined terrestrial and oceanographic climate records and concluded that the amount of climate variability explained by orbital insolation variation was at maximum 20% of the record. Moreover, a number of long-term climate records show variations mostly at the obliquity and eccentricity frequencies; only a small fraction of the variance is linked to precession, despite the fact that the insolation signal at many latitudes occur at that frequency (e.g., Raymo and Nisancioglu, 2003; Huybers, 2006). This apparent inconsistency, plus other unsolved issues, such as the 41 and 100 ka problems (e.g., Raymo and Nisancioglu, 2003; Hays *et al.,* 1976; Imbrie *et al*., 1992), document the presence of other climate mechanisms and feedbacks capable of amplifying the insolation signal.

A major unsolved problem regarding Milankovitch orbital forcing is the apparent synchronous timing of ice ages in both hemispheres (e.g., Mercer, 1984; Steig *et al*., 1998; Schaefer *et al*., 2006). Mercer (1984) noted that, if one follows the Milankovitch model, the implication is that glaciations in both hemispheres should be out of phase. However, existing data suggest that ice ages in both hemispheres may have occurred synchronously (e.g., Mercer, 1984; Schaefer *et al*, 2006), a problem that Broecker (1978) called "a fly in the insolation ointment" and Mercer (1984) "a fly in the ointment of the Milankovitch theory." For instance, the global Last Glacial Maximum (LGM, 23-19 cal ka, Mix *et al*., 2001) coincided with insolation intensity minima in the NH and insolation maxima in the southern hemisphere (SH), but glaciers, as shown by available records

(e.g., Denton *et al.*, 1999b; Clapperton, 2000; Sugden *et al.*, 2005), may have been at their outer positions in both hemispheres at this time, thus raising the question: what drives SH glaciations?

If the insolation cycle controls the pace of ice ages, then one or more internal physical mechanisms must be responsible for producing or maintaining glacial conditions in the hemisphere with unfavorable insolation. A commonly cited mechanism is an albedo feedback, resulting from growth of NH ice sheets, which would overcome insolation maxima in the SH, and thereby expand the glacial conditions beyond the NH (e.g., Clark *et al.*, 1999; Kawamura *et al.*, 2007). However, atmospheric climate models for the LGM do not reproduce this scenario (e.g., Broccoli and Manabe, 1987). Other ideas include the inventory of atmospheric water vapor, together with major shifts in thermohaline circulation, as drivers of symmetric climate change in both hemispheres (e.g., Denton *et al.*, 1999a). Recently, Huybers and Wunsch (2005) and Huybers (2006) disagreed that precession is the dominant orbital control on glacial-interglacial cycles. They argued that the intensity of precession is offset by its duration (by Kepler's second law: duration of summer is proportional to the Earth-sun distance). Obliquity, on the other hand, being the same in both hemispheres, could account for synchronous climate changes. Furthermore, Huybers (2006) and Denton and Huybers (2008) showed that at least during the last 80 ka, obliquity cycles appear to control the total summer energy available for melting glacier ice at middle latitudes in both polar hemispheres.

Terminations are prominent warming events at the end of ice ages. Despite the fact that they are recorded by paleoclimate proxies throughout the planet, terminations are not well understood and cannot be explained by direct Milankovitch forcing. Glacial

evidence from mid-latitudes of both hemispheres suggests that Termination I, the largest climate change of the last 100,000 years, occurred abruptly and nearly synchronously around the globe (Schaefer *et al*., 2006). During this time (~17.5 ka) when Antarctic ice cores showed a warming trend, glaciers in both hemispheres began a rapid retreat from their LGM positions. This implies that "the message" of termination was transported across the globe near instantaneously through the atmosphere and/or the ocean. For instance, Schaefer *et al*. (2006) proposed that the last termination responded to a global rise in summer temperature, probably in close interaction with increasing atmospheric CO_2 concentrations. Overall, terminations have been associated with high summer incoming solar radiation in the NH (Broecker, 1984; Imbrie *et al*., 1993; Raymo, 1997), although some records, such as Devil's Hole (Winograd *et al*., 1992), show terminations preceding insolation intensity maxima. Raymo (1997) suggested that terminations occur when high summer insolation in the NH coincides with excess ice, promoting ice-sheet instability (Denton and Hughes, 1981). Huybers and Denton (2008) suggested that this ice-sheet instability, together with a long SH summer and an intense NH summer, combine to trigger terminations. Alternatively, Huybers and Wunsch (2005) proposed that obliquity acting together with a stochastic forcing was responsible for the abrupt end of ice ages. Leaving the influence of orbital pacing aside, the termination of glacial ages also may respond to several mechanisms which affect the mass balance of ice sheets, such as enhanced meridional heat transport by oceans and the atmosphere, rising eustatic sea level, changing albedo, and increases in CO_2 concentration (Imbrie *et al*., 1992).

Paleoclimate records show that Termination I (18-11.5 ka) occurred with a two-step warming pulse, interrupted by a late-glacial return to cold conditions. The late-

glacial cold events are prominent in ice-core records in Antarctica and Greenland (Antarctic Cold Reversal – ACR and Younger Dryas – YD, respectively). Mean annual temperatures in some places reached values close to glacial maxima (lowering of 15ºC mean annual temperature in central Greenland, Severinghaus *et al*., 1998). Ice and ocean sediment-core records show an out-of-phase interhemispheric phasing during these abrupt climate-change events (Sowers and Benders, 1995; Charles *et al.*, 1996). For example, cooling in Antarctica during the ACR (14.5-12.8 kyr BP) coincided with warm temperatures in the NH (i.e., Bölling/Alleröd) and ended at the peak of the northern YD (12.9-11.7 kyr BP) when Antarctica resumed the warming trend towards the present interglacial (e.g., Sowers and Benders, 1995). More recent ice-core records in Antarctica (EPICA Members, 2006) suggest a closer phasing of these events, with the ACR cooling coincident with the late Allerød cooling trend towards the YD; however, these new data still indicate that Antarctica warmed during most of the YD.

The cause of these late-glacial climate reversals remains uncertain. Younger Dryas cooling may have responded to changes in the conveyor meridional circulation, which affected the climate of the North Atlantic region, particularly Europe, located downwind (i.e., Brauer *et al*., 2008). For instance, Greenland and European $\delta^{18}O$ records from ice-core and lake sediments, respectively, show identical climate shifts during deglacial times, indicating that both regions followed the same climate driver (Dansgaard *et al*., 1989). To explain the out-of-phase pattern between the hemispheres, Broecker (1998) proposed an oceanic bipolar seesaw, in which the near shutdown of the North Atlantic conveyor produced enhanced deep-water production and climate warming in the SH. Such a shutdown could have come from catastrophic discharge of meltwater from

proglacial Lake Agassiz into the North Atlantic (Teller et al., 2002), although evidence for such a flood is elusive (e.g., Lowell *et al.*, 2005). Alternative views to explain the YD cold reversal include global control of North Atlantic deepwater formation by the Southern Ocean (Knorr and Lohmann, 2003).

In short, glacial chronologies and preliminary data from mid-latitudes in both hemispheres (e.g., Denton *et al.*, 1999b; Balco *et al.*, 2002; Schaefer *et al.*, 2006; Doughty, 2008) suggest that glaciers fluctuations in the southern hemisphere did not respond linearly to local summer insolation minima as would be expected based on current Milankovitch Theory (1941). The magnitude, abruptness and synchrony of Termination I in mid-latitudes of both hemispheres cannot be explained by the Milankovitch model without additional (as of yet unknown) feedbacks. Furthermore, the abrupt climate changes (e.g., millennial scale variability), including those present during the termination, also remain a mystery. These facts reflect the state of our understanding of ice ages and identify several unanswered questions, one of them- the focus of this research- is: What drives glaciations in the SH?

One way to address this question is to assess the global timing and synchrony/asynchrony of the discussed above climate events and their relationship to potential forcing factors, such as insolation, CO_2, and changes in North Atlantic circulation. My research addressed this and other problems outlined above through a global stratigraphic comparison using a glacial geologic and geochronologic study in the Torres del Paine region, southern Patagonia. For purposes of this work, the Torres del Paine region (50°45'-51°35' S and 73°30"-71°50' W; Plate 1, pocket) is defined as the area between the Andes Cordillera to the west and the outer moraine belts deposited to

the east in Argentina during the last glaciation (Plate 1, pocket). Lago Argentino and Última Esperanza glacial basins define the northern and southern limits, respectively, of the Torres del Paine region. This research planned to determine important aspects of the glacial history of Torres del Paine and thereby address fundamental questions regarding the origin of ice ages in the SH, including: when did the onset and termination of the LGM occur in Torres del Paine? How does this temporal range compare with other SH sites and with the LGM in the NH? What was the pattern of deglaciation during and after Termination I in this region of the SH? Was it an abrupt or steady process? Was it interrupted by cold reversals that promoted glacial still-stands or re-advances? If a cold stadial occurred in southern South America during the termination, how does the timing of this event compare with those reversals that occurred in the NH? This terrestrial glacial record from Torres del Paine improves the paleoclimate dataset in southern South America, and affords a solid basis for a better understanding of 1) the regional atmospheric conditions during the last glaciation, 2) the regional structure of climate change, and 3) the mechanisms involved during the last glacial-interglacial transition in the SH. Moreover, this research affords new evidence for the phasing of climate changes during the last glacial period with direct impact on our understanding of the astronomical theory of ice ages.

Torres del Paine National Park (51ºS, 73ºW) at the eastern foothills of the southern Andes forms the core of the study area. Here, active glaciers flow from the Southern Patagonian Ice Field (48º-51ºS). During the LGM and earlier glaciations, the Patagonian ice sheet, which developed along the southern Andes from about 38-56ºS (Glasser *et al*., 2008), produced large outlet piedmont glaciers that advanced through the Andes and left

a strong imprint on the surrounding topography (Caldenius, 1932; Marden and Clapperton, 1995). The preservation of glacial deposits (e.g., moraines) from the LGM and earlier glaciations at this latitude is excellent. For example, suites of moraines dating to the last glaciation and previous Quaternary glacial events occur adjacent to the large lakes that punctuate the eastern Andes (e.g., Lago General Carrera/Buenos Aires, Lago Cochrane/Pueyrredón, Lago Argentino) (e.g., Caldenius, 1932; Meglioli, 1992; Singer *et al.*, 2004; Douglass *et al*., 2006; Kaplan *et al*., 2008; Hein *et al*., 2010). Moreover, the geographical location of Patagonia means that it has great potential for climate-change research. The region is on the opposite side of the globe from 65ºN, the latitude used by Milankovitch, as well as from the North Atlantic, which is thought to be a key player for abrupt climate change (e.g., Broecker and Denton, 1989; Alley *et al*., 2002). The region occupies an isolated and unique geographic position- no other continental mass exists at these latitudes. Moreover, Patagonia occurs in a climatic zone dominated by the prevailing westerly wind belt, which correlates strongly with the regional precipitation patterns (Garreaud, 2007) and glacier accumulation rates (Cassasa *et al*., 2002). Isolated from any major mechanism controlling NH climate, the Patagonian ice sheet should afford a clear record of Late Pleistocene climate change in the SH, which can be compared to New Zealand and Antarctic records to highlight any prominent SH climate features, such as an early termination or the late-glacial ACR.

A primary goal of my research was to produce a geomorphologic map (Plates 1-5 in pocket). I used satellite imagery and aerial photographs to produce a preliminary map. In the field, I completed detailed mapping through a combination of stereoscopic aerial-

photo analysis and extensive ground coverage. Among many uses, this map provided the basis for the ^{10}Be chronology program developed here.

To produce a robust chronology, I used both surface-exposure and radiocarbon methods to date moraines accurately. Surface-exposure age dating has been shown to be precise in semiarid regions (Kaplan *et al*., 2008), such as this part of Patagonia. I always tried to sample boulders lacking pervasive signs of post-depositional weathering and erosion and located on stable moraine crests. I also looked for boulders containing a sufficient amount of quartz for ^{10}Be measurements. Quartz is highly suitable mineral to measure ^{10}Be, because of its extensive presence in the lithosphere, its efficiency in excluding other elements, its extraordinary resistance to environmental weathering and erosion, and its feasibility for producing pure samples. To improve the precision of measurements, the ^{10}Be sample preparation protocol, carried out at the Lamont-Doherty Observatory Cosmogenic Lab, included a very low background ^{9}Be carrier. Also, the high-energy currents used in the accelerator mass spectrometer (AMS) at LLNL made possible a highly precise atomic separation of ^{10}Be, ^{9}Be and ^{10}B, and thus permited accurate ^{10}Be/^{9}Be ratios (Appendix A).

Data from scattered studies suggest that Patagonian glaciers may have been at or near their outermost positions during the local LGM between about 28.0-17.5 ka (Hein *et al*., 2010, 2009; Kaplan *et al*., 2004, 2008; Douglass *et al.*, 2006; Sugden *et al.*, 2005; McCulloch *et al*. 2005), before, during and after the global LGM (23-19 ka, Mix *et al*., 2001). In the Chilean Lake District, using a stratigraphic-based approach, Denton *et al.* (1999b) dated the local LGM to be between about 35-17.5 ka, which is a longer maximum than suggested by other data along Patagonia. Nevertheless, sites with

chronologic control are sparse in Patagonia. In many cases, the existing glacier records predate recent technological advances in exposure-age dating (Nishiizumi *et al.,* 2007) and are not sufficiently precise for stratigraphic comparisons.

The pattern of late-glacial climate in southern South America is puzzling. Whereas records on the lee side of the Andes suggest the existence of a glacial re-advance at the end of the ACR (Strelin and Denton, 2005), the sparse records on the western side do not (Lumley and Switsur, 1993; Mercer, 1976; Hall *et al*., in prep). Previous data from Torres del Paine suggest the existence of a glacial re-advance or still-stand during the ACR chronozone (Moreno *et al*., 2009; Fogwill and Kubik, 2005), although age uncertainties precluded firm conclusions about the duration and overall structure of the event. Several hundreds of kilometers to the south, McCulloch *et al*. (2005) and Sudgen *et al*. (2005) suggested the development of an extensive late-glacial episode in the Strait of Magellan that formed a lake dammed by ice terminating at Isla Dawson. However, recent evidence (Hall *et al*., in prep.) suggests that glaciers at this time may have been close to their present-day margins and therefore any advance at this time in southwestern Patagonia was minimal. Pollen records in Patagonia records are also inconclusive regarding the timing and size of any late-glacial event (e.g., Markgraf, 1991, Heusser *et al*. 1998, 2000; Moreno *et al*., 2001; Bennett *et al*., 2000).

Marden (1993) provided the first detailed mapping of Torres del Paine National Park (Chile). In this thesis, I confirm most of the mapping aspects of Marden's work, particularly the number, position and geographical extent of moraine belts in the area. His description and association of moraine belts between different lake basins provided a solid foundation for this thesis and the ^{10}Be chronology presented here. This thesis then

builds on Marden's and other previous work by presenting important changes and improvements on our knowledge of the last glaciation in the area, including the age of moraine belts, reconstruction of paleolake environments and the extent of the ice during the last glacial period in the area.

This thesis also builds on the work of Solari (2010), who, following Caldenius (1932), and based on glaciolacustrine evidence in Torres del Paine, proposed the name of Lake Tehuelche for a prominent paleolake that accompanied the fluctuations of the Patagonian ice sheet in the region. Although my reconstruction of the extent of the lake is similar to that in Solari's work, fundamental differences exist in the timing and association of moraines/ice margins with distinct lake levels.

This Ph.D. dissertation includes five chapters that address the issues above. Chapter 2 describes the glacial geomorphology of the Torres del Paine region. The main objectives of the chapter are 1) to reconstruct former glacial and proglacial environments, including paleolakes that accompanied local Patagonian ice-sheet fluctuations, 2) to gain understanding on the pattern of glaciation and deglaciation, and 3) to provide a geomorphological and geological base for the ^{10}Be chronological program. This chapter provides detailed description and discussion of glacial landforms and sediment sequences, which were the basis for constructing the geomorphological map (Plates 1-5, pocket).

Chapter 3 focuses on the age of moraines dating to the last glaciation and their glaciological, geomorphological and climatological implications. This chapter first documents extensive glacial fluctuations during MIS 2 and MIS 3, the latter being one of

the first pieces of evidence for early glacial expansion in southern South America. Then the chapter discusses the differences in age between TDP I moraines at Lago del Toro and Laguna Azul, as well as the local termination. The chapter then compares the local glacial record with that from other sites in Patagonia and the southern hemisphere, and elaborates on the hemispherical pattern of climate change and the role of insolation and the southern westerly winds.

Chapter 4 presents the late-glacial (ACR) age of the TDP II, III and IV moraines, which are the main focus of this Ph.D. dissertation. This chapter shows that the southern mid-latitude glaciers expanded and collapsed throughout the entire ACR in close relationship with Antarctic climate. This close correspondence suggests teleconnections that likely incorporated the southern westerly wind belt.

Chapter 5 enumerates the main conclusions of this research.

CHAPTER

2. GLACIAL GEOMORPHOLOGY OF THE TORRES DEL PAINE REGION: IMPLICATIONS FOR GLACIATION, DEGLACIATION AND PALEOLAKES

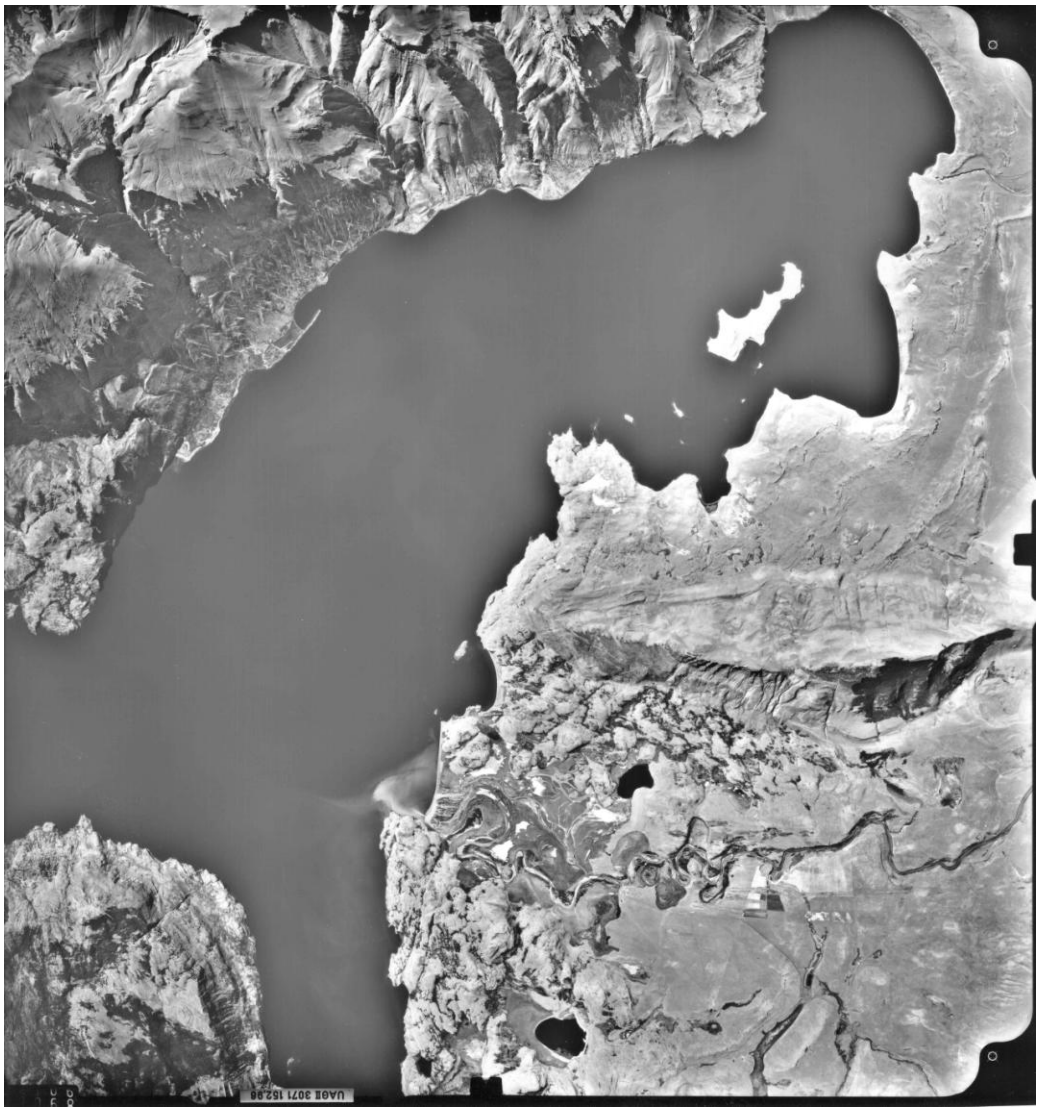

2.1 Abstract

The processes affecting paleoclimate variability in the southern mid-latitudes remain poorly understood, mostly because of the lack of precise records. Glacial landforms are invaluable for reconstructing past ice-sheet and climate changes along the southern Andes, but there are significant gaps in existing data. This paper presents the results of our geomorphological mapping in the Torres del Paine region (51ºS), southern South America. We show that during Marine Isotope Stages 3 and 2, the Patagonian ice sheet experienced major fluctuations in the region and deposited at least seven moraine belts, roughly 50-100 km from present ice margins. The Tehuelche paleolake accompanied each of these ice-sheet fluctuations. Three main phases describe the development of this paleolake, which drained eastward to the Atlantic Ocean: Early Phase, represented by two independent lakes at 300 m a.s.l. and 420 m a.s.l., associated with the outer Río de las Viscachas and Arroyo Guillermo moraines, respectively; Middle Phase, linked to a lake at 250-280 m a.s.l., formed after retreat from these same moraines; Late Phase, represented by a lake at 125-155 m a.s.l. The Late phase may have merged with paleolake Consuelo in Última Esperanza (Sagredo *et al.*, 2011) during advance and retreat from the TDP I moraines at Lago del Toro towards the end of the Last Glacial Maximum. The Tehuelche paleolake likely had drained by the late-glacial period, suggesting that ice southwest of Torres del Paine may have retreated back into the mountains by this time.

2.2 Introduction

The Milankovitch theory, the most widely accepted model for the origin of ice ages, proposes that changes in latitudinal and seasonal insolation from variations in Earth's orbital parameters give rise to climate changes (e.g., glacial-interglacial cycles) (Milankovitch, 1941). The theory is focused on the northern hemisphere and affirms that ice ages begin as a response (e.g., Raymo and Nisancioglu, 2003) to minimum insolation intensity occurring at 65ºN during summer, allowing ice to survive the ablation season and begin a positive feedback growing process.

Despite the fact that the northern and southern mid-latitudes show opposing insolation intensity signals, ice-core and marine records from both hemispheres appear to display broadly synchronous glacial-interglacial climate changes at orbital time scales (EPICA members, 2004; Jouzel *et al*., 2007; Lisiecki and Raymo, 2005). In addition, several investigators have used moraine records to argue for (near) synchronous global glacial activity during the Last Glacial Maximum (LGM) and Termination I (Schaefer *et. al* 2006; Denton *et al.* 1999a, Sugden *et al*., 2005; Clapperton, 2000). Yet, southern hemisphere glaciers apparently advanced in the face of unfavorable summer insolation, a problem Mercer (1984) referred to as "the fly in the ointment of the Milankovitch theory". What then are the drivers of southern hemisphere glaciations? Precisely dated glacial and climate records from both hemispheres afford a means for isolating the causes behind the ice ages and abrupt climate changes, but are scarce in the southern hemisphere. In order to address the problem of the cause of southern hemisphere glaciation, we have begun a mapping and chronologic program in the Torres del Paine region (51ºS), southern South America, which has well-preserved sets of moraines that

are suitable for exposure-age dating. Torres del Paine has insolation opposite to that of the North Atlantic region and is located in the core of the southern westerly wind belt, a main component of present-day climate (Markgraf, 1998; Cerveny, 1998). Shifts in these winds are thought to have constituted a central mechanism for climate change in the southern latitudes in the past (Denton *et al*., 2010; Hall *et al*., 2010; Anderson *et al*., 2009; Moreno *et al*., 2009). This paper presents the results of our geomorphological mapping in the Torres del Paine region and provides foundation for (1) reconstructing the proglacial environments present in the area, (2) understanding the local pattern of glaciation and deglaciation, and (3) determining the timing of glacial events in the region during the last glacial cycle and transition to the Holocene. We want to address the following questions: How extensive was ice during the last glacial cycle in Torres del Paine? When and how did it fluctuate? What environments existed at the terminus of the Patagonian ice sheet in Torres del Paine? What was the spatial and temporal extent of paleolakes, and how did they relate to the different glacial pulses in the area? Does the geomorphic evidence support collapse of the Patagonian ice sheet in the Torres del Paine region during Termination I?

For purposes of this work, the Torres del Paine region (50°45'-51°35' S, 73°30"-71°50' W; Fig. 2.1, Plate 1 pocket) is defined as the area between the Andes Cordillera to the west and the outer moraine belts deposited to the east in Argentina during the last glaciation. Lago Argentino and Última Esperanza glacial basins define the northern and southern limits, respectively, of the Torres del Paine region. Torres del Paine National Park, which constitutes the core of the field area, is located at the southeastern tip of the Campo de Hielo Patagónico Sur (Southern Patagonian Ice Field, Horvath 1997; Cassasa

et al., 2002). During the Quaternary glaciations, the Patagonian ice sheet was the main source of ice in the Torres del Paine region and, together with the Cordillera Paine alpine system (3,248 m a.s.l. at its highest point), nourished eastward fast-flowing outlet glaciers (Glasser *et al*., 2008). These coalesced to form an ice sheet that, in general, has become less extensive over time (cf. Kaplan *et al.,* 2009).

The westerly winds transport cyclones originating in the Antarctic Frontal Zone and are associated with elevated precipitation levels (Garreaud, 2007) that directly affect climate and glacier mass balance all along the southern Andes (Cassasa *et al.,* 2002). The present ice fields in the region (Northern and Southern Patagonian Ice Fields) cover 17,200 km^2 (Aniya *et al.,* 1996; Aniya and Wakao, 1997). The equilibrium line altitude (ELA) on the Southern Patagonian Ice Field, although not known thoroughly, ranges from about 900-1400 m a.s.l. (Cassasa *et al.*, 2002). Cloudiness and precipitation occur year round (Carrasco *et al*., 2002; Miller, 1976), with the greatest amounts of precipitation, as much as 10 m per year, occurring at high elevations (Garreaud, 2007). Cassasa *et al.,* (2002) suggested that this high precipitation rate allows the Northern Patagonian Ice Field to survive at a relatively low latitude (47ºS).

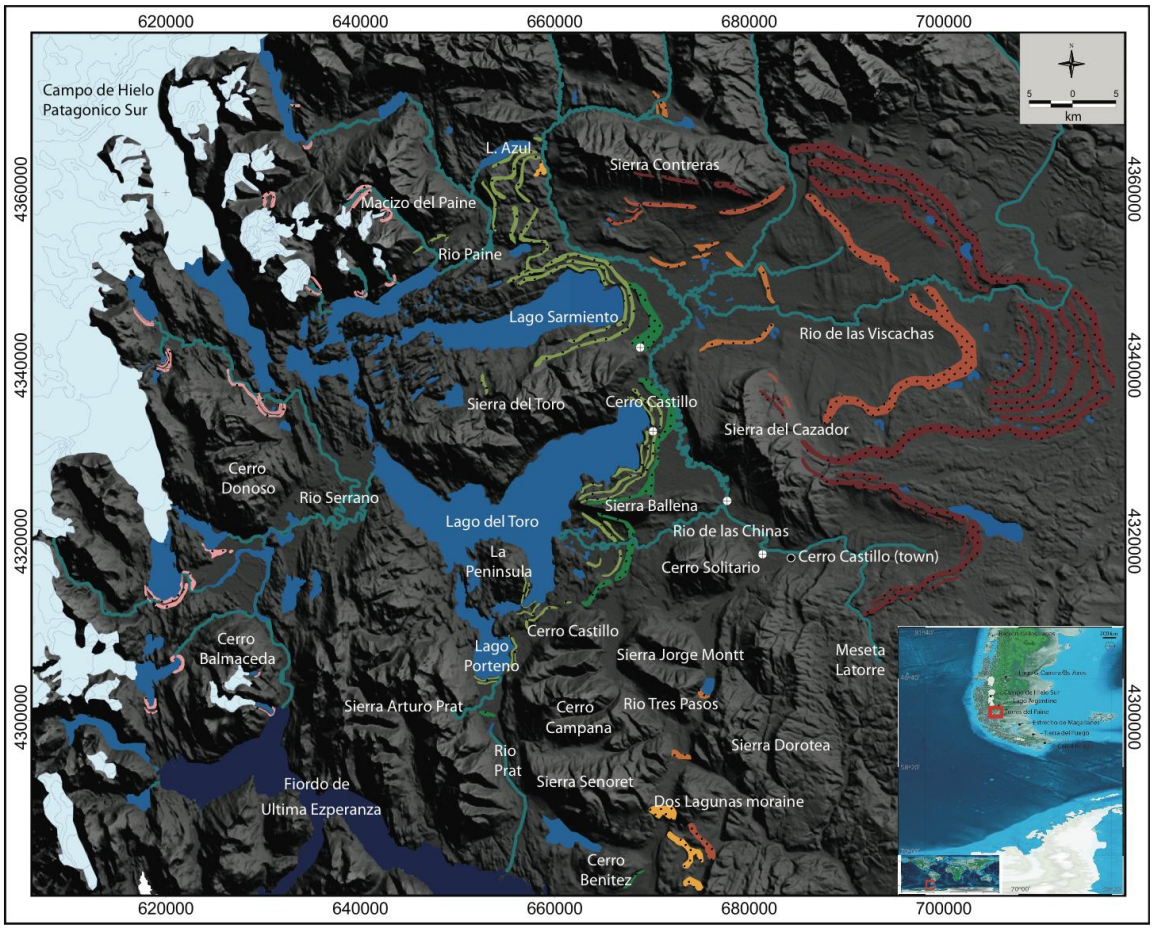

Figure 2.1. Physiographic attributes of the Torres del Paine region. Inset shows southern South America, including the location of the Torres del Paine region (red box). The map depicts each of the moraine belts deposited during the last glaciation.

The southern Andes do not form the hydrologic divide between the Pacific and Atlantic Oceans in the Torres del Paine region. Rather, the moraines themselves form the divide. This condition, along with local bedrock topography, has resulted in the Última Esperanza and Torres del Paine basins being hydrologically connected. A suite of interconnected valleys and lakes in the Torres del Paine region forms a complex network that ultimately drains to Fiordo Última Esperanza through Río Serrano. Thus, the

paleolake histories of Torres del Paine and Última Esperanza are related (Fig. 2.1; Plate 1, pocket).

Nordenskjöld (1898), Hauthal (1905) and Caldenius (1932) produced the first glaciological observations and physiographic maps that included glacial landforms from the Torres del Paine region. Caldenius (1932) defined four main moraine belts, from outer to inner: *Initioglacial, Daniglacial, Gotiglacial,* and *Finiglacial*, with the latter enclosing present-day lakes in Torres del Paine National Park (i.e., Laguna Azul, Lago Sarmiento and Lago del Toro; Plate 1, pocket). Because of the freshness and preservation of landforms, Caldenius (1932) assumed that they were analogues to the Scandinavian glacial record, and he suggested that all four moraine belts dated to the last glaciation. Marden (1993, 1997) and Marden and Clapperton (1995) subsequently separated the *Finiglacial* moraine of Caldenius (1932) into four distinct belts (A-D), which they thought were deposited during the LGM (B-D moraines) and Marine Isotopic Stage 4 (MIS 4) (A moraines). The same authors separated two additional ice-marginal positions (E and F) from less distinct and discontinuous ice–marginal landforms proximal to the D moraines and linked them to the late glacial period, or *post-Finiglacial* in Caldenius's (1932) nomenclature. Fogwill (2005) and Fogwill and Kubik (2005) further mapped and modified the inner D limit of Marden and Clapperton (1995) near Lago Nordenskjöld. Based on four cosmogenic ^{10}Be ages, Fogwill and Kubik inferred D was deposited during late glacial time, in contrast to the conclusions of Marden (1993) and Marden and Clapperton (1995). This finding was supported by the subsequent study of Moreno *et al*. (2009). Because of our concentration on the last glaciation and late glacial period, we focus here on moraine sets A-D. We also made a preliminary study of outer/older

moraines (*Gotiglacial moraines*) located to the east. To avoid confusion with sites elsewhere in southern South America that use similar labels to refer to different glacial events (i.e, Sugden *et al*., 2005; Clapperton, 1993), we name the A-D moraines here accordingly: TDP I= A, TDP II= B, TDP III= C, and TDP IV= D. The outer three moraine belts (*Gotiglacial moraines*, Caldenius, 1932) are named Río de las Viscachas (RV) I, II, III. In addition, a southern ice lobe of the Patagonian ice sheet built another moraine belt, the Arroyo Guillermo (AG) moraines (Fig. 2.1. Plate 5), whose position suggests coeval deposition with the RV I moraines (e.g., Caldenius, 1932).

2.3 Methods

A primary goal of our research was to produce a geomorphologic map (Plates 1-5, pocket). We constructed the map first from stereoscopic analysis of aerial photographs (Vuelo Geotec 1998, 1:70.000) covering most of the study area. We then checked our preliminary mapping during four field campaigns between 2007 and 2010. We focused on ice-marginal positions, as defined by glacial and proglacial features (e.g., moraine ridges, glaciofluvial and glaciolacustrine complexes), built during the last glacial period and transition to the Holocene. The final map was created in the ARC VIEW GIS program at a scale of 1:70,000. We used hand-held global positioning systems (GPS) to measure the elevation of glaciolacustrine terraces multiple times (+/- 5-10 m). We complemented these measurements with Shuttle Radar Topography Mission (90 m horizontal resolution) (vertical uncertainty <15 m) and Google Earth elevation data. We analyzed stratigraphic outcrops associated with different landforms wherever possible.

We divided stratigraphic sections into discrete sediment units, based on physical observations, such as sediment texture, color, sorting, fabric and structures. The chronological investigations are described in Chapter 3 and 4.

2.4 Results

2.4.1 Moraine belts

At least seven moraine belts occur in the study area and are described here (Plates 1-5, pocket). These belts are, from outer to inner, RV (RV= Río de las Viscachas) I, II and III and TDP (TDP= Torres del Paine) I, II, III, and IV. These moraines all occur within 50 km of each other and are located 50-100 km from the present ice-field margin. The TDP II, III, and IV moraines are distinctly smaller in size and relief than the TDP I and RV I, II, and III landforms. In addition, whereas the TDP I-IV systems are associated with the east-west trending lakes in Torres del Paine National Park (Chile), the RV I, II, and III moraines were formed when the Patagonian ice sheet extended farther east in what is today Argentina. At least the inner four moraine belts (TDP I-TDP IV) at Lago del Toro and likely Lago Sarmiento were deposited at the end of the LGM and transition to the present interglacial (Chapter 3, 4). We infer that the outer three moraine belts formed during the last glacial period (Marine Isotope Stages, MIS 3-2), but chronological control is sparse or lacking (Chapter 3).

2.4.1.1 The inner Torres del Paine moraines

As mentioned earlier, the *Finiglacial* moraines of Caldenius (1932) in the Torres del Paine region include four distinct belts: TDP I, II, III and IV, from outer to inner position (Plates 2-4, pocket). In this section, we describe each of them, building on previous work in the area (e.g., Nordenskjöld, 1898; Hauthal, 1905; Marden, 1993; Marden and Clapperton, 1995). These moraine systems occur within three kilometers of each other and fringe the eastern shores of Laguna Azul (220 m a.s.l.), Lago Sarmiento (75 m a.s.l.) and Lago del Toro (25 m a.s.l.) (e.g., Marden, 1993), ~45 km from present-day ice margins and about midway between the outer RV I terminal moraines and the existing Southern Patagonian Ice Field.

2.4.1.1.1 TDP I moraines

We delineated the TDP I moraines based on position and preservation, following Marden (1993). These moraines are distinct from the TDP II, III, and IV landforms, particularly in terms of morphology and relief. For instance, the TDP I moraines are as much as one kilometer wide and have 30-50 m of relief (e.g., at Lago Sarmiento), which is several times the size of the TDP II, III, and IV ridges.

The TDP I moraine belt can be followed along the eastern shores of Laguna Azul, Lago Sarmiento, and Lago del Toro. Whereas at Lagos Sarmiento and del Toro TDP I occurs as well-defined moraine ridges, at Laguna Azul broad landforms form a rolling hilly topography. In the Laguna Azul area, broad, low-relief moraines occur in open areas

west of Río de las Chinas and small ridges span narrow basins that punctuate a local north-south topographic barrier (~500 m a.s.l.).

At Lago Sarmiento, the TDP I moraine is a five-kilometer-long prominent ridge, crosscut by a younger TDP II moraine and breached by a large, two-kilometer-long meltwater channel. The steep ice-contact slope, both here and at Lago del Toro, has as much as 40 m of relief, which has been produced, in part, by glaciofluvial erosion. The TDP I moraine at Lago Sarmiento has a flat, wide crest at about 115-125 m a.s.l., that distally is made up of outwash, as revealed by sandy pebbles that crop out at the Estancia Site (51º03'51'' S and 72º33'51''W, ~125 m a.s.l.; Fig. 2.2; Plate 2, pocket). At this site, well-stratified sandy pebble beds (facies B in Fig. 2.2) are intercalated with massive to crudely bedded coarse sediment up to cobble size (facies A in Fig. 2.2). The sandy pebble beds are well sorted and can be traced laterally for tens of meters. They occur as horizontally and cross-bedded units and are likely channel deposits. In contrast, the massive to crudely bedded sediment contains clasts (≤30 cm in diameter), which are subangular to subrounded in shape. Sorting is poor and the overall aspect is chaotic. We interpret this deposit as debris flows from the ice margin.

At the eastern margin of Lago del Toro, the TDP I moraine belt consists of a composite landform made up of three ridges. From here to Sierra Ballena, there is only a single moraine ridge, and it has been eroded and buried by the main glaciofluvial plain. In the northern foothills of Sierra Ballena, the TDP moraine belt splits again into five ridges but from here continues again as only a single ridge along the western front of Sierra Ballena. South of Sierra Ballena, the TDP I moraine is represented by a wide discontinuous arc. The moraine may be present as far west as the Río Prat valley, south of

Lago Porteño (Plate 4, pocket), but it is hard to be sure that the landform there corresponds to the TDP I moraine system.

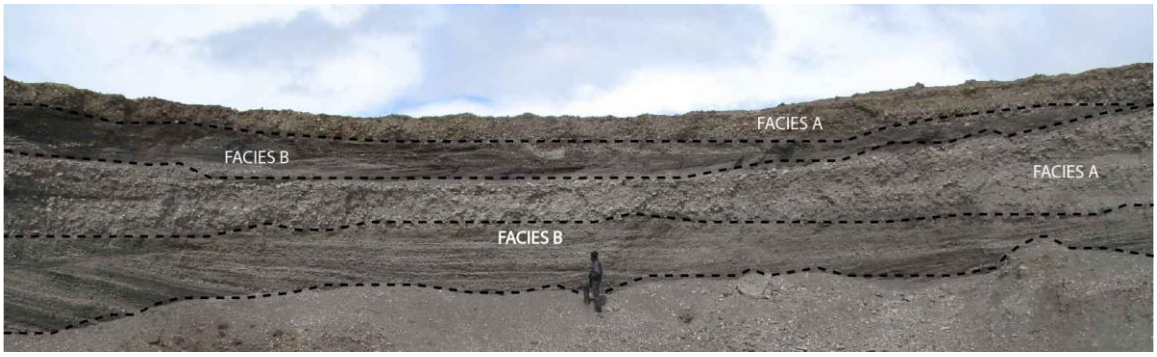

Figure 2.2. Estancia Site stratigraphic section at Lago Sarmiento (TDP I moraine). Facies A: Ice-proximal massive gravelly cobbles. Massive B: sandy gravel glaciofluvial sediments. See text for details.

2.4.1.1.2 TDP II and III moraines

We describe these two moraine systems together, because they closely parallel each other along the eastern margins of the lakes in the Torres del Paine National Park area and are morphologically similar. Each of the TDP II and TDP III moraine belts at Laguna Azul and Lagos Sarmiento and del Toro comprise five-to-ten sharp, well-defined ridges, which preserve their slopes close to the angle of repose. The former landforms are significantly more bouldery and appear more fresh than the TDP I moraines.

At Laguna Azul, it is difficult to distinguish between the TDP II and III belts, because they were deposited close together on a hillside. Here, ice-marginal meltwater channels, as much as thirty meters wide and several hundreds meters long, separate each of the moraines. Between Laguna Azul and Lago Sarmiento, the moraine systems are generally continuous for more than 25 km and cross a low-relief, bedrock-controlled

topography. Meltwater channels, such as in Cañadon del Macho, and small lake basins, such as Laguna Amarga, locally dissect the moraines. The outermost TDP II moraine between Laguna Azul and Lago Sarmiento defines a sharp drift limit. To the east of this limit, glacially scoured bedrock is draped with scattered glacial erratics. Near Cañadón del Macho, this sharp drift limit occurs as an uninterrupted line of boulders a few kilometers long (e.g., Marden, 1993). Between Laguna Amarga and Lago Sarmiento, TDP III moraines crosscut TDP II ridges. Here, TDP III landforms split into two moraine belts, one fronting Laguna Amarga basin and the other Lago Sarmiento.

At the eastern fronts of Lago Sarmiento and Lago del Toro, the organization and morphology of the TDP II and III moraines are similar. Here, the ridges are sinuous and continuous for hundreds of meters. At some locations, the TDP III moraines are higher in elevation and are of greater relief than those of the TDP II, which have been partially buried by outwash from TDP III.

At Lago del Toro, TDP II and III moraines fringe the lake along its eastern and southern margin from Sierra del Toro to La Península promontory. Between Sierra Ballena and Lago Porteño, TDP II and III moraines have been breached and partially infilled by glaciofluvial sediments. Farther south, the TDP II and III moraines are distinct at Bahía del Bote, particularly on the eastern slope of La Península promontory.

Outwash plains are associated with the TDP II and III moraines east of Laguna Amarga, Lago Sarmiento and Lago del Toro. A prominent outwash plain grades from the TDP II moraine in front of Laguna Amarga. Here, the head of outwash is at about 165 m a.s.l. The plain grades distally, at approximately 140 m a.s.l., into the outwash plain from

the TDP II moraines at Lago Sarmiento. The Laguna Amarga outwash plain is dissected by a meltwater channel, which displays several small terraces.

At Lago del Toro, outwash sediments from the inner TDP III moraines are sufficiently thick in places to bury partially the TDP II landforms and give them a discontinuous appearance. Here, meltwater channels that head at the innermost TDP III ridge cut through the TDP II moraines and distally grade into the main outwash plain. One of the main channels in front of Lago del Toro (locally know as El Canal; Plate 3, pocket) dissects the TDP II outwash plain and displays four small outwash terraces similar to those described east of Laguna Amarga. Along the southern margin of Lago del Toro, glaciofluvial sediments occur in patches separated by bedrock hills.

Overall, the elevation of the main outwash plain decreases steadily between Laguna Amarga (160 m a.s.l.) and the Río Prat Valley (~25 m a.s.l.). The outwash records the route of glacial drainage into the Pacific Ocean (i.e., Fiordo de Última Esperanza) at times of TDP II, III, and IV moraine deposition.

2.4.1.1.3 TDP IV moraines

TDP IV deposits commonly form the innermost distinct moraine belt along the present shore of Laguna Azul and Lagos Sarmiento and del Toro. TDP IV moraines are less prominent, less continuous, and smaller than those of the TDP II and III systems and commonly occur as two parallel, well-defined ridges at Laguna Azul, Río Paine and Lago Sarmiento. At Laguna Azul, a double kame terrace parallels the south coast of the lake and marks the TDP IV ice margin (e.g., Marden, 1993). Along the north side of Lago

Sarmiento, the TDP IV moraines crosscut the TDP III ridges, and it is not always possible to differentiate the two sets of landforms. At the eastern front of Lagos Sarmiento and del Toro, the TDP IV moraines form subtle ridges that define the present shorelines. Commonly, there is no space separating the TDP III and TDP IV belts in these areas. A prominent ice-contact slope that can be followed as kame terraces along the southern slope of the Maciso del Paine near Lago Nordenskjöld (Moreno *et al*., 2009; Fogwill and Kubik, 2005; Marden, 1993) is included in the TDP IV landforms.

2.4.1.2 The outer Viscachas and Guillermo moraines

In the Torres del Paine region, Caldenius (1932) locally named the *Gotiglacial* landforms the Río de las Viscachas (RV) and Arroyo Guillermo (AG) moraines. Both are composite terminal moraines, made up of several, wide, arcuate ridges, and located ~100 km from present margin of the Southern Patagonian Ice Field (Fig. 2.1; Plates 1 and 5, pocket).

2.4.1.2.1 Río de las Viscachas (RV) moraines

The RV moraines are located between, and to the east of, Sierra Contreras and Sierra del Cazador (Plate 5). We separate them into three groups (I, II, III), based on their different positions. Bedrock topography most likely conditioned the deposition of these landforms, particularly affecting the inner Río de las Viscachas II and III moraines (Plate 5, pocket). The Río de las Viscachas I (RV I) is the outermost moraine complex and includes at least 20 ridges over a distance of about 13 km. Moraines are on the order of

hundreds of meters wide and are separated by gentle depressions and ice-marginal meltwater channels. The lateral moraines of the RV I system can be traced westward to Sierra del Cazador in the south (maximum elevation= 640 m a.s.l.) and to the vicinity of Sierra Contreras in the north (maximum elevation= 750 m a.s.l.). Landforms and sediments are well-preserved, although relief is low and the crests are broad, particularly when compared with the TDP I–TDP IV moraines to the west. There are only scattered surface boulders. Both glaciofluvial and loess infilling have exerted an important role in leveling the local topography after ice retreat (Caldenius, 1932).

The Río de las Vischachas II (RV II) moraines are located a few kilometers inboard of the RV I ridges and form a continuous belt about two kilometers wide. The moraine belt reaches 300 m a.s.l. at its easternmost point. Whereas the left lateral can be traced along the southern slope of Sierra Contreras (maximum elevation of 380 m a.s.l.), the right lateral moraine only can be followed to about four kilometers east of Sierra del Cazador, where apparently it has been eroded by fluvial activity.

The Río de las Vischachas III (RV III) landforms delineate a discontinuous arc between Sierra Contreras and Sierra del Cazador, about 20 km inboard from the RV II system (Plate 5, pocket). Two or, in places, three ridges make up RV III belt, which is associated with sandy gravels of glaciofluvial origin (Hauthal, 1905). At its eastern front, this moraine reaches 110 m a.s.l. and is about 500 m wide. RV III lateral moraines occur on the flanks of Sierra Contreras (~150 m a.s.l.) and Sierra del Cazador (~150 m a.s.l.), but are difficult to follow because of post-depositional slope processes. On the south slope of Sierra Contreras, the RV III lateral moraines are on the foothills below RV II drift. The right-lateral moraine dams an irregularly shaped lake just north of Sierra del

Cazador; from here, the moraine continues westward along the slope of the mountain where it disappears ~0.5 km before reaching Río de las Chinas.

In the upper Río de las Chinas Valley, north of Sierra Contreras, a group of moraines is located at a position similar to the RV III landforms. These moraines have subtle relief and appear as hilly topography, with scattered boulders. Based on the shape of these landforms and their position, we suggest that they may correspond to the same event that deposited the RV III moraines south of Sierra Contreras.

2.4.1.2.2 Arroyo Guillermo (AG) moraines

As described by Caldenius (1932), the horseshoe-shaped Arroyo Guillermo terminal moraine belt occurs between Sierra del Cazador and Meseta Latorre, south of the RV I moraine arc and about 85 km east of the present-day ice field (Fig. 2.1; Plates 1 and 5, pocket). Several wide, low-relief ridges constitute this moraine belt, which can be traced for more that 30 kilometers. It reaches a maximum elevation of 425 m a.s.l. at its eastern end. Because both the RV I and the AG lateral moraines seem to merge on the eastern slope of Sierra del Cazador (500 a.s.l.), I infer that they were deposited during the same advance (e.g., Caldenius, 1932).

2.4.2 Evidence for paleolakes

Today, drainage to the Pacific Ocean in the Torres del Paine area is through Río Serrano (25 m a.s.l.). When Río Serrano Valley was occupied by ice, Río Prat Valley, a

low-elevation pass between Lago Porteño and Fiordo de Última Esperanza, was used as a meltwater conduit (Plate 5, pocket). Each time the former Patagonian ice sheet advanced eastward in Torres del Paine or northward in Última Esperanza and closed these two drainages to the Pacific Ocean, a proglacial lake formed in the Torres del Paine region. Glaciolacustrine terraces and sediments are common and reflect this important aspect of the geomorphic history. In this section, we describe the locations and attributes of the glaciolacustrine terraces and sediments present in the region, with the goal of reconstructing their relationship to ice-sheet fluctuations.

2.4.2.1 Glaciolacustrine terraces

In the vicinity of Torres del Paine National Park, numerous mountains east and south of Lago del Toro, such as Sierra del Cazador, Sierra Ballena, and Sierra Arturo Prat, exhibit on their flanks discrete, single and, rarely, double systems of glaciolacustrine terraces (e.g., Solari, 2010, Solari *et al*., in press; Figs., 2.3, 2.4; Plates 3-5, pocket). Although some of these landforms resemble kame terraces, we interpret them as being lacustrine features, because their elevations do not change over distances of several kilometers. Also, no trace of former fluvial features (e.g., channels) is evident on them. Terraces can be continuous for several kilometers (e.g., five kilometers at Sierra del Cazador), but more commonly are discontinuous fragments that range in length from hundreds of meters to one to two kilometers. These discontinuous glaciolacustrine landforms are at higher elevation in the western area of the park than in the east. For instance, terraces occur at 125, 140 and 155 m a.s.l., in the eastern, central and western

parts of the Torres del Paine National Park, respectively. Most terraces have been carved into bedrock and lack sediment. On steep hillsides, such as at Cerro Castillo, these shorelines are narrow (e.g., tens of meters) and slope from the back to the front of the landform. In other locations, such as at Sierra del Cazador, terraces are wide (e.g., several hundred meters) and low gradient.

Figure 2.3. Double glaciolacustrine terrace systems in Torres del Paine National Park area. Images display shorelines at 280-250 m a.s.l. and 155-125 m a.s.l. on Cerro del Cazador (upper photos) and Cerro Castillo (lower photos).

Figure 2.4 155-125 m a.s.l. glaciolacustrine terraces in Torres del Paine National Park area. From upper to lower: Perched delta at Río Prat valley; Río Prat Valley; Sierra Jorge Montt; Cerro Solitario; southern Sierra Ballena.

Shorelines range from 280 m a.s.l. to 125 m a.s.l., but those at about 125 m a.s.l. are the most common, particularly in the eastern half of the Torres del Paine National Park and adjacent areas. On the western slope of Sierra del Cazador, two terrace levels were carved by glacial lakes, one at about 250 m a.s.l. and other at 125 m a.s.l. (Fig. 2.3; Plate 5, pocket). Whereas the lower terrace is very prominent and laterally continuous for about five kilometers, the upper level is less extensive. To the west, on the northern slope of Cerro Castillo, levels are present at 280 m a.s.l. and 155 m a.s.l. (Fig. 2.3; Plate 5, pocket). Distal to the TDP I moraine and on the eastern side of Sierra Ballena there is a terrace at 125 m a.s.l. (Fig. 2.4). The same level is also present on the north flanks of Cerro Solitario. Where it parallels Río de las Chinas, the road that connects Bahía del Bote and the town of Cerro Castillo was built on top of a nearly continuous terrace, also at ~125 m a.s.l. Less prominent, but clear in aerial photographs, are narrow terraces at 140 m a.s.l., which occur on the northwest corner of Sierra Jorge Montt (Fig. 2.4; Plate 4, pocket). A flat, extensive plain at 140 m a.s.l. also occurs between Cerro Margarita and Sierra Jorge Montt. On the eastern slopes of Cerro Campana, in the Tres Pasos River Valley, relict deltas occur at 155 m a.s.l. and plains at similar elevations also are present. In addition, we detected terraces and deltas with the same elevation (155 m a.s.l.) in Río Prat Valley (Fig. 2.4; Plate 4, pocket). To the south and east of this valley, entering the Última Esperanza region, a terrace occurs at 150 m on the slopes of Cerro Benitez (e.g., Sagredo *et al.*, 2011; Stern *et al.*, in press). Here, several caves and notches, including the well-known Cueva del Milodón (Saxon, 1976), were carved by lake waves in the Upper Cretaceous conglomerate (e.g., Winn and Dott, 1977). The same level crosses the western and southern slope of Sierra Dorotea.

The Río de las Viscachas moraines are made up of till interbedded with both proximal and distal (e.g., varves) glaciolacustrine sediments that Caldenius (1932) linked with large proglacial lakes formed during ice advance and retreat. Río de las Viscachas, which today drains towards the Pacific Ocean, served at this time as the spillway that conducted into the Atlantic Ocean from lake at 300 m a.s.l. In the Arroyo Guillermo basin to the south, a shoreline at 420 m a.s.l. on the proximal face of the outer moraines formed after glacier retreat from the maximum AG position (e.g., Caldenius, 1932).

2.4.2.2 Glaciolacustrine sediments

In this section, we describe localities where stratigraphic-based findings provide evidence for the existence of glacial lakes formed during the last glaciation and deglaciation.

The Las Mascaras site (51º12’41’’S and 72º26’14’’W; ~70 m a.s.l.) is exposed in the northern bank of Río de las Chinas before it reaches Las Mascaras bridge (Lago del Toro basin, Fig. 2.5; Plate 5, pocket). Here, the site reveals several meters of rhythmically bedded silt and clay (facies A in Fig. 2.5) and gravel sediments (facies B in Fig. 2.5). The gravel beds, which are more abundant in the lower part of the section, are clast-supported, very well sorted, and can be followed laterally for tens of meters. They show cross bedding. Ripples may be present within fine gravel. Isolated peebles locally distort the laminations. The silt and clay are very well laminated and form horizontal beds several meters long. Rare, isolated cobbles that locally deform underlying laminations occur within the fine sediment and are interpreted as dropstones.

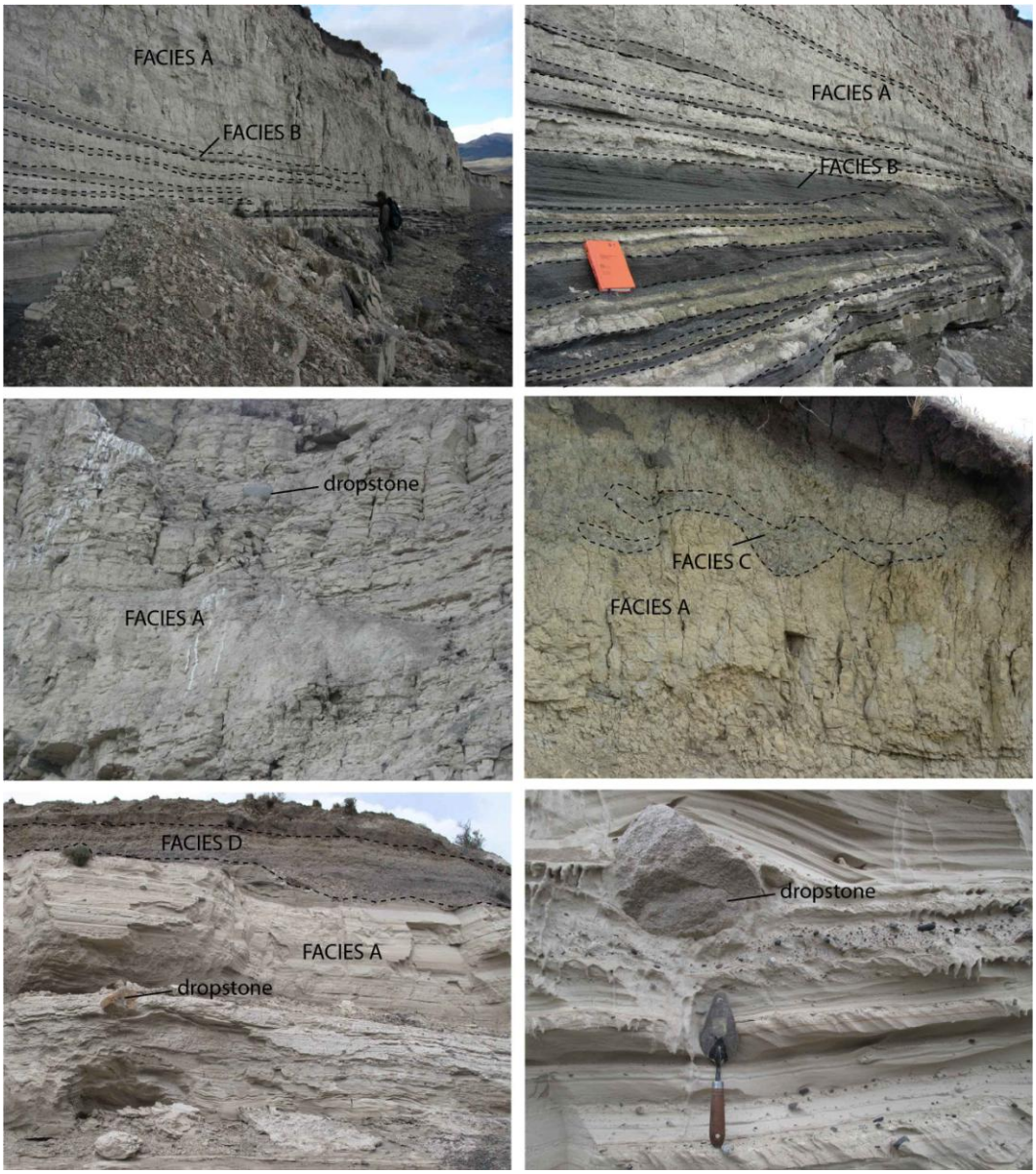

Figure 2.5. Glaciolacustrine sediments in Torres del Paine National Park area. Top and middle left images: Las Mascaras Site; Middle right image: Arroyo Guillermo Site; Bottom images: El Canal site. Facies A: well-laminated glaciolacustrine sediments, which may contain dropstones and gravel layers. Facies B: well-sorted gravel displaying crossbedding and traction structures. Facies C: irregularly shaped gravel lenses embedded within facies A at Arroyo Guillermo Tributary section. Facies D: fluvioglacial gravelly pebbles.

The Arroyo Guillermo Tributary site (51º15’25’’S and72º22’10’’W; ~110 m a.s.l.) is located about seven kilometers southeast of Río de las Chinas, where a small tributary of Arroyo Guillermo cuts into a flat plain and exposes glaciolacustrine sediments (Fig. 2.5; Plate 5, pocket). The section is only about three meters thick and consists of finely laminated clay and silt (facies A in Fig. 2.5). Clayey laminae may contain mud cracks. Rare isolated cobbles, probably dropstones, and rare irregular gravel beds (facies C) are present in this fine sediment unit. Clasts are up to cobble size and the sorting ranges from intermediate to poor.

An artificial channel, El Canal (51º08’30’’S and 72º32’19’’W; ~65 m a.s.l.; e.g., Caldenius, 1932; Marden, 1993; Solari *et al*., in press), was excavated about a century ago within a natural meltwater channel crossing the TDP moraine belts in front of Lago del Toro (Caldenius, 1932; Marden, 1993) (Fig. 2.5; Plate 5, pocket). Along its length of ~2.5 kilometers, there are proximal and distal glaciolacustrine sediments, including delta packages, underflows deposits, and ice-rafted debris sediments, together with subaerial glaciofluvial sediments (Fig. 2.5).

Glaciolacustrine sediments in El Canal consist of generally well-laminated (although the sediment is massive in some sections), mostly pure silt forming planar beds (facies A in Fig. 2.5). In some sections, these are interbedded with distinct gravel layers (few mm to cm thick) that laterally reach tens of centimeters to meters long. Undulating laminae may occur. Silt laminae drape over the gravel beds, which, in places, show normal gradation. Isolated clasts as much as one meter in diameter are embedded in the fine, well-laminated sediment. Commonly, the sediments are glaciotectonized (e.g., folded beds), particularly where associated with diamicton units.

Several types of diamictons, interpreted here as waterlain sediments and till (e.g., flow till and lodgement till) can be differentiated along El Canal section. Diamictons range from poorly sorted, coarsely bedded sediment to massive units that vary in the proportion of clasts/matrix and clast size. The coarsely stratified, deformed diamictons that occur interlayered with silt beds are usually associated with moraine landforms. These diamictons include folded and deeply distorted dipping gravel beds. Another type of diamicton consists of irregularly shaped, coarsely stratified, poorly sorted beds of gravelly cobbles. Beds can be several decimeters thick, subhorizontal or dipping as much as 15º eastward, and commonly occur overlying massive diamicton. Clasts are subrounded to subangular. A third diamicton type consists of massive sediment. Clasts, which are subangular to subrounded (maximum diameter to 25 cm and on average 5 cm), occur sparsely in an indurated, silt matrix. This sediment unit is not common in the sequence but where present, occurs at the base of the section.

Well-sorted sandy gravel makes up horizontal, parallel beds that can be traced laterally for several tens of meters (facies D in Fig. 2.5). Although mostly well-sorted and clast-supported, this sediment varies significantly along a west-east transect. For instance, at some locations it attains a massive to coarsely bedded structure, commonly associated with poor sorting. This contrasts with distinct parallel, horizontal bedding at other locations. Clasts are rounded to subrounded. Cobbles make up the average size, although rare boulders occur. These units are interpreted as fluvioglacial deposits that, where present, occur at the top of the sediment sequence.

2.5 Discussion

2.5.1 Glacial advances

2.5.1.1 RV I-III moraines

Two ages from the outer RV I moraine belt are within 1 sigma and yielded a mean age of 49,000 ka BP (Chapter 3). Taken at face value, these ages imply that this landform was deposited during the early to middle part of the last glaciation. In light of this age coming from only two samples, we consider it preliminary, because it could represent a minimum age due to effects of erosion. At the time of RV I deposition, the margin of the Patagonian ice sheet in Torres del Paine was about 100 km beyond its present position. The broad morphology and low relief of the moraines resulted in part from glaciolacustrine sediments infilling inter-moraine depressions. The well-organized suite of smaller, concentric moraine ridges just proximal to the RV I belt probably may have been deposited during deglaciation from the maximum RV I ice position. This suggests that after the Patagonian ice sheet reached its terminal position at or somewhat earlier than 49, 000 years ago, it fluctuated near its maximum before gradually retreating westward.

The size and continuity of the RV II and RV III moraine belts, plus their isolated position between the RV I and the TDP I systems, suggest that these landforms represent important readvances of the Patagonian ice sheet. Although degraded in some sections by post-depositional fluvial erosion, the RV II and RV III arcs are prominent and larger than

the inner RV I landforms, indicating that ice lingered at these positions at times of the last glacial period.

Although no absolute chronologic data are available at this time for RV II and III moraine belts, we hypothesize that they were deposited during the last glacial period, because of their position between the RV I and TDP I moraines in del Toro basin, which have been dated to ≥49,000 and 16,500 years ago, respectively. The good preservation of the RV II and RV III moraines, where not affected by post depositional fluvial erosion, is consistent with this interpretation.

2.5.1.2 TDP I-IV moraines

The TDP I moraines are prominent landforms comparable in size and morphology to the RV III ridges. However, there are distinct differences in the morphology of the TDP I moraines between the basins. For example, at Laguna Azul the landforms are broad and form a low-relief topography, in contrast with those at Lagos Sarmiento and del Toro, where TDP I occurs as well-defined moraine ridges. In addition to morphological differences, ^{10}Be exposure dates suggest that not all of the TDP I moraines are the same age. Whereas samples from the TDP I moraine belt in the Laguna Azul area yielded a mean age of 41,300 ± 1,300 years ago (n=5), at Lago del Toro they produced a mean age of 16,500 ± 600 years ago (n=5) (Chapter 3). This significant gap in time, as well as the morphological differences, suggests that TDP I moraines at Laguna Azul and Lago del Toro, although originally mapped as the same moraine belt, actually were deposited during different pulses within the last glaciation (Plates 2, 3, pocket).

In contrast to the moraines at Laguna Azul, the TDP I moraines at Lagos del Toro and Sarmiento are similar to each other in terms of number, size, geographic pattern, morphology and position of ridges. The outer TDP I moraines are nearly continuous between the two basins, separated by only three kilometers of foothills. This morphological evidence seems to suggest that TDP I moraines at Sarmiento and del Toro basins were deposited during the same glacial event and both landforms are younger than the TDP I moraines at Laguna Azul.

The TDP I moraines at Laguna Azul mark the most extensive glacial advance in this basin. Our ^{10}Be data from these landforms (Chapter 3) reveal that this position was gained by ice during pre-global LGM times, specifically during MIS 3 (60-25 ka). The next inner deposits preserved at Laguna Azul after TDP I are represented by the late glacial TDP II moraines.

Because of the new ^{10}Be ages (Chapter 3) of the landforms preserved in Lago del Toro, we suggest that the TDP I moraines in the del Toro and Sarmiento basins most likely denote the last readvance or stillstand of the Patagonian ice sheet in Torres del Paine before the local termination. These moraines occur in a position that is similar to other moraines in Patagonia that mark ice extent at the end of the LGM, such as the D moraines in the Strait of Magellan (Kaplan *et al*., 2008; Sugden *et al*., 2005), the Fenix I-Menucos moraines at the Lago Buenos Aires (e.g., Douglass *et al.*, 2006; Kaplan *et al*., 2004) and the Third and Final limit at Lago Pueyrredón (Hein *et al.*, 2010).

As inferred from their geomorphological similarities and identical age of 14,200 yr BP (Chapter 4; Moreno *et al.*, 2009), TDP II, III, and IV moraines all represent a

distinct stadial. Based on the number and size of moraines, we infer the ice at this time was very active, capable of eroding, transporting and depositing most of the glacial drift that fringes the eastern shores of Laguna Azul and Lagos del Toro and Sarmiento. The next inner prominent ice-marginal landforms in Torres del Paine National Park flank Lago Margarita (Lago Grey area) and correspond to the F moraines of Marden (1993) and Marden and Clapperton (1995). Similarly, a double moraine system (F moraines) encloses Lago Dickson. Likely, these "F" multiple moraine arcs (Marden and Clapperton, 1995) represent early Holocene glacial fluctuations of the Southern Patagonian Ice Field. New evidence from the innermost moraine belts adjacent to the ice field (García, unpublished data) has linked these landforms to the latest Holocene.

2.5.2 Torres del Paine ice extent

Whereas Caldenius (1932) proposed that the Patagonian ice sheet during the last ice age deposited four main moraine arcs (*Initioglacial, Daniglacial, Gotiglacial* and *Finiglacial*) that occur 160 km east of the present-day ice margin, Marden and Clapperton (1995) postulated that LGM ice was rather small and only filled present-day lake basins in the national park (i.e., Laguna Azul, Lago Sarmiento, Lago del Toro). These two opposite views were founded mainly on glacial geomorphology. Here, based on the same landscape units and new age control data, we propose an intermediate scenario for Torres del Paine ice during the last glaciation.

In this new reconstruction, the Patagonian ice sheet extended about 100 kilometers east of the current margin in Torres del Paine and deposited seven moraine

belts within a 50-km-wide band beginning at or before 49,000 ka (Fig. 2.1; Plates 1 and 5). If this interpretation is correct, it suggests that Torres del Paine ice already was at the maximum extent of the last glaciation by ≥49,000 ka and 41,000 ka, and was more extensive during the early stage of the glaciation rather than during the global LGM (19-23 ka; Mix *et al*., 2001). These data afford evidence for an advance of the Patagonian ice sheet during MIS 3, which has been reported only for limited sites in southern South America (Sagredo *et al*., 2011; Denton *et al*., 1999b).

This situation does not necessarily imply that ice volume in Torres del Paine was significantly larger during MIS 3 than during the LGM. Several factors, such as local topography (e.g., Glasser *et al*., 2009), steepness of the ice profile (Oerlemans, 1989; Furbish and Andrews, 1984), and glacier bed conditions (e.g., Boulton and Jones, 1979), may have played an important role in ice extent during different phases of the last glaciation. For example, each successive glaciation probably excavated the lake basins, and thus ice during the LGM may have occupied deeper basins than the previous expansions and did not advance as far to the east. However, if lake basins were infilled with sediments between each expansion, it would result in no net excavation, and therefore this geomorphologic factor would not account for significant differences in glacial extent.

2.5.3 Glacial paleolakes

Caldenius (1932, page 100) stated that an understanding of glacial lakes in the Torres del Paine region "..is one of the most interesting and complicated glaciolacustrine

problems in the Andean Cordillera." This is because the hydrological continental divide here is defined by moraines, which control the elevation of drainage to the east into the Atlantic Ocean. In addition, the geographical connection between Torres del Paine and Última Esperanza basins results in ice extent to the south having the potential to control lake level in Torres del Paine. Therefore, ice advancing from the southern Andes or retreating from the RV moraines prompted the formation of glacial lakes. Drainage today to Última Esperanza basin is through Río Serrano. However, during full and late-glacial times, this drainage was blocked by ice. Instead, Río Prat Valley (south of Lago Porteño), when deglaciated, was used as the main route for meltwater escaping to Última Esperanza (Plate 4, pocket). However, during the last glaciation, each time ice extended to Cerro Castillo, the Río Prat pass remained blocked and a lake formed in the Torres del Paine region. Solari (2010) referred to this sequence of glacial lakes in the Torres del Paine region as paleolake Tehuelche. Paleolake Tehuelche had different phases linked to distinct elevations, as defined by outlets that conducted water to the Atlantic Ocean. In our interpretation, during the entire glacial period represented by the TDP and RV moraine systems, paleolake Tehuelche attained elevations that ranged from 420 to 125-155 m a.s.l., both as individual lakes formed at the Río de las Viscachas and Arroyo Guillermo basins, and as united lakes covering a significant part of the region.

Because of the geographic connection, the reconstruction of paleolakes in the Torres del Paine region, particularly at the end of the last glaciation (i.e., post-deposition of the RV moraines), needs to be done in conjunction with evidence from Última Esperanza; drainage of the lake was controlled by the extent of the Patagonian ice sheet in both areas.

Normally, in temperate climatic regions, such as Torres del Paine, input from precipitation is higher than output from evaporation, and therefore the formation of wave-cut platforms occurs when lake level is stable at the elevation of a spillway. One important question regarding the littoral terraces present in the vicinity of Torres del Paine National Park (i.e., west of the RV moraines) is whether all of them (125 m a.s.l., 140 m a.s.l., 155 m a.s.l., 250 m a.s.l and 280 m a.s.l. shorelines) correspond to different lake phases or if some of them, despite differences in elevation, correspond to the same lake. The fact that these terraces are discontinuous makes it difficult to distinguish between these two options.

By one scenario, each of the terrace elevations (i.e., 280 m a.s.l, 250 m a.s.l., 155 m a.s.l., 140 m a.s.l. and 125 m a.s.l.) would represent a distinct phase of paleolake Tehuelche, meaning that the Patagonian ice sheet retreated, allowing a drop in lake level, but that this recession was punctuated by stable ice and hence lake positions. However, an alternative is that differential isostatic crustal rebound caused the relatively small differences among terrace elevations (cf. Stern *et al*., in press; Hein *et al*. 2010). No location displays more than two shorelines. This fact, along with the pattern of landform elevations, suggests that there may be only two levels, one at 250-280 m elevation and the other at 125-155 m elevation. Because terraces occur as landform fragments, we cannot trace them continuously all the way from east to west to confirm this hypothesis. Nonetheless, as mentioned above, our multiple measurements indicate an increase in elevation over long east-west distances (30 km) with higher elevations towards the present ice field to the west, where ice was thicker and lake water deeper the last glaciation. Because of the differential loading, the crust may have suffered more extreme

vertical movements to the west, resulting in unequal amounts of rebound. If this second scenario is correct, it implies a vertical shoreline offset of about 30 m over approximately 30 km of distance, which is slightly greater than values reported previously for southern Patagonia (Stern *et al.*, in press; McCulloch *et al.*, 2005; Ivins & James, 1999). For instance, just south of Torres del Paine in Última Esperanza, Stern *et al.* (in press) estimated 45 m of vertical change along 65 km of east-west distance. Based on the elevation of glaciolacustrine terraces in the Strait of Magellan, McCulloch *et al*. (2005) estimated a similar difference of ~35 m of vertical displacement along ~70 km. In summary, differential postglacial uplift is a common theme along the east side of the southern Andes. Although more study regarding postglacial uplift and crustal rebound in the Torres del Paine region is important, we favor this second scenario to explain the spatial pattern of shorelines related to the Tehuelche paleolake.

2.5.3.1 Tehuelche paleolake phases

Here, we provide a tentative reconstruction that links littoral terraces, spillways and moraines in the Torres del Paine region. We use available exposure-age data (Chapters 3 and 4; Sagredo *et al*., 2011) to infer possible temporal scenarios, although we do not intend to tie undated landforms to an absolute age. Our interpretation suggests that the evolution of the Tehuelche paleolake can be divided into three phases: Early Phase (lake levels at ≥300 m a.s.l., Fig. 2.6b-c), Middle Phase (lake level at 250-280 m a.s.l., Fig. 2.6d) and Late Phase (lake level at 125-155 m a.s.l., Fig. 2.6e-f). Because our data from the outer RV and AG moraines and associated lacustrine sediments are preliminary,

we focus on the lower lake phases (i.e., 250-280 and 125-155 m a.s.l.) that occurred after the deposition of RV III moraines. Two dependent factors are relevant for the reconstruction of paleolake Tehuelche: (1) the position of the ice both in Torres del Paine and Última Esperanza, which dammed the lake and altered drainage, and (2) the elevation of spillways.

The Middle Phase is associated with a lake level at 250-280 m a.s.l. (Fig. 2.6d) likely tied to the elevation of the Río Turbio-Tres Pasos spillway (Plate 4, pocket). Although there is no shoreline that can be traced to this spillway, based on similarity in elevation, we infer that the spillway and the 250-280 m a.s.l. shoreline are linked. During this phase, ice had retreated sufficiently from the Arroyo Guillermo and Río de las Viscachas basins to clear the Río Turbio-Tres Pasos spillway and to allow a united lake to form (Fig. 2.6d). The exact ice position during this phase is unknown, but we infer that it must have formed a continuous front in Lago del Toro basin, west of Sierra Dorotea, allowing waves to carve terraces on both Cerros del Cazador and Castillo. To the south, the Patagonian ice sheet may have lingered at the Dos Lagunas moraine between Sierra Señoret and Sierra Dorotea, where an ice-contact delta at 270 m a.s.l. grades from the moraine, built when the Patagonian ice sheet stood at this site (~38 ka; Sagredo *et al.*, 2011). While ice fluctuated at this position, it blocked drainage and prompted lake formation at 250-280 m a.s.l. and the associated shoreline in Torres del Paine.

Based on the wide (e.g., 1-2 km), flat top of the TDP I moraine at Lago Sarmiento, together with its elevation (115-125 m a.s.l.) and association with proximal subaerial glaciofluvial sediments at ~125 m a.s.l. at the Estancia site (Fig. 2.2; Plate 2, pocket), we infer that part of this landform represents an ice-contact delta. Thus, the

proximal glaciofluvial sediments cropping-out at the Estancia site indicate that at least the upper part of this feature was deposited under subaerial conditions, adjacent to a proglacial lake at 125 m a.s.l. The fact that subaerial outwash sediments occupy the whole sequence at the Estancia site indicates that a deep lake never covered this site after TDP I moraine deposition. Because deep lake sediments are lacking, we infer that the Middle Phase (e.g., 250-280 m a.s.l.) of the Tehuelche paleolake must predate the TDP I glacial pulse at Lago Sarmiento and it probably occurred at ~38 ka, as inferred from three exposure ages that date the Dos Lagunas moraines and associated ice-contact delta (Sagredo *et al*., 2011).

The Late, and final, Phase of paleolake Tehuelche at 125-155 m a.s.l. probably occurred during the advance to and retreat from TDP I moraine at Lagos Sarmiento and del Toro (Fig. 2.6e-f). This scenario is consistent with the ice-contact delta described at Estancia Site that marks a lake level at 125 m a.s.l. contemporaneous with moraine formation. In contrast, our mapping identified outwash plains grading to the late-glacial TDP II, III, and IV moraines (Chapter 4). From this evidence we infer that the Patagonian ice sheet in Torres del Paine terminated under subaerial conditions during the Antarctic Cold Reversal and that paleolake Tehuelche had drained by this time (Fig. 2.6g). This implies that ice had retreated sufficiently in Última Esperanza to open a new lower spillway. Therefore, the time for the lake at 125-155 m a.s.l. is bracketed to during and after the TDP I event, but before the TDP II advance.

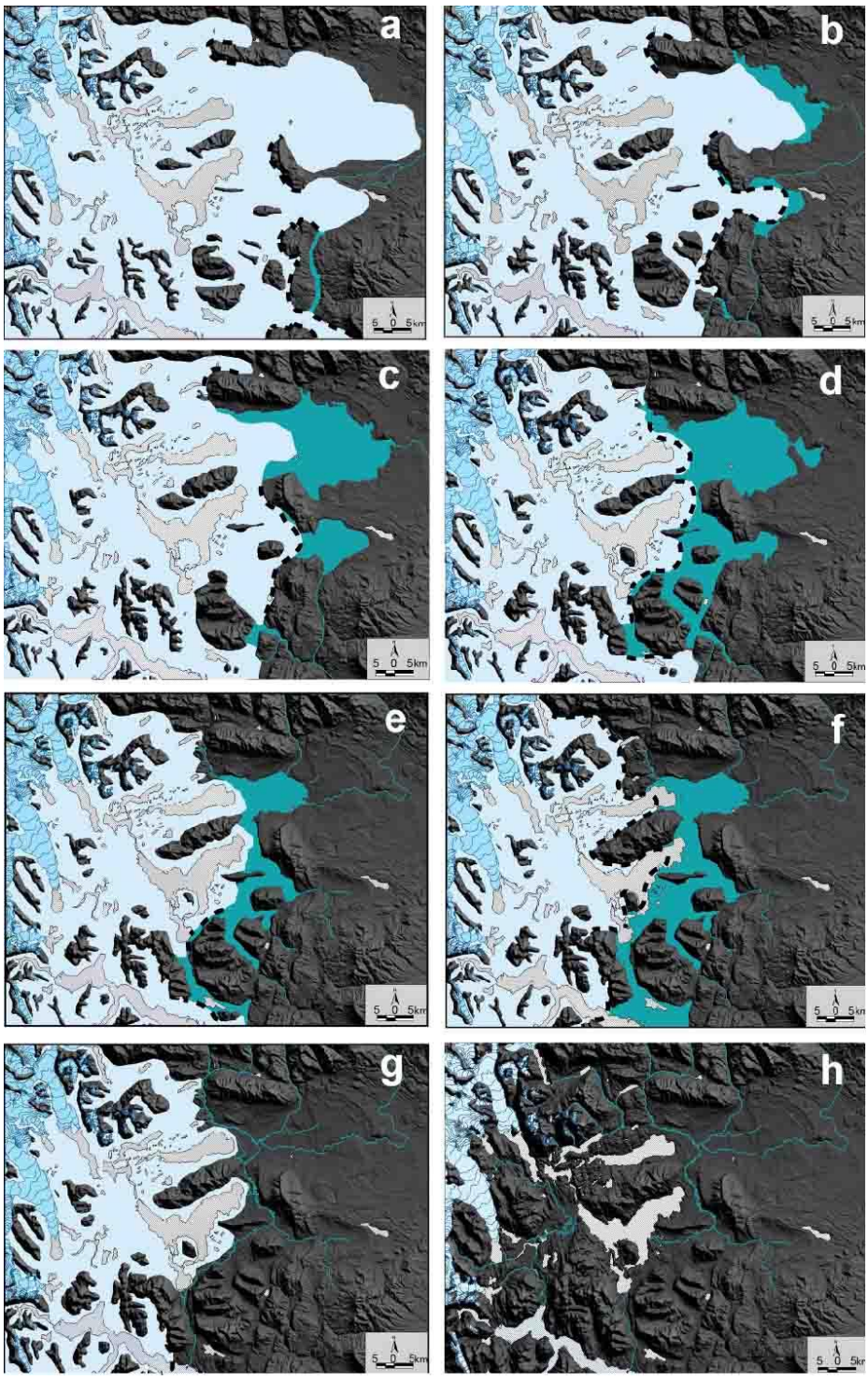

Figure 2.6. Evolution of the Patagonian ice sheet and paleolake Tehuelche throughout the last glacial period. a: RV I glacial maximum; **b-c**: Early Phase (RV II and RV III readvances); **d**: Middle Phase (TDP I Laguna Azul/Dos Lagunas moraines readvance: ~40 ka); **e-f**: Late Phase (TDP I Lago del Toro moraine readvance ≥16.5 ka and Termination); **g**: TDP II-IV readvance (ACR phase); **h**: present. Dashed line: inferred ice margin.

In order for the lake to drain from 250-280 m a.s.l. (Middle Phase) to 125-155 m a.s.l. (Late Phase), the Patagonian ice sheet must have retreated from a pass between the ice front and Cerro Castillo in Río Prat Valley (Plate 4, pocket). It also must have receded from the LGM age Arauco moraines (e.g., Sagredo *et al.,* 2011) and Sierra Dorotea in Última Esperanza in order to leave a gap between ice and topography that allowed a passageway to the Frontera spillway to the Atlantic Ocean (~125 m a.s.l., e.g., Sagredo *et al.,* 2011). If ice in Torres del Paine during the TDP I advance had buttressed against Cerro Castillo, a lake draining through Río Turbio-Tres Pasos spillway (i.e., 250-280 m a.s.l.) would have formed instead. Our evidence from the Estancia Site does not support this scenario. Based on prominent shorelines and muddy sediments present in cores, Sagredo *et al.,* (2011) suggested the existence of ice-dammed paleolake Puerto Consuelo at Última Esperanza. This lake formed at 150 m elevation during retreat from the Dos Lagunas moraine and Sierra Dorotea and probably merged with paleolake Tehuelche during the Late Phase.

Although we know the Late Phase had begun by the time TDP I moraines at Lagos del Toro and Sarmiento were deposited and was over before the deposition of TDP II landforms, the exact timing is not known. Sagredo *et al.* (2011) obtained two calibrated radiocarbon ages of 17.6 and 17.3 cal ka (recalibrated here using INTCAL09, Reimer *et al*., 2009) at Vega Benitez and Lago Dorotea, respectively, which they interpreted as minimum ages for glacial retreat from LGM positions, at or near Dos Lagunas moraine. If this interpretation is correct then the date of 17.6 ka represents a close-minimum age for clearing of the 125-155 m a.s.l. Frontera spillway and formation of Lago Puerto Consuelo at 125-150 m a.s.l. (Sagredo *et al*., 2011; Stern *et al.,* in press). However, ice

retreat from Dos Lagunas moraines could have occurred somewhat earlier, because direct dating of these landforms indicate it was formed at ~38 ka (Sagredo *et al*., 2011), 20 ka before the minimum ages obtained from Vega Benitez and Lago Dorotea. An alternative is that during the Late Phase the Patagonian ice sheet could have been buttressed against an undated inner ice-marginal position at Cerro Benitez few kilometers south of the Dos Lagunas moraines (Plate 4, pocket). This position is defined by a delta at 150 m a.s.l. and a moraine (Sagredo *et al*., 2011), suggesting that the ice front was at this position during the existence of Lake Puerto Consuelo, which would have merged with Tehuelche. Regardless of when ice pulled back from the Dos Lagunas position and Sierra Dorotea, this glacial retreat opened the Frontera spillway, allowed the formation of paleolake Tehuelche at 125-155 m a.s.l., and eventually led to subaerial outwash sediments being deposited at the Estancia Site.

Based on available chronological evidence, the complete drainage of Lago Tehuelche may have occurred at ~16.5 ka. Because of the elevation of the TDP I moraines at Lago del Toro (i.e., ~80-110 m a.s.l.), we infer that the lake at 125-155 m a.s.l. may have covered this moraine. Shielding of the boulders by lake water may have resulted in its exposure age of 16.5 ka being slightly younger than the true landform age (Chapter 3). One possibility is that the age may represent the drainage of the lake during the termination. This mean age is in close agreement with the proposed drainage age for Lago Puerto Consuelo by Sagredo *et al.,* (2011) of 16.8 ka (recalculated using INTCAL09, Reimer *et al*., 2009) obtained from a core in Lago Pintito. This age represents a close-minimum age for ice pulling back from the Lago Pinto moraines, at the SW sector of Última Esperanza basin, which likely led to the opening of lower outlet that

allowed lake drainage. The minimum age of 16.8 ka for lake drainage also corresponds well with calibrated radiocarbon ages of milodón remains (dung, hair and skin) found at 150 m a.s.l. (i.e., Cueva del Milodón, Long and Martin, 1974). These ages also imply that Lake Puerto Consuelo had drained by 16.8 ka. Based on this chronological and morphological evidence for glacial lakes at both Torres del Paine and Última Esperanza basins, we suggest that paleolake Tehuelche during the Late Phase merged with glacial lake Puerto Consuelo and that this phase began some time before 17.6 ka and ended by 16.5-16.8 ka.

Las Mascaras (~70 m a.s.l. Fig. 2.5; Plate 5, pocket) and Arroyo Guillermo Tributary (~110 m a.s.l. Fig. 2.5; Plate 5, pocket) sites are located between the RV III and the TDP I moraines. The sediment sequences recorded at these sites show well-laminated fine sediments and well-sorted gravelly sediments that represent lake environments. The absence of till in these sequences implies that ice never covered the sites after lake sediments were settled, and therefore these sediments were deposited after ice had retreated from the RV III moraine. Based on the crossbedding features of gravel beds (e.g., several meters long) and distinct encroachment structures, together with the good sorting, we interpret these sediments as traction beds formed subaqueously by density undercurrents not far from the ice front (e.g., Brodzikowski & van Loon, 1991). Poorly sorted gravel beds and isolated cobbles within the well-laminated, muddy sediments at both Las Mascaras and Arroyo Guillermo sites represent ice-rafted debris due to melting or turnover of icebergs.

We infer from outwash plains grading to the late glacial TDP II, III, and IV moraines, at different elevations (~75-90 m a.s.l.), that the Patagonian ice sheet in Torres

del Paine terminated under subaerial conditions and that paleolake Tehuelche had drained by Antarctic Cold Reversal time (Fig. 2.6g). Subaerial drainage probably extended all the way to the Pacific Ocean, because the highest outwash plain grading from the TDP II, III, and IV moraines in front of Lago del Toro occurs at ~80 m a.s.l. This outwash plain can be traced discontinuously to Fiordo de Última Esperanza through Río Prat Valley, where glaciofluvial plains occur at ~25 m a.s.l. (Plates 3-4, pocket). Therefore, any potential late glacial lake must have been below this elevation. This reconstruction does not agree with Solari's interpretation (2010), who, based on lacustrine sediments in El Canal and moraine location, proposed that TDP I, TDP II, III glacial fluctuations were acompained by a lake at 240-260 m a.s.l. and that TDP IV was accompanied by a lake at 150-160 m a.s.l.

Based on dating and interpretation of pebbly mud and clay sediments at Pantano Dumestre (77 m a.s.l.) and Pantano Eberhard (68 m a.s.l.), respectively, Sagredo *et al*., (2011) suggested a lake existed at ~80 m a.s.l. in the Última Esperanza area between 15.4 ± 0.2 and 12.6 ± 0.04 ka. Any glacial lake in Última Esperanza at this time should have extended east of Lago del Toro through the Río Prat Valley and covered the TDP II, III and IV moraines. Yet, our mapping and chronology show that drainage east of Lago del Toro during deposition of these moraines was subaerial. Glaciolacustrine and fluvioglacial sediments exposed in El Canal Site at Lago del Toro show that only local, shallow lakes formed during retreat from TDP II moraine and that they were infilled later by fluvioglacial sediments deposited on top of the section. One possibility is, given that ice filled the Lago del Toro basin during late glacial time (Chapter 4 shows that the TDP II, III, and IV moraines date to this period), the Río Prat was blocked by ice and the ~80

m a.s.l. lake could not reach Torres del Paine. However, such an ice position would have prompted the formation of a separate lake in Torres del Paine, for which there is no evidence at present. These facts, together with the apparent absence of distinct shorelines at ~80 m in Torres del Paine and Última Esperanza (Sagredo *et al.*, 2011; Stern *et al*., in press), question this widespread aspect of the history of a 80-m lake level at Última Esperanza and raises the need for more data to test this hypothesis.

2.6 Conclusions

During the last glacial period, the Patagonian ice sheet in the Torres del Paine region experienced significant fluctuations and deposited multiple moraine systems 50-100 kilometers from the present ice front. Our reconstruction puts ice farther east than generally thought for the last major glacial period (i.e., Marden and Clapperton, 1995), but less extensive than some early interpretations (Caldenius, 1932). At least seven glacial advances occurred during the last glacial cycle between ≥50,000 and 14,000 years ago.

Glacial advances and retreats in the Torres del Paine region were accompanied by the formation of prominent paleolakes, because the continental divide at this latitude is located east of the main crest of the Andes. In the vicinity of Torres del Paine National Park, geomorphic and sedimentologic evidence documents at least two main lake phases: Middle Phase, represented by a lake at 250-280 m a.s.l. that used the Río Turbio-Tres Pasos spillway during retreat from the RV III and AG moraines and readvance to the

TDP I (Laguna Azul) at 41 ka and Dos Lagunas moraines at 38 ka; and Late Phase, represented by a lake at 125-155 m a.s.l. that, as defined by local topographic conditions, must have merged with paleolake Consuelo in Última Esperanza and drained though the Frontera spillway. The Late Phase of paleolake Tehuelche coincided with the deposition of TDP I moraine at Lagos del Toro and Sarmiento but was over by the time TDP II was deposited.

Complete drainage of paleolake Tehuelche early in the termination indicates the Patagonian ice sheet had retreated sufficiently to open a new outlet in western Patagonia that triggered drainage of paleolake Tehuelche/early phase of Puerto Consuelo in Torres del Paine and Última Esperanza.

CHAPTER

3. RECONSTRUCTING THE LAST GLACIATION IN THE TORRES DEL PAINE REGION (51ºS): IMPLICATIONS FOR THE DRIVERS OF ICE-AGES CYCLES IN THE SOUTHERN HEMISPHERE

3.1 Abstract

Stratigraphic comparison of paleoclimate records from the northern and southern hemispheres reveals approximately synchronous glacial changes at orbital time scales, despite the fact that these regions have the opposite insolation signal. However, because of the scarcity of lack of precisely dated glacier records in the southern hemisphere, this apparent synchrony has not been tested adequately at both orbital and shorter time scales, which are important for understanding abrupt climate change and for predicting future climate scenarios. Here, we present ^{10}Be cosmogenic ages, along with careful mapping, that show that the Patagonian ice sheet in the Torres del Paine region (51ºS) advanced at ~49,000, 41,000, and slightly before 16,500 years ago during the last ice age. The data indicate that the glaciers expanded to their maximum during Marine Isotopic Stage 3, much earlier than the global Last Glacial Maximum. Comparison with ice-core and marine records suggests that the stadial conditions documented here were synchronous with ocean-atmosphere reorganizations that took place in the middle and polar southern latitudes during MIS 3 and 2.

3.2 Introduction

Insolation intensity, traditionally thought to be the main pacer of ice ages (Milankovitch, 1941), is of opposite sign in the mid-latitudes of the two hemispheres. Despite this insolation contrast, ice-core and marine records from both hemispheres show approximately synchronous glacial-interglacial climate changes at orbital time scales

(EPICA members, 2004; Jouzel *et al*., 2007; Lisiecki and Raymo, 2005). In addition, moraine records also show (near) synchronous glacial activity during the Last Glacial Maximum (LGM) and Termination I (Schaefer *et. al* 2006; Denton *et al.* 1999a, Sugden *et al*., 2005; Clapperton, 2000). For instance, despite the decreasing local insolation intensity, southern hemisphere glaciers apparently retreated in near lock-step with northern glaciers during the termination (i.e., Mercer, 1984; Schaefer *et al.,* 2006). Furthermore, recent records have shown that glaciers in the southern hemisphere already were at their maximum positions before the global LGM (Mix *et al.* 2001; Clark *et al*., 2009) and that the ice maintained this position for more than one precession cycle (Sagredo *et al.,* 2011; Doughty, 2008; Kelley, 2009; Denton *et al*., 1999b, Barrows *et al*., 2001, 2002), implying that factors other than local insolation intensity must play an important role in the wax and wane of southern glaciers.

The Milankovitch model for ice ages focuses primarily on the extensive northern hemisphere ice sheets (Milankovitch, 1941). In this scenario, the northern ice sheets translate the orbital radiative forcing into a climate signal and prompt feedbacks that expand the ice-age realm globally (Clark *et al*., 2009; Imbrie *et al.*, 1992, 1993). Nevertheless, models (e.g, Manabe and Broccoli, 1987) have not reproduced any widespread effect in the southern hemisphere from growth of northern hemisphere ice sheets, and the origin of the southern glacial events remains elusive, despite its essential implication for understanding climate change.

Resolving the cause of ice ages requires well-dated paleoclimate records from the southern hemisphere. Yet, such records are sparse. To address this problem, we present a well-dated record of moraines in the Torres del Paine region (Southern Patagonia,

50°45’-51°35’ S and 73°30”-71°50’ W, Fig. 3.1; Plate 1, pocket) that were deposited during the last glaciation. This work aims to answer the following questions: What was the timing, structure and duration of the local LGM in the Torres del Paine region? Is the glacier record identical in the three glacial catchments studied? How does the timing of glaciation in the Torres del Paine region compare to other sites in Patagonia and in the southern and northern mid-latitudes? What can this tell us about the drivers of ice-age climate in the southern hemisphere?

3.3 Setting

Torres del Paine is situated ideally for gaining a better understanding of the mechanisms driving ice ages. The region is located in the only mid-latitude continental landmass south of 43ºS and is distant from the North Atlantic Ocean and the northern latitudes that are believed to play an active role in ice-age inception and termination (e.g., Alley *et al*., 2002; Broecker and Denton, 1989; Milankovitch, 1941). Moreover, the insolation signal is opposite that of the northern mid-latitudes. The Torres del Paine region is under the influence of the Sub-Antarctic climatic zone (Belkin and Gordon, 1996) and is affected strongly by seasonal latitudinal fluctuations of the westerly wind belt that transports low-pressure systems and associated precipitation into the region (Garreaud, 2007). Torres del Paine is located in the lee of the Andes, where an effective rain shadow produces an abrupt transition from cold rain forest to semiarid steppe (Luebert and Pliscoff, 2006). The mean annual precipitation is 700 mm within the boundaries of Torres del Paine National Park (Carrasco *et al*., 2002). Precipitation

decreases rapidly to the east. For instance, in Cerro Castillo (125 m a.s.l.), about 45 km to the southeast and distant from the mountains, precipitation is only about 350 mm. Mean annual temperature in the park is about 7ºC, with a winter mean minimum of 1ºC and summer mean maximum of 13ºC (Carrasco *et al*., 2002).

During the LGM, the Patagonian ice sheet was continuous from 38ºS to 56ºS in western South America (Glasser *et al.,* 2008). The Patagonian ice sheet produced outlet glaciers that flowed both east and west of the divide. In the Quaternary, eastward-flowing glaciers excavated deep, elongated lake basins; those flowing westward scoured the Chilean fjord landscape and terminated offshore. Today, there are three discrete remnant ice fields in the southern Andes: Campo de Hielo Sur (Southern Patagonian Ice Field), Campo de Hielo Norte (Northern Patagonian Ice Field) and the Cordillera Darwin ice cap.

The preservation of glacial landforms in Patagonia is excellent, particularly in semi-arid areas east of the southern Andes. Suites of moraines dating to the last glaciation and previous Quaternary glacial events occur adjacent to the large lakes that punctuate the eastern Andes (e.g., Lago General Carrera/Buenos Aires, Lago Cochrane/Pueyrredón, Lago Argentino) (e.g., Hein *et al*., 2010; Kaplan *et al*., 2008; Douglass *et al*., 2006; Sugden *et al*., 2005; McCulloch *et al*., 2005; Singer *et al*., 2004; Caldenius, 1932). Data from scattered studies suggest that Patagonian glaciers may have been at or near their outermost positions of the last glaciation during the local LGM between about 28.0-17.5 ka (Hein *et al*., 2010, 2009; Kaplan *et al*., 2004, 2008; Douglass *et al.,* 2006; Sugden *et al.,* 2005; McCulloch *et al.,* 2005). Denton *et al.* (1999b), based on stratigraphic records, dated the local LGM farther north in the Chilean Lake District to about 35-17.5 ka, which

is a longer glacial maximum than suggested by data in Patagonia. However, well-dated glacial records are sparse in Patagonia. In addition, in some cases, the available chronologic data predate recent technological progress in exposure-age dating (Nishiizumi *et al.*, 2007) and are not sufficiently precise for stratigraphic comparisons of glacial events.

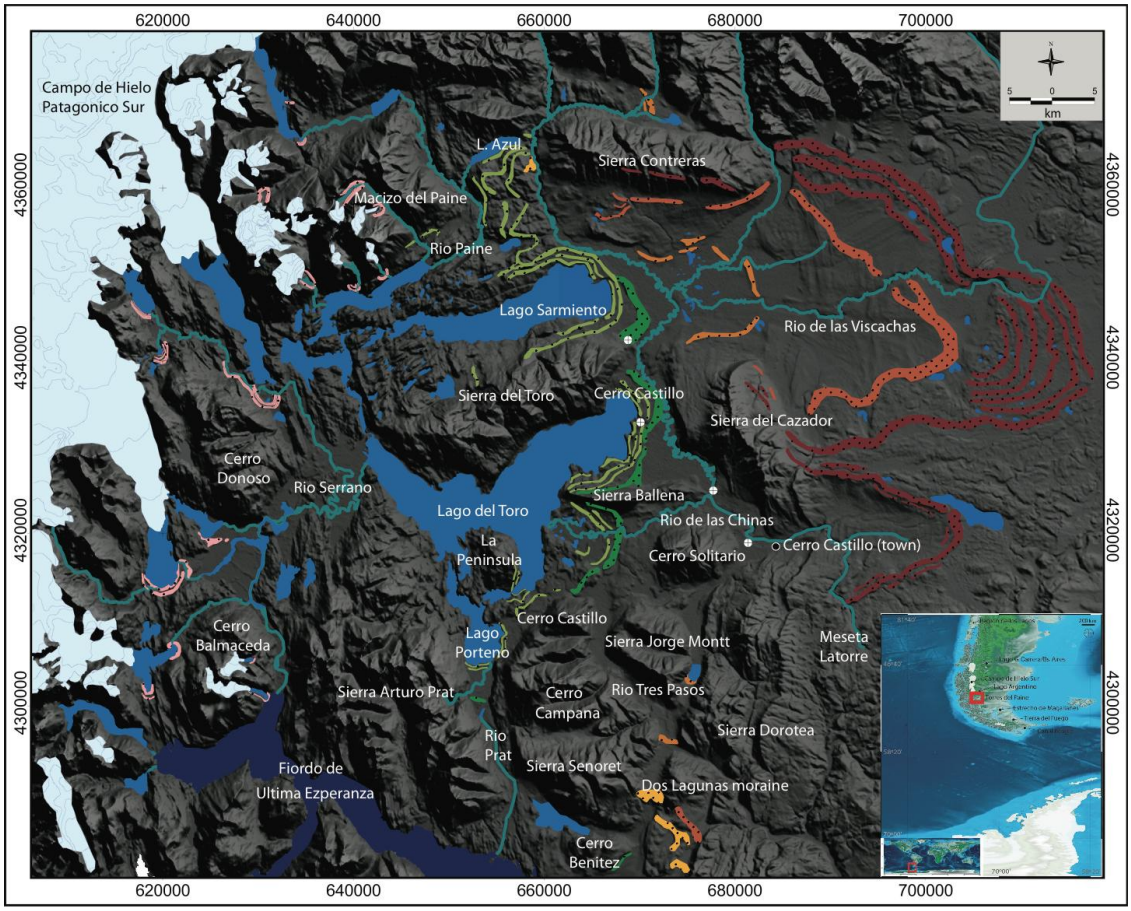

Figure 3.1. Physiographic attributes of the Torres del Paine Region. Inset shows a map of southern South America, including the location of the Torres del Paine region (red box). The map depicts each of the moraine belts deposited during the last glaciation in the region.

3.3.1 Torres del Paine moraines

Similar to previous workers in the Torres del Paine region (e.g., Marden and Clapperton, 1995; Marden, 1993), we distinguished moraine belts based on position, morphology, and number and geographic pattern of ridges. We identified at least seven prominent moraine belts deposited during the last glacial period and transition to the Holocene (Fig. 3.1; Plate 1, pocket). These moraines occur within 50 km of each other and are named from outer to inner: Río de las Viscachas (RV) I, II, and III, and TDP I, II, III, and IV (Chapter 2; TDP I-IV = A-D of Marden, 1993; Marden and Clapperton, 1995) (Fig. 3.1; Plate 1, pocket). Previous work dated the TDP II, III (e.g. Chapter 4) and IV (Chapter 4; Moreno *et al*., 2009; Fogwill and Kubik, 2005) moraines to the late-glacial period. Because our interest for this study was primarily the local LGM, we focused on the extent and age of moraines distal to the late-glacial landforms, such as the TDP I deposits. Although they lacked chronologic data, Marden and Clapperton (1995) suggested that the TDP I landforms (which they called the 'A' moraines) dated to Marine Isotope Stage (MIS) 4. We also included preliminary data for the RV I moraine system, which allowed us to bracket the early part of the last glaciation in the Torres del Paine region.

TDP I terminal moraines (Plates 2-4, pocket) extend along the eastern shores of the three main east-west-trending lakes in Torres del Paine National Park: Lago del Toro (25 m a.s.l.), Lago Sarmiento (75 m a.s.l.) and Laguna Azul (220 m a.s.l.). It is not always possible to trace TDP I lateral moraines in these three lake basins.

In Laguna Azul basin, the TDP I moraines are discontinuous and separated by bedrock relief reaching ~500 m a.s.l. The moraines occur as a hilly topography, with both large and small ridges present. Whereas large moraines (e.g., hundreds meters wide and tens meters high) appear as wide and shallow landforms deposited in open areas to the west of Río de las Chinas, small moraines (e.g., few meters high) occur across narrow basins used during later glacial advances as meltwater conduits (Plate 2, pocket).

The TDP I landform at Lago Sarmiento is preserved only as one prominent, wide (e.g., 300 m), flattish ridge, which represents an ice-contact moraine delta that still preserves glaciofluvial morphology (Chapter 2). The ice-contact slope, with as much as 40 m of relief, has been reworked and steepened by post-depositional glaciofluvial erosion. Well-preserved meltwater channels that head at the TDP II deposits occur alongside the TDP I moraine.

The TDP I moraine at the eastern margin of Lago del Toro is a prominent composite feature, which includes from three to five ridges (e.g., Marden, 1993; Chapter 2). This wide, arcuate moraine belt can be traced for several kilometers along the eastern and southern ends of the lake. As at Lago Sarmiento, this composite moraine features a steep ice-contact slope of about 40 m of relief that was reworked by post-depositional glaciofluvial erosion.

Caldenius (1932) mapped the outer RV I moraines (Plate 5, pocket) and suggested that they, along with the RV II and III landforms, belong to a glacial period he named the *Gotiglacial*. RV I consists of a composite terminal moraine complex, made up of at least 20 distinct, wide (e.g., hundreds meters), concentric ridges that reach a maximum

elevation of ~300 m a.s.l at their easternmost point. This moraine belt is located between Sierra Contreras and Sierra del Cazador (Fig. 3.1; Plate 1, pocket), about 85-100 kilometers from the present ice margin. Lateral moraines commonly are well developed on the slopes of these mountains. Overall, the RV I moraine relief is low (e.g., ≤15 m) and distinctly less sharp than that of the TDP I moraines at Lagos Sarmiento and del Toro.

A flat, open terrain, punctuated by moraine belts (RV II and III), separates the TDP I landforms at Lago Sarmiento from the RV I ridges. Whereas the RV II moraine belt occurs only few kilometers inboard from the RV I landforms, the RV III moraines are located halfway between the RV II and TDP I deposits at Lago Sarmiento. Both RV II and RV III moraine belts are prominent composite features. At their easternmost points, these moraines occur at 290 and 115 m a.s.l., respectively.

3.4 Methods

We constructed a geomorphologic map from stereoscopic analysis of aerial photographs (Vuelo Geotec SAF 1998, 1:70.000) that included most of the study area. Our preliminary mapping was checked and corrected in the field during four campaigns between 2007 and 2010. We focused on the description of ice-marginal features built during the last glacial cycle (e.g. moraine ridges, glaciofluvial and glaciolacustrine complexes) and analyzed, wherever possible, stratigraphic sections to complement our geomorphological approach. We concentrated on delineating former positions of the

Patagonian ice sheet from moraine belts occurring in the Torres del Paine region. This map (Chapter 2) served as a foundation for our ^{10}Be chronology (Plates 2, 3, 5, pocket).

We collected samples from 14 quartz-rich boulders (mostly granite, greywacke and dacite) for ^{10}Be cosmogenic exposure-age dating, using a hammer and chisel. Our sampling protocol included the selection of boulders with well-preserved surfaces (e.g., no or only slight signs of weathering or erosion) that were embedded on stable moraine crests (Figs. 3.2). In the field, we determined sample boulder height, length, width, geometric and topographic shielding, latitude and longitude and elevation above sea level (Appendix B). We made notes and observations regarding the local setting, such as moraine position and continuity, meltwater drainage routes, and relationships with other samples. Samples in the Lago del Toro basin were obtained from the TDP I terminal moraines, which consist of three ridges. We collected samples from each ridge. At Laguna Azul, boulders came from both well-formed moraine crests and low-relief landforms. RV I samples were from the outer ridges (Fig. 3.2).

Sample preparation and beryllium extraction were carried out in laboratories of the Earth Sciences Department and Climate Change Institute at the University of Maine (UMAINE), and in the Geochemistry Cosmogenic Nuclide Laboratory at Lamont-Doherty Earth Observatory (LDEO). We followed laboratory protocols of the Cosmogenic Isotope Laboratory at the University of Washington (http://depts.washington.edu/cosmolab/chem.html) and an updated version of Licciardi (2000). Details on the ^{10}Be chemistry are in Appendix A.

For calculating ages, we used the ^{10}Be production rate (PR) based on New Zealand's Macaulay site (43ºS; Putnam *et al*., 2010), which recently has been replicated in the Lago Argentino area, less than 100 km from Torres del Paine (50ºS; Kaplan *et al*., accepted pending revision). To allow comparisons both among Patagonian sites and with other southern hemisphere studies, all ^{10}Be ages included here from prior work have been recalculated using the New Zealand PR (Putnam *et al*., 2010) and the time-dependent scaling model of Lal/Stone (Stone, 2000). In our discussion, we use calculated ages with no correction for erosion.We identified outliers using Grubbs test (1969) and the two-sigma rule. We applied recent technological advances, including very low background ^{9}Be carrier and the application of high-energy currents during AMS ^{9}Be/^{10}Be measurements, which often allowed us to obtain mean uncertainties of ~3%. Calculation of ages and associated assumptions are described in detail in Schaefer *et al*. (2009, supplementary note) and Appendix A.

In addition to sampling for cosmogenic isotopes, we collected sediments from mires between the TDP I and II moraines using a modified Livingston piston corer in order to obtain minimum ages for glacier retreat. Here, we report results from one of these cores in Vega Chulengo. We used CALIB 6.0.1 and the IntCal09 dataset (Reimer *et al*., 2009) for calibrating radiocarbon ages. All radiocarbon ages are presented in calendar years with 1σ error.

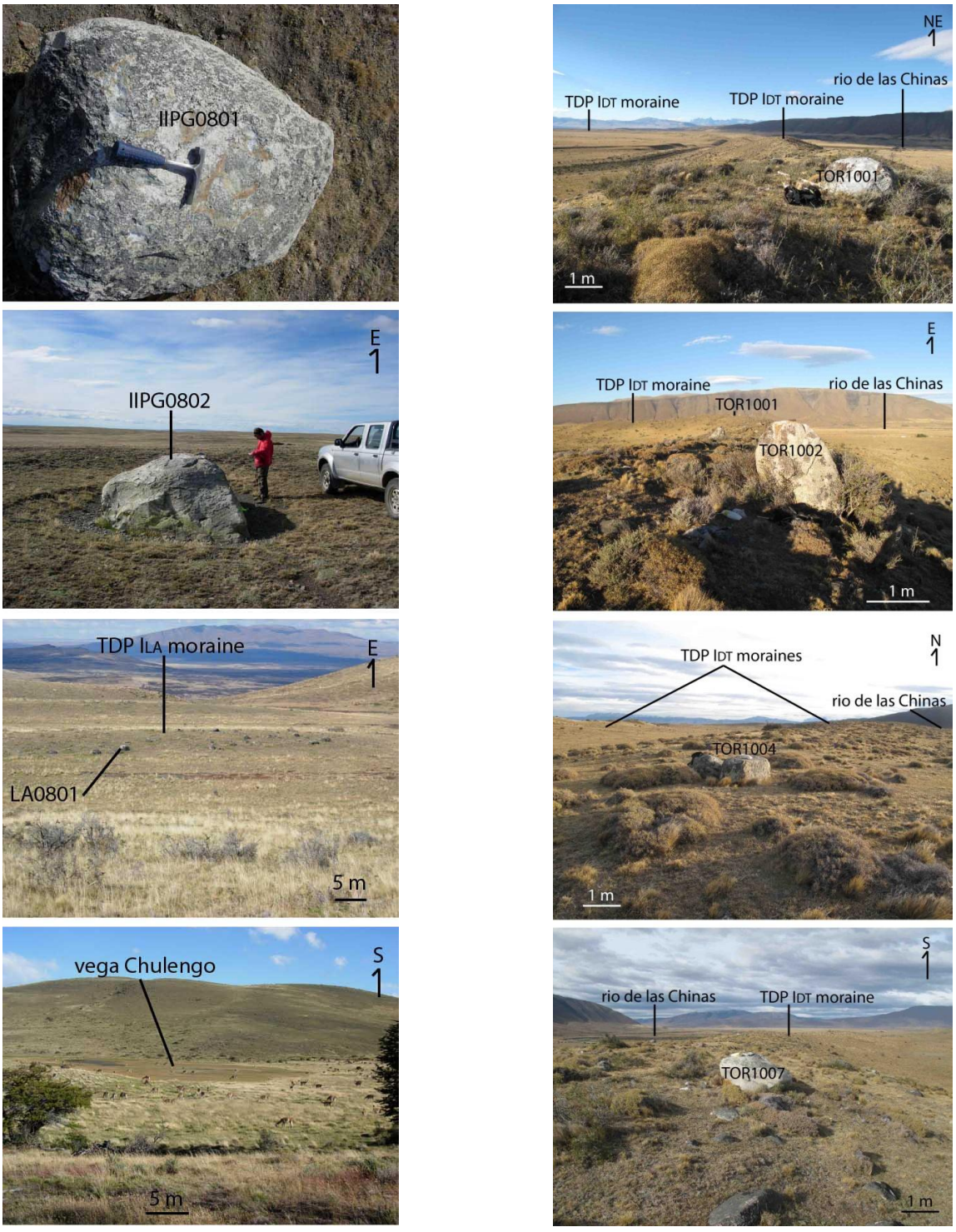

Figure 3.2. Boulders, moraines and ^{14}C site geographical context. This page: Left panel: RV moraines and boulders; TDP I_{LA} moraine (sample LA0801) and Vega Chulengo (17.4 ± 0.2 kcal yr B.P.) in the Laguna Azul area; Right panel: TDP I_{DT} moraines and boulders in Lago del Toro basin. Next page: TDP I_{LA} moraines and boulders in the Laguna Azul area.

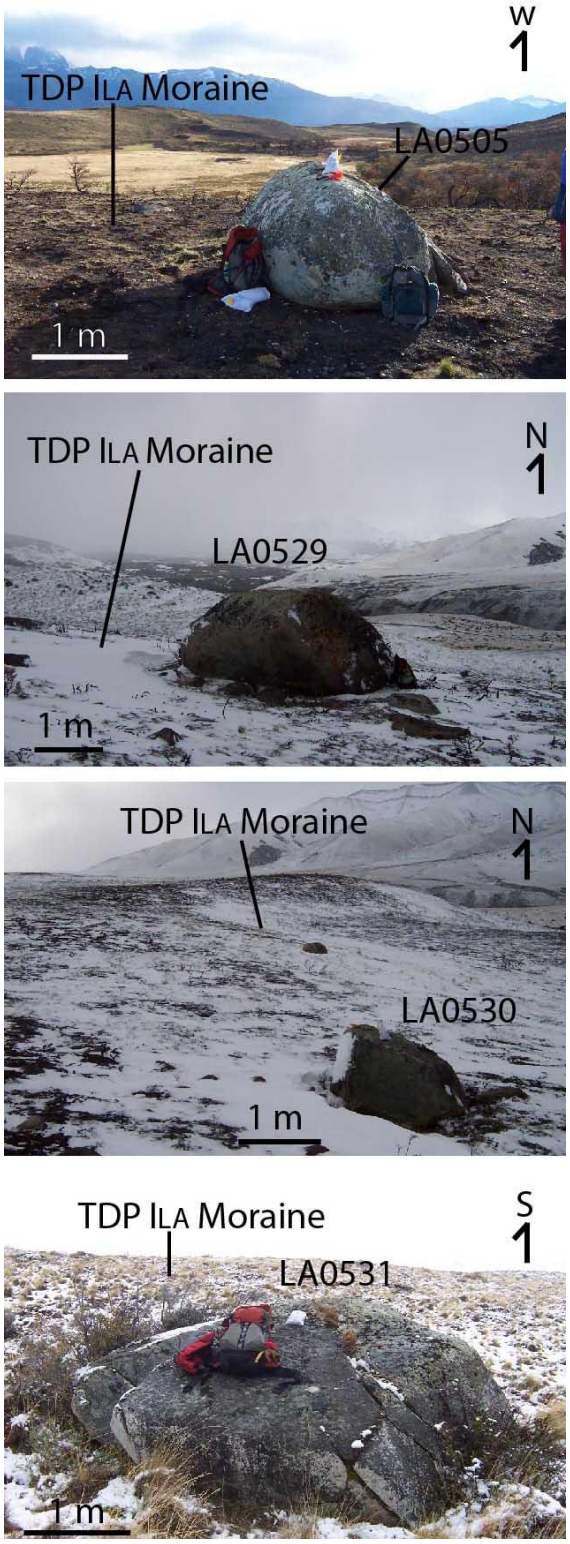

Figure 3.2. Continued.

3.5 Results

Table 3.1 includes geographic and ^{10}Be analytic data for TDP I and RV I cosmogenic samples. Table 3.2 presents all ^{10}Be ages obtained in this study as calculated with the different scaling schemes (Balco *et al.*, 2008). Six samples come from the TDP I moraine at Lago del Toro (Plate 3, pocket), six from the moraines at Laguna Azul (Plate 2, pocket) and two from the outermost RV I moraine (Plate 5, pocket) (Fig. 3.2). We detected two outliers in the data set, one from the Laguna Azul moraines (LA0702) and one from the moraines at Lago del Toro (TOR1008).

The resulting ages of the TDP I moraines at Laguna Azul range from 40.6 to 42.7 ka and yield a mean age of 41.3 ± 1.3 ka (n=5, Fig. 3.3a). In contrast, the ages from the TDP I moraines at Lago del Toro fall between 16.0 ka and 17.1 ka and yield a mean age of 16.5 ± 0.6 ka (n=5, Fig. 3.3b). The two dates from the RV I moraines (48.3 and 49.5 ka) produce a mean age of 49.0 ± 1.5 ka (Fig. 3.3c) (Plates 2-3, 5, pocket).

We obtained a sediment core from Vega Chulengo (50º54’32’’S; 72º43’53’’W, 370 m a.s.l.; Fig.3.2; Plate 2, pocket), located in the Laguna Azul basin, between the TDP II and TDP I moraines. The base of the sediment sequence in core from Vega Chulengo is organic-poor, sandy silt. Plant remains from the lowermost centimeters of this unit yielded an age of 17.4 ± 0.2 (1σ) kcal yr B.P. (OS-74486, radiocarbon age 14,350 ± 70, Fig. 3.4). The basal unit grades upward to laminated inorganic clay and then gravel. The sediment again becomes finer upwards, with a transition to organic-poor silt sediment that, in turn, grades to the present organic-rich, fibrous peat.

Figure 3.3. Relative probability plots and statistics for each moraine (TDP I_{LA}, TDP I_{DT}, RV I). Relative probability plots of ^{10}Be exposure-age distribution for each moraine. Probability plots without outliers are presented for each moraine belt. The thin curves represent individual sample ages ± 1σ. The thick curve is the normalized probability distribution of the moraine age population. Central vertical lines in plots denote the arithmetic mean ±1σ (yellow rectangle), 2σ (red vertical line) and 3σ (green vertical line). Values used in the text are arithmetic means and associated uncertainties obtained after rejecting outliers. Uncertainties used (bolded values) include propagation of the analytical and production-rate errors. We used a 2.4% uncertainty from the ^{10}Be production rate as defined in Putnam *et al*. (2010). **a** – TDP I_{LA} moraines; **b** – TDP I_{DT} moraines; **c** – RV I moraines.

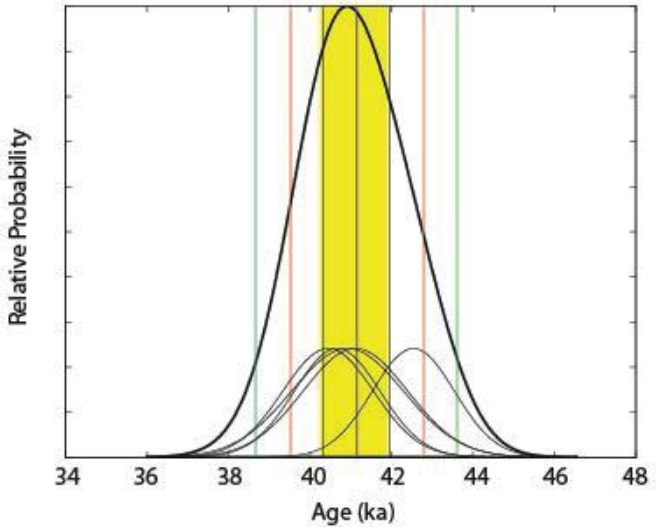

a) TDP I_{LA} moraines. Samples (n=5): LA0505, LA0529, LA0530, LA0531, LA0801

Statistics
Arithmetic mean/1 sigma uncertainty: 41,100±820 yrs
Including production rate uncertainty: **41,100±1280 yrs**
Weighted mean/weighted uncertainty: 41,200±510 yrs
Peak age: 40,900 yrs
Median/Interquartile Range: 40900±860 yrs
Reduced χ^2: 0.6

Figure 3.3. Continued

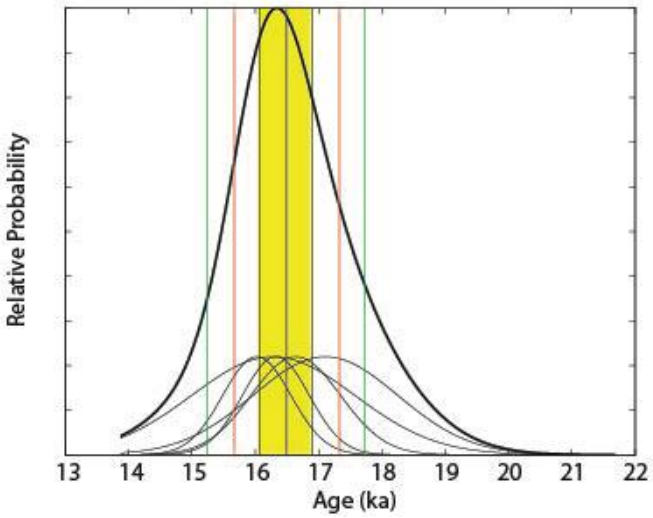

b) TDP I_{DT} moraines. Samples (n=5): TOR1001, TOR1002, TOR1004, TOR1005, TOR1007.

Statistics
Arithmetic mean/1 sigma uncertainty: 16,500±410 yrs
Including production rate uncertainty: **16,500±570 yrs**
Weighted mean/weighted uncertainty: 16,300±310 yrs
Peak age: 16,300 yrs
Median/Interquartile Range: 16,300±540 yrs
Reduced χ^2: 0.3

Figure 3.3. Continued

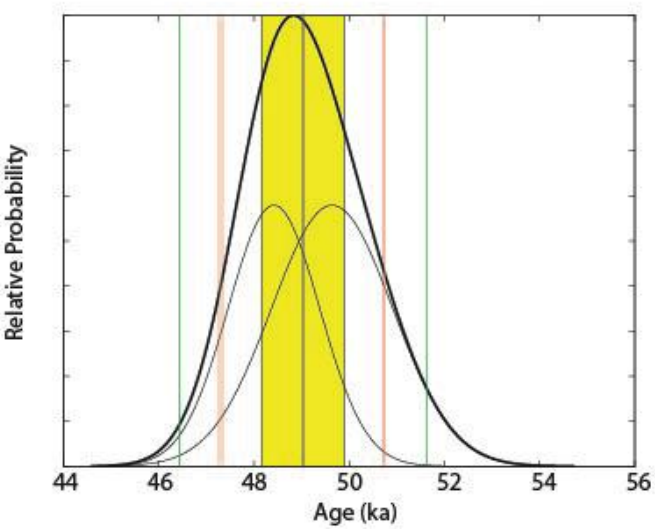

c) RV I moraine. Samples (n=2): IIPG0801, IIPG0802

Statistics
Arithmetic mean/1 sigma uncertainty: 49,000±870 yrs
Including production rate uncertainty: **49,000±1460 yrs**
Weighted mean/weighted uncertainty: 48,900±770 yrs
Peak age: 48,700 yrs
Median/Interquartile Range: 49,000±1220 yrs
Reduced χ^2: 0.6

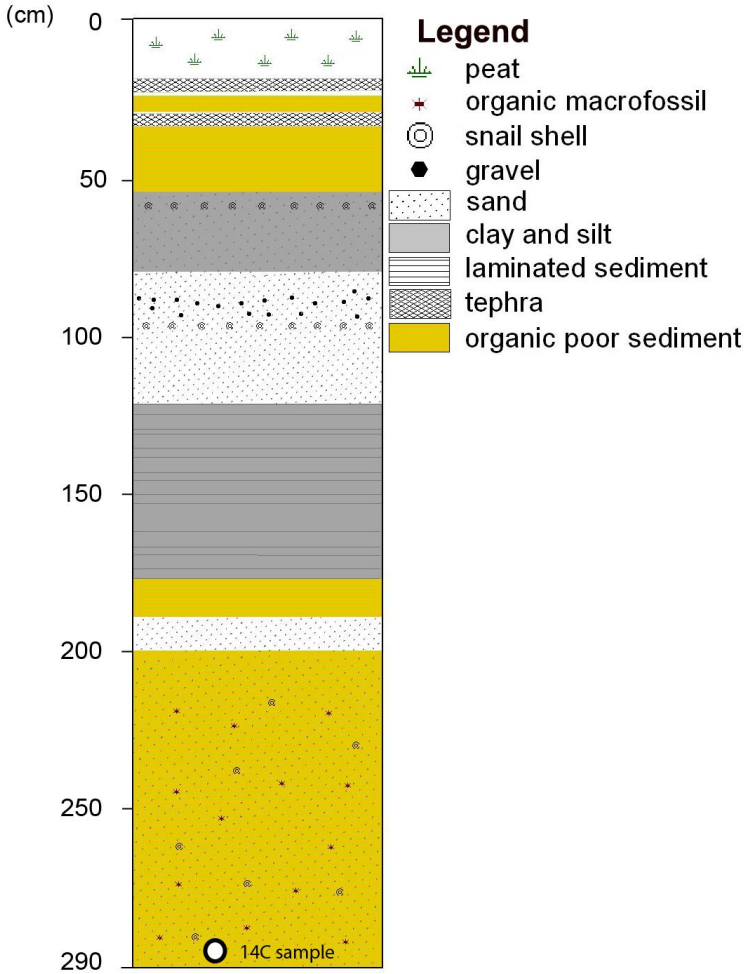

Figure. 3.4. Stratigraphic column from a core obtained from Vega Chulengo (50º54'32''S; 72º43'53''W). A ^{14}C wood piece sample was obtained from close to the base (cm 289) of this section and yielded a calibrated age of 17.4 ± 0.2 (1σ) kcal yr B.P. (OS-74486, radiocarbon age 14,350 ± 70 years B.P.).

Table 3.1 Geographical and 10Be analytical data for TDP I and RV moraines cosmogenic samples*.

SAMPLE ID	Lat ºS	Long ºW	Elevation (m a.s.l.)	Sample thickness (cm)	Boulder height (cm)	Shielding correction	^{10}Be ±1σ (10^4 atoms g^{-1})	^{10}Be/^{9}Be ratio ± error
TDP I_{LA} moraine								
LA0505	-50.8946	-72.7432	466	1.5	101	0.999	27.38 ± 0.64	2.12E-13 ± 4.98E-15
LA0529	-50.8995	-72.7316	455	1.2	166	1.000	26.01 ± 0.67	8.75E-14 ± 2.13E-15
LA0530	-50.8991	-72.8980	409	1.0	88	0.990	24.9 ± 0.83	6.28E-14 ± 2.09E-15
LA0531	-50.9004	-72.7235	366	2.5	129	1.000	23.99 ± 0.74	9.88E-14 ± 2.98E-15
LA0702	-50.8936	-72.7331	417	1.0	223	0.990	29.88 ± 0.65	1.53E-13 ± 3.28E-15
LA0801	-50.8991	-72.7380	434	1.1	78	0.990	25.16 ± 0.69	8.04E-14 ± 2.16E-15
TDP I_{DT} moraine								
TOR1001	-51.1484	-72.5267	102	1.1	105	1.000	7.7 ± 0.33	4.26E-14 ± 1.80E-15
TOR1002	-51.1495	-72.5323	91	1.2	175	1.000	7.83 ± 0.52	2.18E-14 ± 1.45E-15
TOR1004	-51.1332	-72.5159	73	1.6	67	1.000	7.29 ± 0.57	1.26E-14 ± 9.94E-16
TOR1005	-51.1322	-72.5150	78	1.6	112	1.000	7.35 ± 0.24	5.04E-14 ± 1.62E-15
TOR1007	-51.1242	-72.5113	103	1.1	98	1.000	7.42 ± 0.25	6.32E-14 ± 2.11E-15
TOR1008	-51.1336	-72.5194	97	2.1	66	1.000	5.16 ± 0.31	3.21E-14 ± 1.90E-15
Río de las Viscachas moraine								
IIPG0801	-51.1057	-71.8733	330	0.7		1.000	28.49 ± 0.72	1.85E-13 ± 4.68E-15
IIPG0802	-51.0993	-71.8686	312	0.9	122	1.000	27.29 ± 0.54	1.88E-13 ± 3.69E-15

*All samples measured at CAMS using the 2.85^{-12} = 07KNSTD3110 standard for normalization (Nishiizumi, 2007).

Table 3.2 ^{10}Be ages for TDP I_{LA}, TDP I_{DT} and Río de las Viscachas moraines.

SAMPLE ID	Du	int	ext	Li	int	ext	De	int	ext	Lm	int	ext	(1)	Lm	int	ext	(2)
TDP I_{LA} moraine ridges																	
LA0505	43600	±	1040 1400	42300	±	1010 1340	43200	±	1030 1380	42500	±	1010 1370		44700	±	1120 1520	
LA0529	41700	±	1080 1400	40400	±	1050 1350	41300	±	1070 1390	40700	±	1060 1380		42700	±	1160 1520	
LA0530	41900	±	1410 1670	40700	±	1370 1610	41500	±	1400 1660	40900	±	1380 1640		42900	±	1520 1810	
LA0531	42100	±	1320 1600	40900	±	1280 1540	41700	±	1310 1590	41100	±	1290 1570		43100	±	1420 1730	
LA0702	50000	±	1110 1540	48500	±	1070 1480	49500	±	1100 1530	48800	±	1080 1510		51800	±	1220 1710	
LA0801	41400	±	1140 1450	40200	±	1110 1400	41100	±	1130 1440	40400	±	1120 1420		42400	±	1230 1570	
TDP I_{DT} moraine ridges																	
TOR1001	17000	±	720 810	16700	±	710 790	16800	±	710 800	16600	±	710 790		17000	±	730 820	
TOR1002	17500	±	1170 1230	17100	±	1150 1200	17200	±	1150 1210	17100	±	1140 1200		17400	±	1190 1250	
TOR1004	16600	±	1310 1360	16300	±	1290 1330	16400	±	1300 1340	16300	±	1290 1330		16600	±	1340 1390	
TOR1005	16700	±	540 650	16400	±	530 630	16400	±	530 640	16300	±	530 630		16600	±	550 660	
TOR1007	16400	±	550 650	16100	±	540 640	16200	±	540 640	16000	±	540 640		16300	±	560 660	
TOR1008	11500	±	690 730	11400	±	680 720	11400	±	680 720	11300	±	670 710		11400	±	690 730	
Río de las Viscachas I moraine ridges																	
IIPG0801	50800	±	1300 1700	49300	±	1260 1630	50300	±	1290 1680	49600	±	1270 1670		52700	±	1430 1880	
IIPG0802	49500	±	980 1450	48000	±	950 1390	49000	±	970 1440	48400	±	960 1430		51300	±	1080 1610	

(1): no erosion (2): 1.4 mm*10^-3 yr erosion

Note: ^{10}Be ages in years calculated with four different scaling protocols (Balco *et al*., 2008). 'Lm' is the time dependent version of Stone/Lal scaling scheme (Stone, 2000). 'Du' is calculated using the scaling scheme of Dunai (2001), 'Li' the scaling based on Pigati and Lifton (2004) and Lifton et al. (2008), and the 'De' scaling scheme presented in Desilets and Zedra (2003). All ages were calculated using a ^{10}Be production rate measured at New Zealand's Macaulay Site (Putnam et al., 2010). We use the Lm scaling scheme in our result discussion (Stone, 2000). Density of rock used for calculating ^{10}Be ages is 2.65 g cm^{-3}. Age uncertainties include internal (int) analytical error only and external error (ext), which includes systematic uncertainties (Balco *et al*., 2008) associated with scaling to the latitude and altitude of Torres del Paine region.

3.6 Discussion

Our surface exposure ages form discrete clusters, which are internally consistent (e.g., with only limited outliers) for each of the dated moraines. The ^{10}Be ages making up each of these respective clusters overlap within 1 sigma. Although the two ages from the outer RV I moraine are statistically identical, the mean age of 49.0 ka for this landform should be taken as preliminary until more data replicate this value. These data, along with the mapping, afford evidence for several glacial fluctuations, starting at least as early as 49.0 ka and 41.3 ka and continuing to the termination at 16.5 ka.

3.6.1 TDP I moraines

The TDP I moraines at Laguna Azul and Lago del Toro differ in age, despite their similar position just outside TDP II landforms (14.2 ka, Chapter 4) in their respective basins. Therefore, in order to avoid confusion in this paper, we rename these landforms accordingly: TDP I at Laguna Azul: TDP I_{LA}; TDP I at Lago del Toro: TDP I_{DT}; TDP I at Lago Sarmiento: TDP I_{SA}.

One hypothesis is that the moraines in all three basins are indeed the same age, but that the boulders at Laguna Azul contain significant prior exposure to cosmic radiation, and therefore their dates appear older than the true age of the landform. We do not prefer this alternative. First, all the samples from Laguna Azul, except for one outlier, are consistent and overlap within one sigma, which suggests that they represent the landform age. In contrast, ages from boulders with previous exposure tend to show

significant scatter (e.g., Kelly *et al.*, 2008) as each boulder embraces an individual unique history. In addition, temperate glaciers, such as the Patagonian ice sheet, generally produce significant erosion on boulders transported subglacially. Although it is difficult to be sure that all our boulders were transported at the glacier sole, the difference in lithological types among samples suggests that they may have been eroded and transported subglacially rather than on the surface from an avalanche point source. In addition, the boulders from Laguna Azul include distinct facteted geometries, some of which with distinct bullet shapes (Fig. 3.2). Moreover, ^{10}Be dates obtained from the TDP II, III, and IV moraines (Chapter 4) indicate that boulders with obvious prior exposure from these deposits were limited to <10% of the cases.

A second alternative is that the Laguna Azul ages are correct, and it is the boulders from the TDP I_{DT} moraines that are flawed. This could occur if the TDP I_{DT} boulders have been eroding at high rates and therefore represent only minimum ages. However, in order to produce ages close to 41.0 ka from TDP I_{DT} samples, erosion rates would need to have been more than ten times higher than the maximum value estimated for the region (cf. Kaplan et al., 2004; Douglass, 2006), which is likely unrealistic. In addition, some boulders in Torres del Paine preserve abrasion marks (e.g., striations) and most of sampled rocks appear to exhibit their original surfaces, indicating low erosion rates.

A third option that may explain why the TDP I moraines do not yield the same age in both basins is that the boulders from TDP I_{DT} were exhumed, and therefore appear younger than the real age of the moraine. In this scenario, the boulders at TDP I_{DT} would have been deposited at the same time as those at Laguna Azul but only exposed to cosmic

radiation at 16.5 ka by exhumation. We do not prefer this option because of the high internal consistency of the age cluster for this moraine.

Thus, the bulk of evidence suggests that the TDP I_{LA} and TDP I_{DT} mean ages, as calculated, are accurate. As mentioned above, we, as have others before us (e.g., Marden and Clapperton, 1995), mapped these two moraines as part of the same TDP I moraine belt, mainly because of their position and morphology with respect to the younger TDP II deposits. Nevertheless, the TDP I moraines are morphologically distinct from each other. For instance, Laguna Azul landforms mostly lack distinct moraine morphology and cannot be traced from basin to basin, as opposed to those at Lago del Toro, which are prominent, well-defined ridges that can be traced for several kilometers. At Laguna Azul, the moraines are wider and more subtle than the sharp TDP I moraines at Lagos Sarmiento and del Toro, suggesting that the former may be older, an aspect confirmed by our ^{10}Be data. We therefore conclude that the original correlation of the TDP I moraines at Laguna Azul and Lago del Toro is not accurate and that both moraines were deposited at different times during the last glaciation. At Lagos del Toro and Sarmiento, the moraine systems are comparable in terms of number and size of moraines ridges, geomorphology and position. The pattern of ridges in both basins suggests that each of the glacial lobes produced about the same moraine clusters. These observations suggest that TDP I_{DT} and TDP I_{SA} moraines likely were deposited during the same glacial event.

3.6.2 RV moraines

Our mapping and chronology suggest that ice from Laguna Azul, Lago Sarmiento and Lago del Toro basins may have expanded to the RV I outer moraine early during the last glaciation. Given only two ages, our conclusions are tentative. However, by ~49.0 ka, the Patagonian ice-sheet margin in the Torres del Paine region may have been about 100 kilometers east of the present-day Southern Patagonian Ice Field, much farther east than generally thought (e.g., Marden, 1993; Marden and Clapperton, 1995; Glasser *et al.*, 2008). The well-organized suite of inboard, smaller and concentric moraine ridges that make up the inner part of the RV I belt likely represent fluctuations close to the maximum position. As inferred from the location and elevation of lateral moraines, re-advances subsequent to deposition of the RV I landforms (e.g., RV II-III moraines) occurred when ice was less extensive and thinner. By the time of TDP I deposition, the ice sheet already had begun to split into individual lobes in the Lago del Toro and Lago Sarmiento-Laguna Azul basins.

3.6.3 The local glacial maximum

Our cosmogenic-exposure data afford evidence for glaciation in Torres del Paine during Marine Isotope Stage 3 (MIS 3; about 60-25 ka) at 41 ka and ~49 ka. This is some of the first evidence for glacial expansion at this time in southern South America. Although the Patagonian ice sheet in Torres del Paine reached its maximum extent during MIS 3, most other glacial records in southern South America show maximum ice extent at ~26-28 ka, when calculated with the New Zealand production rate (Putnam *et al.*,

2010). This latter age is slightly earlier than the global LGM at 19-23 ka (Mix et al., 2001; Hein *et al*., 2010, 2009; Kaplan *et al*., 2004, 2008; Douglass *et al.*, 2006; Sugden *et al.*, 2005). The only other location showing extensive MIS 3 ice in Patagonia is at Última Esperanza (52ºS), where dated moraines record maximum ice expansion at 38.0 ka (Sagredo *et al.*, 2011).

Why have only scattered sites in Patagonia revealed glacial expansion during MIS 3? Most available studies have dated the LGM moraine sequence, as well as moraines immediately distal to the LGM landforms, without finding evidence of MIS 3 advances. One exception is the Chilean Lake District, where a glacial event was dated at ~35 ka (Denton *et al.*, 1999b); However, evidence for this MIS 3 glacial advance comes only from stratigraphic sections (Denton *et al*., 1999b); the full extent of ice is not known, but may have been relatively close to the outermost terminal limit. In contrast, at Última Esperanza MIS 3 moraines are dated directly with ^{10}Be and occur ~seven kilometers distal to the moraines thought to date to the LGM. If glacial fluctuations occurred in both the Lake District and the Torres del Paine/Última Esperanza areas, which are separated by ~10 degrees of latitude, it seems reasonable to suggest that glaciation occurred throughout the region during MIS 3. One possibility is that LGM advances erased the morphological evidence for MIS 3 ice expansions in most locations.

Is this early glacial maximum at Torres del Paine related to greater temperature depression at 41 ka and perhaps at 49 ka than during the global LGM in southern Patagonia? Or can the pattern of moraines be explained by non-climatic factors? As a hypothesis, we suggest that the location of the southern westerly wind belt, which transports both cold temperatures and humid air masses into the mid-latitudes of the

southern hemisphere (Garreaud, 2007), may have affected the relative size of glaciations in the Torres del Paine region. From present-day records, we know that the core of the westerly wind belt is located at about 50ºS and that precipitation rates decrease from this point south and north (Miller, 1976). In general, the westerly wind belt shifted north during the LGM (e.g., Heusser, 1989), but it also may have moved rapidly between low and high latitudes several times during the last glaciation and deglaciation in connection with stadials and interstadials in both polar hemispheres (Anderson *et al.,* 2009; Denton *et al*., 2010; Hall *et al*., 2010). Figure 3.5 shows that glacial advances recorded in the Torres del Paine region (Fig. 3.5b) occurred during stadial periods in Antarctica (Fig. 3.5f), which in turn were associated with cooler sea-surface temperatures (SST; Fig. 3.5d) and lower rates of opal-derived, wind-driven upwelling in the Southern Ocean (Anderson *et al*., 2009; Fig.c). These conditions imply a northern shift of the westerly winds and expansion of cold conditions into the southern mid-latitudes (e.g., Kaiser *et al*., 2005, Fig. 3.5d). Therefore, ice extent in Torres del Paine would have been affected not only by temperature depression, but also by the position of the westerly belt, which would have controlled precipitation amounts. Existing data and models suggest drier conditions in the Torres del Paine region during the global LGM (cf. Hulton *et al.,* 2002; Rojas *et al*., 2009), consistent with the idea that the westerly wind belt shifted north into the Chilean Lake District (e.g., Heusser, 1989). The reduction in precipitation may have resulted in a smaller advance during the global LGM than at 41 ka and ~49 ka, when the westerly wind belt may not have been pushed so far north. Better-dated paleoclimate records in Patagonia would help test this hypothesis and contribute towards understanding MIS 3 advances in the local glacial history.

In addition to climate, the morphology of deep lake basins also may have affected glacial extent. For example, each glaciation may have excavated the lake basins and thus ice during the LGM, although possibly similar in volume to the early advances, occupied deeper basins and thus could not extend as far to the east. However, the formation of glacial lakes during retreat (e.g., interglacial periods) would have resulted in the deposition of thick glaciolacustrine sediments and thus it is not certain that the basins became progressively deeper over time.

3.6.4 The Global Last Glacial Maximum

Our ^{10}Be data lack evidence for moraines dating to the global LGM (24-19 ka BP, Mix *et al.*, 2001). Where was ice during this time in the Torres del Paine region?

3.6.4.1 Lagos del Toro and Sarmiento basins

With the data available, we cannot pinpoint the position of the Patagonian ice sheet in the Lago del Toro/Lago Sarmiento basins during the global LGM. One possibility is that the ice was at one of the prominent undated moraine belts to the east of these basins (e.g., RV II-III moraines), which likely date between ~49 ka (RV I moraine) and 16.5 ka (TDP I_{DT} deposits). An alternative is that after deposition of the RV I moraine at ~49 ka, ice retreated into the Torres del Paine National Park area and remained at or near the TDP I_{DT} position throughout the global LGM. This scenario implies that the TDP I_{DT} moraine is a composite landform produced during several

pulses. The mean age of 16.5 ka would represent only the last glacial incursion to this landform. This scenario would be consistent with the apparent moraine pattern at Laguna Azul, where most identified glacial advances reached a similar position (e.g., TDP I_{LA}-TDP IV)

3.6.4.2 Laguna Azul basin

Our moraine-based ^{10}Be chronologies, together with detailed mapping, show that ice at Laguna Azul advanced both at 41.3 ± 1.3 ka (TDP I_{LA} moraines) and at 14.2 ± 0.6 ka (TDP II-IV moraines, Chapter 4). No other moraines exist between the TDP II and TDP I_{LA} landforms, raising the question of where was the ice margin in this basin during the global LGM?

There are several possible hypotheses to explain the absence of moraines dating to the global LGM in the Laguna Azul basin. One alternative is that LGM ice overrode the TDP I_{LA} deposits, merged with ice from Lago Sarmiento and Lago del Toro, and extended to a position farther east, perhaps to the RV III moraines. However, because of the consistency of the TDP_{LA} exposure-age dates (41 ka), this scenario would imply that ice during the LGM was cold-based and neither eroded the TDP I_{LA} moraines nor deposited boulders on their surfaces of younger age. We find this scenario unlikely because of the temperate maritime regime that would have favored wet-based ice (cf. Evans, 2003). Moreover, we did not find other evidence of cold-based ice, such as thrust-block moraines or permafrost structures, and we are not aware of previous work reporting this type of glacial deposits at this latitude, except for Benn and Clapperton (2000) in the

Strait of Magellan (53ºS) >200 km south. Moreover, commonly boulders that have been covered by cold-based ice produce exposure age datasets with significant scatter (Kelley *et al*., 2008; Briner *et al*., 2005), unlike our Laguna Azul dataset (Fig. 3.3a).

A second, and preferred, line of thought is that LGM ice at Laguna Azul was of an extent similar to that during the late glacial period (i.e., TDP II). Circumstantial evidence supports this alternative. First, within the late-glacial ^{10}Be dataset for the TDP II, III, and IV moraines, there are outliers dating to the LGM chronozone (Chapter 4). These outliers may indicate that late glacial ice reworked LGM boulders, some of which were not eroded sufficiently to reset the ^{10}Be cosmogenic clock. Second, we obtained an age of 17.4 ± 0.2 ka (1σ) for the base of the Vega Chulengo core, located between the TDP I_{LA} and TDP II moraines in Laguna Azul basin (Fig. 2, pocket). The date, from gastropods within the lowest silt, affords a minimum age for deglaciation from the TDP I_{LA} position. More important, the basin was fed by meltwater from an ice position close to the TDP II moraine belt, suggesting that ice at 17.4 ka was similar in size to that during the TDP II advance.

3.6.5 The Last Termination

The position of the TDP I_{DT} moraine, as well as its age of 16.5 ± 0.6 ka, suggests that this landform marks the end of the LGM in the Torres del Paine region. However, the mean age of TDP I_{DT} seems slightly younger than ages from other late LGM moraines in the southern hemisphere when those ages are recalculated using the New Zealand production rate (Putnam *et al*., 2010; cf. Kaplan *et al*., *accepted*). For instance, the Fenix

I-Menucos moraines at Lago Buenos Aires (Douglass *et al*., 2006; Kaplan *et al*., 2004), the third and final limit of the Río Blanco moraines at Lago Pueyrredón (Hein *et al.*, 2010), and the D_2 moraines at the Strait of Magellan and Bahía Inútil basins (Kaplan *et al*., 2008; McCulloch *et al.*, 2005), all show recalculated ages between about 18.5-21 ka. In addition, our minimum age of 17.4 kcal yr B.P. for deglaciation in the Laguna Azul basin is at least 1000 years older than the TDP I_{DT} moraine but in close agreement with minimum-limiting data obtained at other sites southern in Patagonia (e.g., Sagredo *et al.*, 2011; McCulloch and Davies, 2001; McCulloch et al., 2005; Hall et al., in prep.), and the Chilean Lake District (Denton *et al.*, 1999b), all of which show that glaciers had abandoned their LGM positions by ~17.0-17.5 ka.

One possibility is that the ^{10}Be data may underestimate slightly the true age of the TDP I_{DT} landform. Several potential problems, such as PR variation, erosion, and snow or lake shielding, could lead to ages being too young.

Production rates for cosmogenic isotopes are average estimations based on calibration sites (Balco *et al.*, 2008). We use the New Zealand PR (Putnam *et al*., 2010), which has been confirmed recently at Lago Argentino (50ºS), because it agrees better with radiocarbon ages marking late-glacial ice retreat in Torres del Paine than other available PR (Chapter 4; Appendix A). Despite use of the most up-to-date PR, it is possible that a significant local air pressure shift concurrent with the southward migration of the westerly wind belt at the end of the LGM (e.g., Anderson et al., 2009; McCulloch *et al*., 2000) could have increased the local ^{10}Be PR producing slightly younger ages. However, a southward shift of the westerly winds also implies a southward shift of the Antarctic Polar Front and sub-tropical convergence, which probably were accompanied

by an overall increase in local barometric pressure (and thus decrease in PR) in south Patagonia during the termination (e.g., Ackert *et al.*, 2003). Therefore, it is not evident that a change in air pressure due to a change in atmospheric circulation would cause exposure ages for TDP I_{DT} moraine to be too young.

When erosion rates are high they also can affect significantly the exposure age calculated for a particular landform. In Patagonia at 46ºS, ~500 km to the north, previous work has estimated a maximum average erosion rate of about 1.4 mm per thousand years over long-term exposures (e.g., $>10^5$) (Kaplan *et al.*, 2004; Douglass, 2005). If we applied this estimation to our samples, the age of the TDP I_{DT} moraine becomes only slightly (~2%) older (Table 3.2). Moreover, our boulders from TDP I_{DT} moraine all had well-preserved surfaces and lacked evidence for significant erosion. Therefore, we conclude that erosion has not affected ages of the TDP I_{DT} significantly.

Snow shielding may affect the production rate of cosmogenic nuclides when a thick snowpack continuously covers the rock surfaces. For instance, Jackson *et al.* (1999) obtained a 5% snow correction assuming a one-meter snow cover during half of the year in southwestern Alberta, Canada. However, average winter temperatures in Torres del Paine where the moraine belts are located is >0ºC today (Carrasco *et al.*, 2002), which makes thick snow accumulation for long periods unlikely, at least during the Holocene. In addition, samples from the TDP I_{DT} moraine were obtained from low elevation (~100 m a.s.l.) in a semiarid region and in locations exposed to wind, which would blow away accumulated snow. Therefore, any effect from snow shielding on local ^{10}Be ages should be negligible.

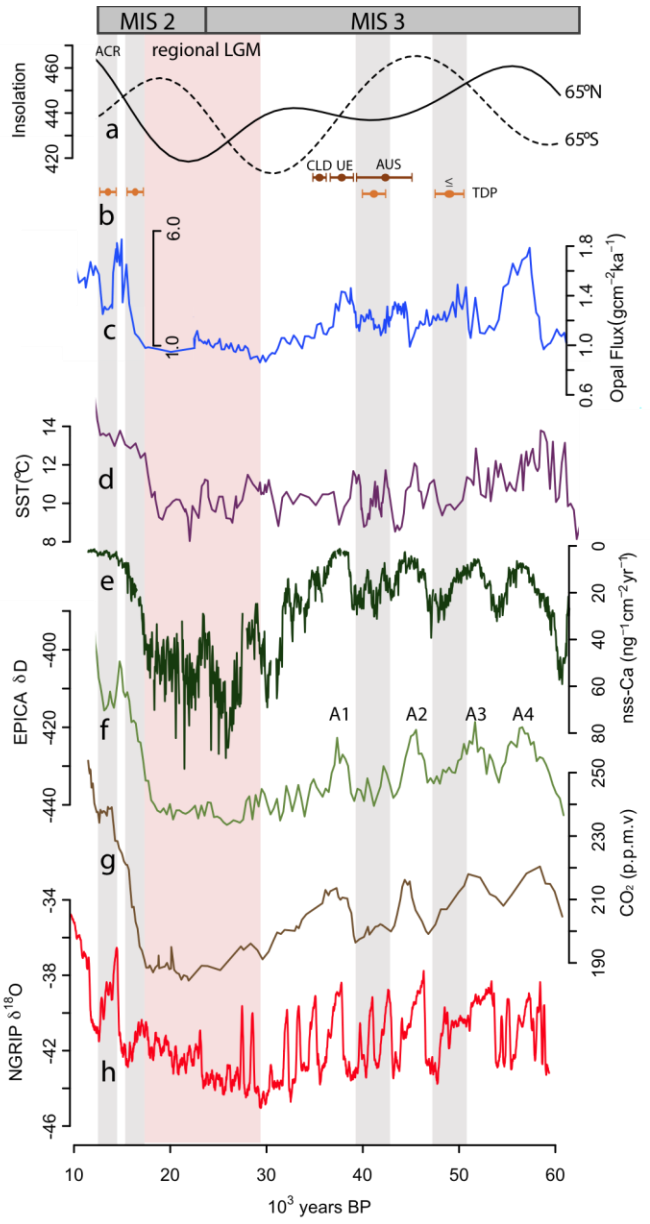

Figure 3.5. Paleoclimate records spanning Marine Isotope Stages 3 and 2. a) Insolation for mid-high latitudes in the northern and southern hemispheres (Berger and Loutre, 1991); **b)** Moraines: TDP= Torres del Paine (this study); UE= Última Esperanza (Sagredo *et al*., 2011); CLD= Chilean Lake District (Denton *et al*., 1999b); Aus= Australia (Tasmanian region; Barrows *et al*., 2002; Mackintosh *et al*., 2006); **c)** Southern Ocean wind-driven upwelling and southern westerly wind belt latitudinal variation interpreted from biogenic opal flux (Anderson *et al*., 2009); **d)** Alkenone-derived sea-surface temperature (SST) at the Southeast Pacific Ocean (site (ODP1233; Kaiser *et al*., 2005); **e)** non sea-salt calcium EPICA Dome C ice-core (Röthlisberger *et al*., 2002); **f)** Antarctic deuterium record (EPICA community members, 2004); **g)** Atmospheric carbon dioxide record from EPICA ice core (Lüthi *et al*., 2008); **h)** Greenland stable oxygen record (North Greenland Ice Core Project members, 2004).

In contrast, shielding by lake water could have resulted in slightly young exposure ages at TDP I_{DT} moraines (80-110 m a.s.l.). As described in Chapter 2, lake terraces and glaciolacustrine sediments record the existence of paleolake Tehuelche in Torres del Paine. Because of the presence of subaerial glaciofluvial sediments grading from the ice front into the TDP I_{SA} ice-contact delta-moraine at the Estancia site, we infer that the TDP I moraines at Lago Sarmiento and likely Lago del Toro were deposited when the Tehuelche lake was at ~125 m a.s.l. A lake at this level would have inundated the TDP I_{DT} moraine and shielded the sampled boulders under as much as 40 m of water. In order to maintain water level at this elevation, this lake must had drained through the Frontera spillway at ~125 m a.s.l. in Última Esperanza (Chapter 2). If this interpretation is correct, paleolake Tehuelche must have been continuous with the Puerto Consuelo paleolake in Última Esperanza (Sagredo *et al.*, 2011), which is dated at about 17.6-16.8 ka (Sagredo *et al.,* 2011; Stern *et al.,* in press; Chapter 2). One possible interpretation then is that the age of the TDP I_{DT} boulders represents not the time of moraine formation, but the drainage of Lago Tehuelche and exposure of the landform at 16.5 ka. This age is comparable to that proposed for drainage of Lago Puerto Consuelo.

In summary, a calibrated radiocarbon date from Vega Chulengo suggests that the termination was underway in the Laguna Azul basin by 17.4 ka, similar to other sites in southern South America (e.g., Sagredo *et al.,* 2011; McCulloch and Davies, 2001; McCulloch *et al.,* 2005; Hall *et al.*, in prep.). The TDP I_{DT} terminal moraine, thought to represent the end of the LGM, yielded an age ~1,000 years younger. Although this age may be correct and reflect differences in glacier response between different basins, an alternative possibility is that the exposure ages were affected by lake-water shielding.

3.6.6 The Last glacial period in Southern South America

As described above, previous work in the Patagonian region (42-53ºS) and Chilean Lake District (39-42ºS) has provided invaluable data that overall afford a generally consistent pattern of glacial and deglacial trends in the region. However, some aspects of the glacial record from Torres del Paine presented in this thesis (Chapter 3 and 4) do not fit entirely with this "Patagonian pattern" and leave open important questions about the glaciation and termination in the region. For example, the record from the Chilean Lake District (Denton *et al*., 1999b; Moreno *et al*., 1999) consistently shows that the local LGM occurred between ~35-17.5 cal ka. Throughout this time glaciers expanded into their LGM positions and only by 17.5 cal ka, at the beginning of the Termination, did glaciers rapidly retreated into the mountains. It is not clear if glaciers at this latitude readvanced during the late glacial, although pollen, and lake and ocean sediment records indicate stadial conditions (Lamy *et al*., 2004; Moreno *et al*., 2001; Ariztegui *et al*., 1997). In Patagonia, glaciers are known to have advanced near synchronously with those in the Chilean Lake District. In addition, the Termination occurred near synchronously throughout the whole region (e.g., Hein *et al*., 2010; Douglass *et al*., 2006; Sudgen *et al*., 2005; Denton et al., 1999b) and was interrupted by a glacial expansion during the Antarctic Cold Reversal (ACR, Strelin and Denton, 2005).

Two aspects of the ^{10}Be record in Torres del Paine need special mention when compared with other sites in Patagonia/Chilean Lake District, because they differ significantly from conslusions reached during previous work: 1) The location of the late glacial moraines just proximal to the 40 ka moraines at Laguna Azul, and 2) the location of the late glacial moraines close to the interpreted late LGM moraines at Lago del Toro

(TDP I_{DT}). These two problems arise from the fact that the position of the LGM ice margin in Torres del Paine is unknown. This is particularly true for the Lago Sarmiento and Lago del Toro areas. Moreover, if the interpretation of the chronology is correct, it implies that glacial advances at least at Laguna Azul reached a similar position several times throughout the last glaciation and late-glacial period, a pattern not seen elsewhere. More data need to be recovered from the outer RV II and RV III, AG and TDP I_{DT} moraines to define better the local structure of the last glaciation and transition to the present interglacial in Torres del Paine. This will allow a better comparison with other sites in southern South America and elsewhere in the southern hemisphere.

3.6.7 The Last Termination in the southern hemisphere

The pattern shown by Patagonian glaciers at the end of the last glaciation matches records acquired from other terrestrial and marine sites in the southern middle and polar latitudes. For instance, glacier reconstructions from several sites in the Snowy Mountains in southeast Australia and Tasmania (Barrows *et al*., 2001, 2002) showed that regional glacial culmination occurred by 20.0 ka, based on the mean age of an inner LGM moraine. Schaefer *et al*. (2006) presented a similar termination scenario, based on a glacier record at Lake Pukaki. Here, they showed retreat into the mountains after deposition of the inner LGM moraine after 19.0 ka. Newer work in the same region has revealed that the LGM culminated at 18.0 ka (Kelley, 2009; Doughty, 2008). The beginning of the Antarctic warming trend, as recorded by deuterium and oxygen isotope variations in the southern ice cores (EPICA Community Members, 2006; Blunier and Brook, 2001), also occurred at about ~18.0 ka , nearly synchronous with retreat of the

southern mid-latitude glaciers. At the same time, atmospheric CO_2 concentration increased (Monnin *et al*., 2001) and the Southern Ocean sea-surface temperatures (SST) (Barker *et al*., 2009) rose. All together, this group of paleoclimate records suggests a hemisphere-wide termination event and climate synchronization between the southern middle and high latitudes.

3.6.8 MIS 3 in the southern hemisphere

Although evidence for MIS 3 glaciation in southern South America is limited, the opposite is true for the western side of the south Pacific. Glacial advances in New Zealand and Australia, as inferred from luminescence, speleothem and exposure-dating methods, have been linked to stadial conditions during MIS 3 (Schulmeister *et al*., 2010; Mackintosh *et al*., 2006; Almond *et al*., 2001; Barrows *et al*., 2001, 2002; Williams, 1996). As shown below, these data suggest that the MIS 3 glacial advances recorded in Torres del Paine (~49 ka and 41 ka), in Última Esperanza (38.0 ka) and the Chilean Lake District (~35 cal ka) have been replicated at other sites in the southern middle latitudes and likely document a hemispheric-wide climate signal.

In Rakaia Valley in New Zealand, Shulmeister *et al*. (2010) obtained infrared stimulated luminescence (IRSL) ages from glacial sediments indicating advances occurring at ca. 48 ka and ca. 40 ka. In addition, luminescence dating from soil profiles developed on moraines at South Westland in New Zealand showed that glacier expansion in the region occurred at some time between 45-50 ka (Almond *et al*., 2001). These MIS 3 glacial expansions likely were broadly coincident with Aurora 4 (40-41 ka) and Aurora

5 (46-48 ka) advances, as interpreted from speleothems at Aurora Cave (Te Anau, New Zealand; Williams, 1996).

A ^{10}Be glacial chronology from the Snowy Mountains of southeast Australia (37ºS; Barrows *et al.*, 2001) revealed that glaciers expanded at some time between ~40-60 ka and deposited the BL-I moraine. The authors suggested that post-depositional snow shielding and exhumation may have affected the boulders, and thus they preferred the oldest age to represent the glacial pulse. The BL-I moraine defined the maximum expansion of ice during the last glaciation in the region.

A ^{36}Cl and ^{10}Be glacial chronology from the Central Plateau in southwest Tasmania (41-43 ºS) (Barrows *et al*., 2002) also affords evidence for glacial expansion between about 39-46 ka at three different sites: Mt. Jukes (40.8±3.5 ka), Mt. Hartz (39.3±2.9 ka, 45.5±2.9 ka) and Mt. Field National Park (43.1±3.0 ka). More recent, , Mackintosh *et al.* (2006) obtained ^{36}Cl ages of boulders on moraines at Mt. Field dating 44.1±2.2 and 41.0±2.0 ka. The extent of glacial expansion at this time was similar to that during MIS 2 (Barrows, et al., 2002, Mackintosh *et al.*, 2006).

Ice and marine-sediment cores record MIS 3 as a transition period with significant climate variability (Jouzel *et al*., 2007; EPICA members, 2006; Kaiser *et al*., 2005; Fig. 3.5). Millennial-scale variability at this time produced δ^{18}O oscillations greater than 3‰ (Blunier and Brook, 2001) and δD fluctuations of 10-15‰ (EPICA members, 2006) (Fig. 3.5f), equivalent to temperature changes of 2 to 3ºC over Antarctica (Jouzel *et al*., 2007). At 41ºS, in the southeast Pacific, alkenone-derived SST records also show variations of 2 to 3ºC (Fig. 3.5d), coincident with the MIS 3 stadials shown by the Antarctic ice cores

(Kaiser *et al.*, 2005). Therefore, isotope maxima and minima throughout MIS 3 in Antarctic ice cores likely mark stadial and interstadial conditions that recorded synchronous ocean and atmosphere changes in the southern mid and high latitudes.

Based on an opal-derived, wind-driven upwelling record from the Southern Ocean (Fig. 3.5b), Anderson *et al*. (2009) proposed that the southern westerly wind belt acted as a main modulator of millennial-scale climate changes during MIS 3. They found that the westerly wind belt shifted southward into the Southern Ocean, driven by intense cooling in the northern hemisphere. This southward migration was coincident with a rise in atmospheric CO_2 concentrations (Fig. 3.5g) and interstadial conditions in Antarctica (Fig. 3.5f). Our glacial chronology suggests that advances in the Torres del Paine region (Fig. 3.5b) were concurrent with Antarctic stadials. These stadials may have promoted northward shifts of the westerly wind belt into Patagonia, which increased precipitation rates in the Torres del Paine region.

3.6.9 Drivers of southern glaciation

Although LGM ice fluctuations are not well represented by moraines in Torres del Paine, glacier records from elsewhere in southern South America suggest the existence of a regional LGM beginning at 28-26 ka, slightly earlier than the global LGM. Glaciers remained at their LGM position until the termination (e.g., Denton *et al*., 2010; Schaefer *et al*., 2006).

Overall, paleoclimate records of the last ice age (MIS 4-2) in the southern hemisphere show that stadial conditions and glacier advances occurred at times when

isolation intensity was both at maxima and minima. (Fig. 3.5a, b) (e.g., this chapter, Hein *et al*. 2010; Kelley, 2009; Doughty, 2008; Vandergoes *et al*. 2005; Suggate and Almond, 2005; Sugden *et al*., 2005; Barrows *et al.*, 2001, 2002; Denton *et al*., 1999b; Heusser *et al.*, 1999). This implies that glacial conditions in the southern mid-latitudes occur irrespective of the insolation intensity phase, and thus other factors must drive southern hemisphere ice ages.

Ice-age conditions during the global LGM could have been transmitted from the northern hemisphere into the south, but models that rely on ice-sheet feedbacks, such as albedo, (e.g., Broccoli and Manabe, 1987), fail to reproduce this scenario. Decrease in atmospheric CO_2 concentrations during the global LGM (Fig. 9g) would have affected both hemispheres simultaneously, but this is thought to have been only a positive feedback in expanding the glacial realm globally (Clark et al., 2009), rather than the primary driver of ice ages (Syktus *et al.*, 1994; Verbitsky and Oglesby, 1992). Huybers and Denton (2008) proposed that duration of summers in the southern polar hemisphere, which covaries with northern summer intensity, might provide the missing factor in driving synchronous global ice ages. During the LGM, shorter summers (and longer winters) prompted cooler mean annual temperatures in the southern polar hemisphere (Huybers and Denton, 2008), which probably were transmitted to lower southern latitudes by northward expansion of the polar front, sea ice and the westerly winds. Longer winters in the Southern Ocean stimulated stable stratification (Sigman and Boyle, 2001) with a direct consequence for sea-ice concentration, extent and duration (Hays and Morley, 2003; Gersonde *et al.*, 2003). The sea ice would have had mainly a winter effect

on climate, complementing the outcome of shorter ablation seasons on glacier expansion (Huybers and Denton, 2008).

The expansion of Antarctic climate into the southern mid-latitudes also may have been achieved through fluctuations of the westerly wind belt, which is a main climate component for this region. The position and intensity of these winds is sensitive to sea-surface temperatures and semi-permanent pressure cells at low and high latitudes (Lamy *et al*., 2004; Markgraf, 1998; Miller, 1976) and therefore rapidly transmit climate fluctuations. In this scenario, the westerly wind belt would have responded as a principal positive feedback to the expansion of the Antarctic Frontal Zone, thus propagating the glacial signal into the lower southern latitudes.

3.7 Conclusions

Our ^{10}Be ages show that the Patagonian ice sheet expanded at ~49,000, 41,000, and slightly before 16,500 years ago during glacial conditions of the last ice age. The TDP I_{DT} moraine probably formed close the end of the LGM, but the absence of other moraines dating to this time period precludes definition of the exact location and overall structure of the LGM in the Torres del Paine region. Additional chronologic work on the RV II and RV III moraines should help resolve this important problem.

The Patagonian ice sheet in the Torres del Paine region reached its maximum extent during MIS 3, something that has been documented only in a few localities southern South American to date but which is more common in Australasia. The greater

extent of ice during this time compared to MIS 2 may result from fluctuations of the southern westerly wind belt between northern and southern Patagonia.

Chronological and mapping evidence suggests that in the Laguna Azul basin, the Antarctic Cold Reversal may have produced the most extensive advance of MIS 2. The Patagonian ice sheet snout seems to have fluctuated near this position during a significant part of the last glaciation. This pattern of glaciation is significantly different from that observed at most other southern hemisphere locations and requires further study.

Southern mid-latitude glacier expansions occurred irrespective of the insolation phase. MIS 3 millennial-scale stadial conditions recorded by glaciers and other paleoclimate proxies in the southern hemisphere suggest rapid oceanic and atmospheric reorganizations that prompted hemispheric-wide simultaneous climate changes. Northern shifts of the Antarctic Frontal Zone, Subtropical Zone and, particularly, the southern westerly wind belt may have played an important role in expanding the Antarctic glacial climate into the southern middle latitudes during MIS 3 stadials. A similar series of marine and atmospheric feedbacks may have occurred during the global LGM, when a combination of shorter ablation seasons (Huybers and Denton, 2008) and longer winters could have decreased mean annual temperature in the southern mid-latitudes.

CHAPTER

4. GLACIER EXPANSION IN SOUTHERN PATAGONIA THROUGHOUT THE ANTARCTIC COLD REVERSAL

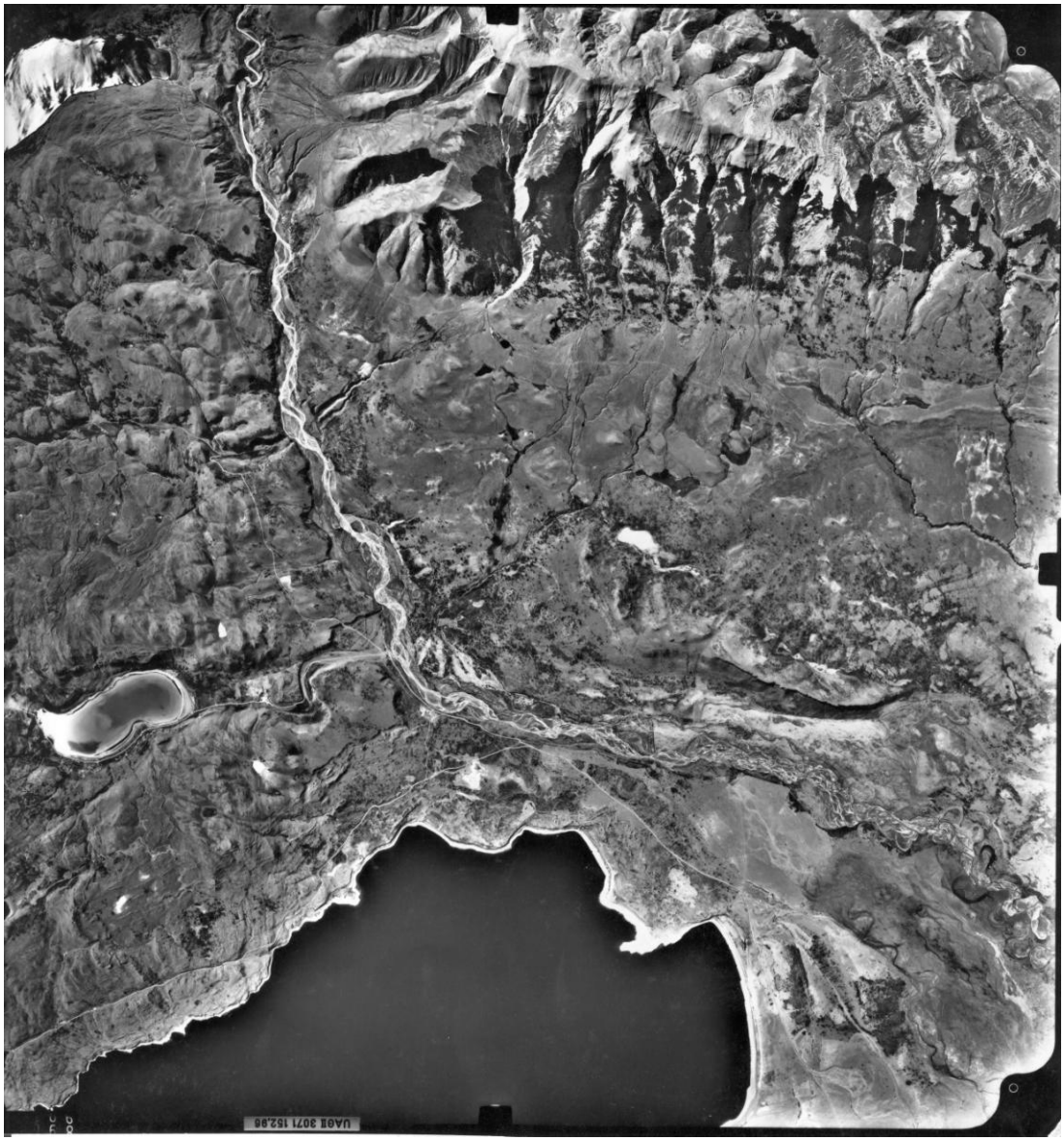

4.1 Abstract

Outlet glaciers of the South Patagonian Ice Field are sensitive to atmospheric temperatures and precipitation (Oerlemans *et al*., 1992). Thus, former margins record the magnitude and timing of the last glacial to interglacial transition and afford a means for resolving both debated climate changes in the southern mid-latitudes (e.g., Ackert *et al.*, 2008; Putnam *et al*., 2010a; Strelin and Denton, 2005) and potential teleconnections between temperate and polar latitudes. Here, we use precise mapping together with ^{10}Be exposure ages of 38 boulders from Torres del Paine (51°S) moraines and radiocarbon ages (e.g., Moreno *et al*., 2009) to date directly an outlet glacier maximum throughout the Antarctic Cold Reversal. This extended 1,600-year-long ice-sheet culmination in Patagonia has remained unappreciated in glacial records, but matches closely atmospheric and marine records from the Southern Ocean and Antarctica that show a close coupling. We hypothesize that late glacial global climate reorganization prompted a northern migration of the westerly wind belt during the early Antarctic Cold Reversal into lower latitudes of southern South America, including Torres del Paine, bringing both cold temperatures and increased precipitation. Furthermore, we conclude that an interhemispheric teleconnection existed, whereby a northward shift of the westerly belt at the start of the Antarctic Cold Reversal followed the northward migration of the thermal equator, which was linked to the onset of the warm Northern Hemisphere Bølling period.

4.2 Introduction

Understanding millennial-scale climate variability that interrupted the last deglaciation (18.0–11.5 ka) affords insight into the nature and cause of the termination of

ice ages. One prominent event, the Antarctic Cold Reversal (ACR, ~14.5-12.8 ka, Lemieux-Dudon *et al.,* 2010) in the high southern polar latitudes, was contemporaneous with the Bølling warm period in the north and ended during the peak of the Younger Dryas stadial (~12.9-11.7 ka, Blunier and Brook, 2001), but its cause remains obscure. Recent studies (Putnam *et al*., 2010a; Strelin and Denton, 2005) show robust evidence for a final late glacial culmination in southern mid-latitudes during the latest ACR about 13.1 ka, followed by substantial glacier recession in the subsequent millennium (Kaplan *et al*., 2010). These studies argue for a regional to hemispheric footprint of the ACR. However, marine and ice-core evidence show an onset of the ACR much earlier than 13.1 ka (Barker *et al.,* 2009; Blunier and Brook, 2001; EPICA community members, 2004), and climate dynamics throughout the remainder of the ACR remain unclear. Resolving the details of this time period, especially on land, is essential for understanding its cause, as well as the cryosphere-atmosphere-ocean links, including the relation between atmospheric CO_2 and ice, that operated during the transition to the Holocene.

Here, we use modern ^{10}Be techniques and radiocarbon dating to establish a detailed and robust reconstruction of ice fluctuations in southern South America during the entire ACR. Precise ^{10}Be ages of boulders on moraines in Torres del Paine National Park (51ºS, 73ºW, Fig. 4.1) afford unequivocal evidence that glaciers in the middle latitudes responded immediately to the onset of this major late glacial climate reversal, that the duration of glacier expansion in the southern mid-latitudes matched that seen in Antarctica, and that there was tight coupling between ocean, atmosphere, and glacial systems through this time.

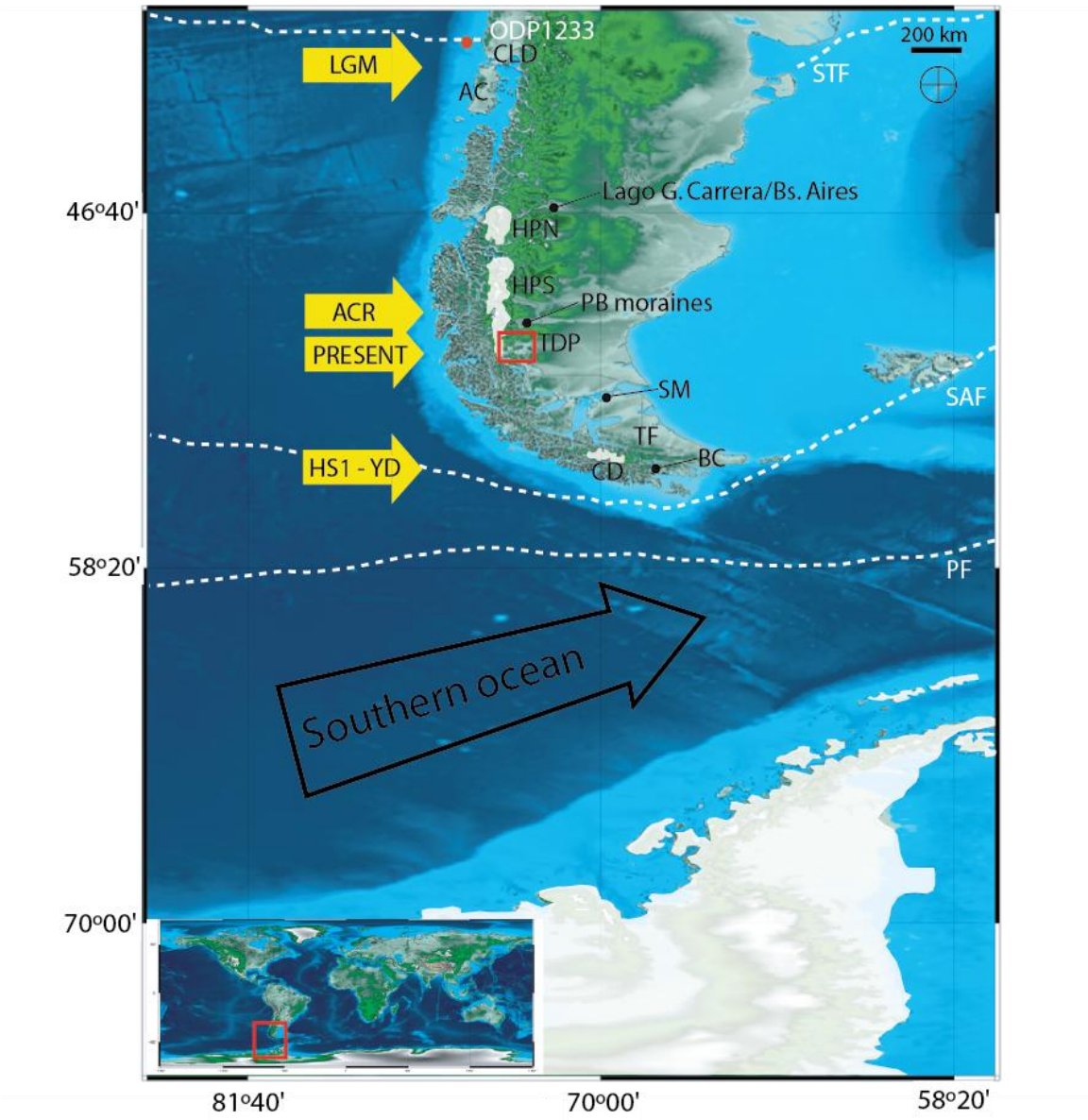

Figure 4.1. Location of Torres del Paine (TDP, red box in main image) in southern South America in the geographic context of the Southern Ocean and Antarctic Peninsula. Inset shows position of main image (red box) in the global context. Solid yellow arrows depict location of the south westerly wind belt (SWW) at different key periods during the last glacial interglacial transition and at present time (Miller, 1976). White dashed lines indicate approximate present position of the Polar Front (PF) and Sub-Antarctic Front (SAF) and Subtropical Front (STF). Past SWW latitudinal shifts and positions are interpreted from paleocological, glacial and sedimentological records mentioned in the text. CLD=Chilean Lake District; AC= Archipiélago de Chiloé; HPN= Hielo Patagónico Norte (North Patagonian Icefield); HPS=Hielo Patagónico Sur (South Patagonian Icefield); PB=Puerto Bandera; SM= Strait of Magellan; TF=Tierra del Fuego; BC= Beagle Channel; CD= Cordillera Darwin Ice Cap; LGM=Last Glacial Maximum; ACR= Antarctic Cold Reversal; HS1= Heinrich Stadial Event; YD= Younger Dryas; ODP= Ocean Drilling Program. Base map modified from *http://ecm.um.maine.edu.*

Torres del Paine has one of the prime late-glacial moraine records in the southern mid-latitudes. The excellent preservation and continuity of suites of moraines and their geographical location make them ideal to test hypotheses of late-glacial climate change (Fig. 4.1; Plate 2, pocket). Previous work (Marden and Clapperton, 1995) defined four distinct moraines belts, named A to D from outer to inner, thought to have been deposited during full-glacial conditions. To avoid confusion with moraines of different ages having similar labels in other sites in southern South America (Sugden *et al*., 2005), we rename these moraines here accordingly: A= TDP I, B= TDP II, C= TDP III and D=TDP IV. These moraine sets occur within three kilometers of each other at both Laguna Azul and Lago Sarmiento (Plate 2, pocket) and are ≥45 km from present-day ice margins. The sharp morphology of the TDP II to IV moraines contrasts from that of the TDP I moraines, which are wide and prominent landforms, possibly implying that a significant time elapsed between the formation of these moraine belts. TDP II–IV moraines can be tracked with only short gaps between both lake basins, suggesting that Laguna Azul and Lago Sarmiento ice lobes merged and formed a single ice sheet with a >20 km continuous terminus (Plate 2; Appendix A supplementary note).

4.3 Results and Discussion

We collected 38 boulders from the TDP II, TDP III, and TDP IV moraines adjacent to Laguna Azul and Lago Sarmiento (Figure 4.2). We applied recent technological advances, affording for improved precision of ^{10}Be analyses ($1\sigma \sim 3\%$; Appendix A - supplementary methods). Our exposure ages are calculated using a ^{10}Be production rate based on New Zealand's Macaulay site (Putnam *et al*, 2010b; Appendix A). This ^{10}Be production rate recently has been confirmed in the Lago Argentino area

(Kaplan *et al*., accepted) north of Torres del Paine. Boulders from the TDP II moraines yielded ages ranging from 13.4–15.0 ka, with an arithmetic mean of 14.2±0.5 ka (n=14) (Fig. 4.3a). The TDP III moraine boulders range from 13.7–15.0 ka, with a mean of 14.1±0.5 ka (n=10) (Fig. 4.3b), whereas those of the TDP IV moraines (including two ages recalculated from Moreno *et al*., 2009) yielded ages of 13.8-15.3 ka, with a mean of 14.1 ± 0.7 ka (n=6) (Fig. 4.3c) (Table 4.1 and 4.2).

For each respective moraine belt, the ^{10}Be boulder ages show a normal distribution and high internal consistency (Fig. 4.3). We detected and rejected outliers by applying the Grubbs test (Grubbs, 1969) and the two-sigma rule (see Appendix A - supplementary methods for discussion on outliers; Fig. A3). The resulting ^{10}Be mean ages indicate that deposition of these three moraine systems occurred relatively rapidly within the same time period, at approximately 14.2 ± 0.6 ka.

The number, size and continuity of the moraine sequences suggest that the ice was active and capable of eroding, transporting, and depositing a large volume of sediment during their formation (Plate 2, pocket). The clearest evidence for this glacial pulse being a readvance comes from the Lago Sarmiento and Río Paine areas. In the former, the TDP II moraine crosscuts the older TDP I moraine, suggesting that at least the most extensive ACR moraine in Torres del Paine represents a glacial expansion, rather than just a stillstand during retreat. In addition, near Río Paine, deformed lake beds occur in the TDP IV moraines, indicating that ice readvanced over its own proglacial lake deposits (Marden and Clapperton, 1995).

Figure 4.2 Examples of boulders sampled for ^{10}Be exposure dating from TDP II, TDP III, and TDP IV moraines at Torres del Paine. Photographs show moraines and boulders at different parts of the study area. See Plate 2 (pocket) for location and ages, and Table 4.1 and 4.2 for sample details.

Figure 4.3 Relative probability plots and statistics for each moraine (TDP II, TDP III, TDP IV). Probability plots without outliers are presented for each moraine belt. The thin curves represent individual sample ages ± 1σ. The thick curve is the normalized probability distribution of the moraine age population. Central vertical lines in plots denote the arithmetic mean ±1σ (yellow rectangle), 2σ (red vertical line) and 3σ (green vertical line). Values used in the text are arithmetic means and associated uncertainties obtained after rejecting outliers. Uncertainties used (bolded values) include propagation of the analytical and production-rate errors. We used a 2.4% uncertainty from the ^{10}Be production rate as defined in Putnam *et al*. (2010b). **a** – TDP II moraine; **b** – TDP III moraine; **c** – TDPIV moraine. TDP IV includes two CAMS recalculated dates from Moreno *et al*. (2009).

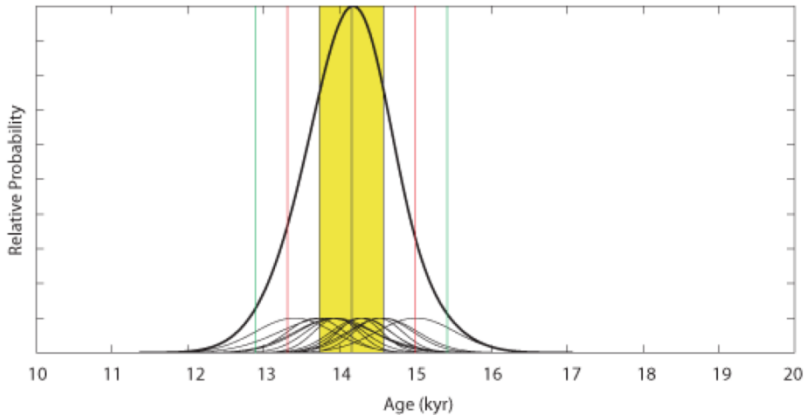

a) TDP II moraine belt. Samples (n= 14):
LA0703, 07, 15, 20, 0901
RP0815, 17, 20
SAR0703, 05, 13, 18, 25, 0907
Outliers: LA0714, 16, 32, SAR0702, 19

Statistics
Arithmetic mean/1 sigma uncertainty: 14,200±420 yrs
Including production rate uncertainty: **14,200±540 yrs**
Weighted mean/weighted uncertainty: 14,200±100 yrs
Peak age: 14,200 yrs
Median/Interquartile Range: 14,100±580 yrs
Reduced χ^2: 0.9

Figure 4.3. Continued

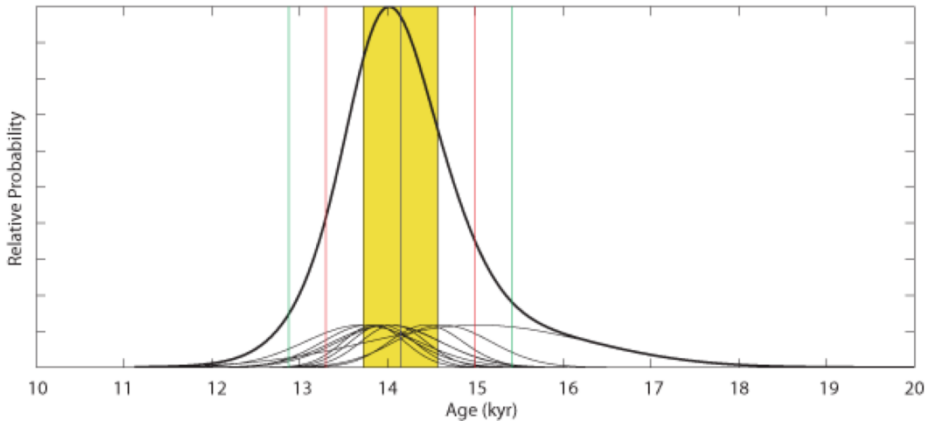

b) TDP III moraine belt. Samples (n=10):
LA0522, 0704, 27, 28
RP0705, 0903, 04, 05, 06
SAR0908
Outliers: LA0512, SAR0701, 24, SAR0906

Statistics
Arithmetic mean/1 sigma uncertainty: 14,100±420 yrs
Including production rate uncertainty: **14,100±540 yrs**
Weighted mean/weighted uncertainty: 14,100±150 yrs
Peak age: 14,000 yrs
Median/Interquartile Range: 14,000±590 yrs
Reduced χ^2: 0.4

Figure 4.3. Continued

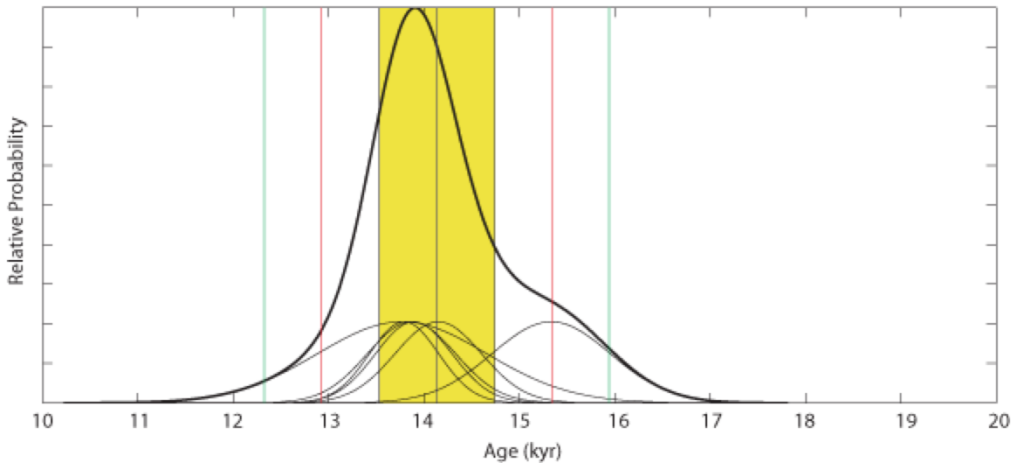

c) TDP IV moraine belt. Includes recalculated ages (samples VN-05-25, 26) from Moreno *et al*. (2009). Samples (n=6):
RP0701, 03
SAR0721, 23
VN0525, 26
Outliers: SAR0722

Statistics
Arithmetic mean/1 sigma uncertainty: 14,100±600 yrs
Including production rate uncertainty: **14,100±690 yrs**
Weighted mean/weighted uncertainty: 14,000±190 yrs
Peak age: 13,900 yrs
Median/Interquartile Range: 13,900±360 yrs
Reduced χ^2: 1.1

Our moraine-based chronology shows that glaciers in Torres del Paine region were far from the present-day ice margin at 14,200 years. Glacier retreat only was underway by 12,600 cal years ago as recorded by radiocarbon ages from sites within the moraine belts (e.g., Moreno *et al*., 2009). Radiocarbon ages date the transition from coarser inorganic to organic sediment, interpreted as the cessation of meltwater activity tied to ice retreat from TDP IV moraines (Plate 2, pocket; Appendix A - supplementary

methods). Our sediment core obtained at the Vega Baguales meltwater conduit (Plate 2, pocket) yielded a close minimum calibrated age of 12,500 ± 70 (Appendix A note, Fig. A2) for glacier retreat, which is in close agreement with previous radiocarbon data from the area for deglaciation of 12,540 ± 40, 12,470 ± 100, and 12,280 ± 100 cal years ago (Moreno *et al.*, 2009).

Collectively, the ^{10}Be and ^{14}C ages indicate that extensive glacier ice in Torres del Paine lingered for ~1600 years at its late glacial position, providing direct evidence for the full duration of the ACR in southern Patagonia, as recorded by glaciers. We hypothesize that during the early phase of the ACR the westerly belt may have been close to 51°S in SSA (Fig. 4.1), which would have brought not only cold conditions, but also peak precipitation to Torres del Paine glacial catchments. Late-glacial pollen records south of 53°S in Tierra del Fuego and the Beagle Channel (e.g., Heusser, 2003), in the southernmost tip of south America, support such a northward shift of the westerly belt and also may imply a concurrent northward shift of the Antarctic Frontal Zone, probably as far as the Strait of Magellan (53°S, Sugden *et al.*, 2005). Our results do not support previous conclusions (Ackert *et al.*, 2008) that glaciers at this latitude were within the cordillera during the ACR, nor that local late-glacial glacier records oppose Antarctic temperature records (Blunier and Brook, 2001). Lake-level fluctuations recorded at Lago Cardiel (49°S) suggest locally dry conditions at the end of the ACR (Stine and Stine, 1990) that seems to agree with our results. Dry conditions on the lee side of the Andes result mostly from an effective rain shadow. While on the windward side a positive correlation between wind flow and precipitation dominates, the opposite is true on the lee side (Garreaud, 2007). Therefore stronger winds during the ACR at this latitude may have enhanced dry conditions on the lee side of the Andes, such as at Lago Cardiel.

We provide precisely-dated moraines demonstrating that glaciers in the southern middle-latitudes responded immediately to the onset of the ACR as recorded in Antarctic ice cores (Blunier and Brook, 2001; EPICA community members, 2004) (Fig. 4.4f). As mentioned above, previous work showed glaciers in the southern mid-latitudes culminating at the least at the end of the ACR chronozone. At Lago Argentino, the maximum age for the deposition of the Puerto Bandera moraines is ~13.1 cal ka (Strelin and Denton, 2005); there is no evidence for earlier glacial expansion during the ACR at the same time as that at Torres del Paine (14.2 ka). This is intriguing, because Lago Argentino is just north of Torres del Paine and both basins share part of the same accumulation area. One alternative that may help to reconcile both records, Torres del Paine and Lago Argentino, is that at the beginning of the ACR, when active ice was building the TDP II, III, IV moraines at Torres del Paine, ice at Lago Argentino was still expanding to the Puerto Bandera moraines. Although, the exact position of the ice just prior to the late-glacial period is unkown, ice was behind the ACR position. It is possible that the early Termination retreat was more extensive at Lago Argentino than at Torres del Paine (maybe because of a local enhanced calving effect in the deeper lake) and thus it took longer for the ice at Lago Argentino to reach its maximum late-glacial position. Our data document that southern glaciers were likely at a maximum throughout the entire ACR period, consistent with sediment records from Última Esperanza (Sagredo *et al*., 2011) and previous work in Torres del Paine (Moreno *et al*., 2009; Fogwill and Kubik, 2005). This glacier signal is also consistent with several recent ocean-atmosphere records shown in Fig. 4.4, supporting the view of a hemispheric-wide ACR and suggesting a close coupling between southern oceanic, atmospheric, and cryospheric systems. The

onset of glacier advance in South Patagonia during the early phase of the ACR, and perhaps elsewhere (Putnam *et al*., 2010a) (Fig. 4.4a), was contemporaneous with a decline in the Southern Ocean upwelling rate (Anderson *et al*., 2009) (Fig. 4.4c) and associated CO_2 degassing into the atmosphere (Monnin *et al*., 2001) (Fig. 4.4e) at 14.5 ka. This glacier advance culminated at 14.2 ka coincident with minimum upwelling in the Southern Ocean and a plateau in atmospheric CO_2 concentrations (Fig 4.4e). After ~1600 yrs, the onset of rise in the Southern Ocean upwelling and atmospheric CO_2 rates at 13.0 ka coincided with rapid glacier retreat in Patagonia and New Zealand (Putnam *et al*., 2010; Strelin and Denton, 2005; Moreno *et al*., 2009; Kaplan *et al*. 2010).

What accounts for the close linkage between the glacial record of Patagonia, Antarctic climate, and Southern Ocean upwelling and temperature records? During the ACR, latitudinal shifts of the Antarctic Frontal Zone and westerly belt linked to Southern Ocean surface temperatures (Anderson *et al*., 2009; Bianchi and Gersonde, 2004) (Fig. 4.4b) were associated with upwelling rates (Anderson *et al*., 2009; Toggweiler *et al*., 2006) and ocean stratification (Bianchi and Gersonde, 2004). During the early stage of the last termination, a southward shift of the westerly belt to the latitude of the Drake Passage led to increased upwelling in the Southern Ocean, increases in both atmospheric temperature and CO_2 values, and glacier collapse in southern mid-latitudes. The ACR interrupted the deglacial trend of the last termination and coincided with oceanic and atmospheric reorganization in the southern hemisphere which expanded the polar realm and shifted north the main oceanic fronts and associated climatic zones.

Table 4.1 Geographical and ^{10}Be analytical data for TDP II, III, IV cosmogenic samples*.

SAMPLE ID	Lat ºS	Long ºW	Elevation (m a.s.l.)	Sample thickness (cm)	Boulder height (cm)	Shielding correction	^{10}Be ±1σ (10^4 atoms g^{-1})	^{10}Be/^{9}Be ratio ± error
TDPII moraine ridges								
LA0714	-50.9064	-72.7486	442	1.8	361.0	0.990	5.76±0.42	1.47E-14 ± 1.08E-15
LA0715	-50.9067	-72.7483	435	1.1	238.0	0.990	8.67±0.31	3.98E-14 ± 1.40E-15
LA0716	-50.9106	-72.7478	379	0.7	338.0	0.990	10.00±0.34	3.98E-14 ± 1.36E-15
LA0720	-50.9119	-72.7481	376	2.6	155.0	0.990	8.06±0.36	2.82E-14 ± 1.24E-15
SAR0718	-50.9869	-72.6919	146	3.2	176.0	0.990	6.54±0.24	3.47E-14 ± 1.29E-15
LA0732	-50.9303	-72.7283	266	1.7	245.0	1.000	11.41±0.42	2.96E-14 ± 1.10E-15
SAR0719	-50.9764	-72.6550	146	1.2	114.0	0.990	6.00±0.31	1.65E-14 ± 8.61E-16
SAR0702	-50.9903	-72.7070	261	1.1	135.0	0.999	6.97±0.20	2.70E-14 ± 7.93E-16
SAR0703	-50.9900	-72.7062	257	1.4	253.0	0.999	7.61±0.21	3.73E-14 ± 1.01E-15
SAR0705	-50.9781	-72.6861	188	1.4	284.0	1.000	6.84±0.19	3.73E-14 ± 1.02E-15
SAR0713	-50.9861	-72.7342	296	1.0	188.0	1.000	7.93±0.20	4.01E-14 ± 1.01E-15
SAR0725	-50.9919	-72.7322	312	1.9	163.0	1.000	7.79±0.21	3.75E-14 ± 1.02E-15
SAR0907	-50.9948	-72.7123	299	0.9	70.0	0.999	7.92±0.16	5.47E-14 ± 1.10E-15
LA0703	-50.8867	-72.7378	386	1.1	178.0	0.996	8.71±0.25	2.90E-14 ± 8.19E-16
LA0707	-50.8892	-72.7286	353	1.9	284.0	0.999	8.40±0.18	4.47E-14 ± 9.74E-16
LA0901	-50.8891	-72.7272	350	1.8	89.0	1.000	8.07±0.17	4.18E-14 ± 8.82E-16
RP0815	-50.9344	-72.7281	227	2.5	145.0	1.000	7.48±0.23	3.90E-14 ± 1.22E-15
RP0817	-50.9483	-72.7321	286	1.2	203.0	0.999	8.22±0.28	4.26E-14 ± 1.46E-15
RP0820	-50.9520	-72.7360	304	1.4	190.0	1.000	7.45±0.28	2.70E-14 ± 1.03E-15

Table 4.1 Geographical and ^{10}Be analytical data for TDP II, III, IV cosmogenic samples (continued)*.

SAMPLE ID	Lat ºS	Long ºW	Elevation (m a.s.l.)	Sample thickness (cm)	Boulder height (cm)	Shielding correction	^{10}Be ±1σ (10^4 atoms g^{-1})	^{10}Be/^{9}Be ratio ± error
TDPIII moraine ridges								
LA0727	-50.9058	-72.7644	350	0.7	146.0	0.990	8.44±0.32	3.53E-14 ± 1.32E-15
LA0728	-50.9033	-72.7592	364	1.0	279.0	0.990	8.04±0.30	4.08E-14 ± 1.53E-15
LA0512	-50.8896	-72.7563	465	2.5	147.0	0.998	7.15±0.34	2.26E-14 ± 1.06E-15
LA0522	-50.8968	-72.7620	423	2.0	83.0	0.990	9.19±0.77	1.52E-14 ± 1.27E-15
SAR0724	-51.0011	-72.7481	311	0.9	149.0	0.990	10.41±0.54	2.58E-14 ± 1.34E-15
LA0704	-50.8867	-72.7378	358	0.8	199.0	0.998	8.10±0.21	4.21E-14 ± 1.07E-15
SAR0701	-50.9906	-72.6971	192	1.3	89.0	0.999	4.38±0.16	3.04E-14 ± 1.12E-15
SAR0906	-50.9929	-72.7016	207	1.6	106.0	1.000	3.77±0.24	1.52E-14 ± 9.51E-16
SAR0908	-50.9975	-72.7273	307	1.4	99.0	1.000	7.83±0.32	4.81E-14 ± 1.99E-15
RP0903	-50.9436	-72.7516	234	0.7	157.0	1.000	7.30±0.19	6.28E-14 ± 1.62E-15
RP0904	-50.9469	-72.7566	245	1.1	94.0	1.000	7.38±0.32	2.30E-14 ± 9.98E-16
RP0905	-50.9482	-72.7575	245	1.2	83.0	1.000	7.23±0.34	3.09E-14 ± 1.45E-15
RP0906	-50.9536	-72.7633	266	0.9	84.0	1.000	7.58±0.20	6.38E-14 ± 1.68E-15
RP0705	-50.9203	-72.7853	441	1.3	161.0	1.000	9.10±0.26	5.94E-14 ± 1.72E-15

Table 4.1 Geographical and ^{10}Be analytical data for TDP II, III, IV cosmogenic samples (continued)*.

SAMPLE ID	Lat ºS	Long ºW	Elevation (m a.s.l.)	Sample thickness (cm)	Boulder height (cm)	Shielding correction	^{10}Be ±1σ (10^4 atoms g^{-1})	^{10}Be/^{9}Be ratio ± error
TDPIV moraine ridges								
SAR0721	-51.0019	-72.7311	242	1.0	142.0	1.000	8.08±0.33	4.99E-14 ± 2.01E-15
RP0701	-50.9097	-72.7998	375	1.2	165.0	0.999	8.19±0.21	6.78E-14 ± 1.78E-15
RP0703	-50.9225	-72.7878	404	1.2	180.0	1.000	8.46±0.28	3.61E-14 ± 1.20E-15
SAR0722	-51.0036	-72.7353	251	2.6	249.0	0.990	8.55±0.49	1.93E-14 ± 1.10E-15
SAR0723	-51.0022	-72.7547	318	2.3	158.0	0.990	7.64±0.49	1.18E-14 ± 7.54E-16
VN-05-25^	-50.9470	-72.7863	218	0.9	135.0	1.000	8.06±0.26	7.37E-14 ± 2.46E-15
VN-05-26^	-50.9489	-72.7879	204	2.8	92.0	1.000	7.71±0.22	7.18E-14 ± 2.04E-15

*All samples measured at CAMS using the 2.85^{-12} = 07KNSTD3110 standard for normalization (Nishiizumi, 2007).
VN samples= Published by Moreno *et al.* (2009) and recalculated here.

Table 4.2 ^{10}Be ages for Torres del Paine TDP II, III and IV moraines.

SAMPLE ID	Lm int ext	Du int ext	Li int ext	De int ext	Global PR* Lm int ext
TDPII moraine ridges					
LA0714	**9300 ± 680 710**	9500 ± 700 730	9300 ± 690 710	9400 ± 690 720	7900 ± 570 890
LA0715	**13900 ± 490 580**	14300 ± 510 590	14100 ± 500 570	14100 ± 500 580	11900 ± 410 1090
LA0716	**16900 ± 580 690**	17300 ± 600 700	17000 ± 590 670	17100 ± 590 690	14400 ± 490 1320
LA0720	**13800 ± 610 680**	14200 ± 630 700	14000 ± 620 670	14000 ± 620 680	11900 ± 510 1130
SAR0718	**13900 ± 520 600**	14300 ± 530 610	14000 ± 520 590	14000 ± 520 600	12000 ± 430 1110
LA0732	**21300 ± 800 920**	21800 ± 820 940	21400 ± 800 900	21500 ± 800 920	18300 ± 670 1690
SAR0719	**12600 ± 660 720**	12900 ± 680 730	12700 ± 670 710	12700 ± 670 720	10800 ± 550 1080
SAR0702	**13000 ± 380 480**	13400 ± 400 480	13100 ± 390 460	13100 ± 390 470	11100 ± 320 1000
SAR0703	**14300 ± 390 500**	14700 ± 400 500	14400 ± 390 480	14400 ± 390 490	12200 ± 330 1090
SAR0705	**13700 ± 380 480**	14000 ± 380 480	13800 ± 380 460	13800 ± 380 470	11700 ± 310 1040
SAR0713	**14300 ± 360 470**	14700 ± 370 480	14400 ± 360 460	14500 ± 370 470	12300 ± 300 1080
SAR0725	**13900 ± 380 480**	14300 ± 390 490	14100 ± 380 470	14100 ± 380 480	12000 ± 320 1060
SAR0907	**14300 ± 290 420**	14700 ± 300 430	14400 ± 290 400	14400 ± 290 420	12200 ± 240 1060
LA0703	**14600 ± 410 520**	15000 ± 420 530	14700 ± 420 500	14700 ± 420 520	12500 ± 340 1110
LA0707	**14500 ± 320 450**	14900 ± 330 450	14600 ± 320 430	14700 ± 320 440	12400 ± 270 1090
LA0901	**14000 ± 300 420**	14400 ± 300 430	14100 ± 300 400	14100 ± 300 420	12000 ± 250 1040
RP0815	**14600 ± 460 560**	14900 ± 470 570	14700 ± 460 540	14700 ± 460 550	12500 ± 380 1130
RP0817	**15000 ± 520 610**	15400 ± 530 620	15100 ± 520 600	15200 ± 520 610	12900 ± 430 1170
RP0820	**13400 ± 510 590**	13800 ± 530 600	13500 ± 520 580	13600 ± 520 590	11500 ± 430 1060

Table 4.2 ^{10}Be ages for Torres del Paine TDP II, III and IV moraines (continued).

SAMPLE ID	Lm int ext	Du int ext	Li int ext	De int ext	Global PR* Lm int ext
TDPIII moraine ridges					
LA0727	**14600 ± 550 630**	15000 ± 570 650	14800 ± 560 620	14800 ± 560 640	12500 ± 460 1160
LA0728	**13800 ± 520 600**	14200 ± 530 610	13900 ± 520 590	13900 ± 530 600	11800 ± 430 1090
LA0512	**11200 ± 530 580**	11600 ± 550 600	11300 ± 540 580	11400 ± 540 590	9600 ± 440 930
LA0522	**15000 ± 1260 1300**	15500 ± 1290 1330	15200 ± 1270 1300	15200 ± 1270 1310	12900 ± 1050 153(
SAR0724	**18700 ± 980 1060**	19200 ± 1000 1080	18800 ± 980 1050	18900 ± 990 1060	16000 ± 820 1590
LA0704	**13800 ± 350 460**	14200 ± 360 470	14000 ± 360 450	14000 ± 360 460	11900 ± 290 1050
SAR0701	**8700 ± 320 370**	9000 ± 330 380	8800 ± 320 370	8800 ± 330 370	7500 ± 270 690
SAR0906	**7400 ± 470 490**	7700 ± 480 500	7500 ± 470 490	7500 ± 470 500	6400 ± 390 670
SAR0908	**14000 ± 580 660**	14400 ± 600 670	14100 ± 590 650	14200 ± 590 660	12000 ± 490 1130
RP0903	**13900 ± 360 470**	14300 ± 370 480	14100 ± 370 460	14100 ± 370 470	11900 ± 300 1060
RP0904	**14000 ± 610 680**	14400 ± 630 690	14100 ± 610 670	14100 ± 620 680	12000 ± 510 1140
RP0905	**13700 ± 650 710**	14100 ± 670 730	13800 ± 650 710	13800 ± 650 710	11700 ± 540 1140
RP0906	**14100 ± 370 480**	14500 ± 380 490	14200 ± 370 460	14200 ± 370 480	12000 ± 310 1070
RP0705	**14400 ± 420 520**	14800 ± 430 530	14600 ± 420 510	14600 ± 420 520	12400 ± 350 1110

Table 4. 2. ^{10}Be ages for Torres del Paine TDP II, III and IV moraines (continued).

SAMPLE ID	Lm int ext	Du int ext	Li int ext	De int ext	Global PR* Lm int ext
TDPIV moraine ridges					
SAR0721	**15300 ± 620 700**	13800 ± 530 600	15500 ± 630 690	15500 ± 630 700	13100 ± 520 1230
RP0701	**13800 ± 360 470**	13801 ± 530 600	13900 ± 370 460	14000 ± 370 470	11800 ± 300 1050
RP0703	**13900 ± 460 550**	13802 ± 530 600	14000 ± 470 540	14000 ± 470 550	11900 ± 390 1080
SAR0722	**16400 ± 940 1000**	13803 ± 530 600	16500 ± 940 1000	16600 ± 950 1010	14100 ± 790 1440
SAR0723	**13800 ± 890 940**	13804 ± 530 600	13900 ± 900 930	13900 ± 900 940	11800 ± 740 1260
VN-05-25	**14100 ± 450 550**	13811 ± 530 600	14300 ± 460 540	14300 ± 460 550	12100 ± 380 1100
VN-05-26	**13900 ± 400 500**	13812 ± 530 600	14000 ± 400 490	14000 ± 400 500	11900 ± 340 1070

* Global ^{10}Be production rate as calculated in Balco *et al.* (2008) (See Appendix A - supplementary methods).
Note: ^{10}Be ages in years calculated with four different scaling protocols (Balco *et al*., 2008). 'Lm' is the time dependent version of Stone/Lal scaling scheme (Stone, 2000). 'Du' is calculated using the scaling scheme of Dunai (2001), 'Li' the scaling based on Pigati and Lifton (2004) and Lifton et al. (2008), and the 'De' scaling scheme presented in Desilets and Zedra (2003). All ages were calculated using a ^{10}Be production rate measured at New Zealand's Macaulay Site (Puatnman et al., 2010), except for last column with asterisk, which is calculated with the the "global calibration data set" (Balco et al., 2008). We use the Lm scaling scheme in our result discussion (Stone, 2000). Density of rock used for calculating ^{10}Be ages is 2.65 g cm^{-3}. Age uncertainties include internal (int) analytical error only and external error (ext), which includes systematic uncertainties (Balco *et al*., 2008) associated with scaling to the latitude and altitude of Torres del Paine region. VN samples= published by Moreno *et al.* (2009) and recalculated here.

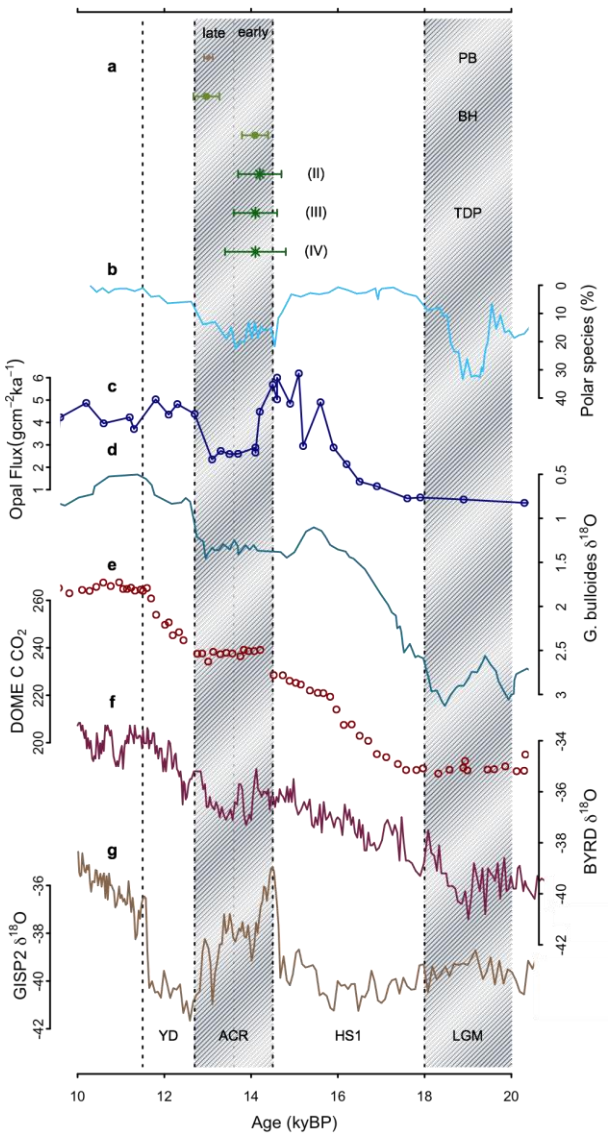

Figure 4.4. Paleoclimate deglacial records discussed in the text. **a)** ^{10}Be moraine ages from the TDP II, III, and IV moraines in Torres del Paine (this study and two ages from Moreno *et al*., 2009), the Birch Hill (BH) moraines in New Zealand (Putnam *et al*., 2010a), and radiocarbon-dated nearby Puerto Bandera moraine (PB) (Strelin and Denton, 2005). **b)** Ocean-water temperatures as inferred from polar foraminiferal species in the South Atlantic (core TNO57-21) (Barker *et al*., 2009). **c)** Southern Ocean wind-driven upwelling and southern westerly wind belt (SWW) latitudinal variation interpreted from biogenic opal flux (Anderson et al., 2009). **d)** Sea Surface Temperatures (SST) in the SE Pacific Ocean (ODP1233) inferred from *G. bulloides* δ^{18}O (Lamy *et al*., 2004). **e)** Atmospheric carbon dioxide concentrations (Monnin et al., 2001) placed on the GISP2 timescale (Marchitto *et al*., 2007). **f)** Polar atmospheric mean annual temperatures derived from the Byrd ice core δ^{18}O isotopic record (Blunier and Brook, 2001). **g)** Polar atmospheric mean annual temperatures derived from the North Atlantic GISP2 ice core δ^{18}O isotopic record (Greenland) (Stuiver *et al*., 2000).

The westerly belt most likely acted as one of the prime positive feedbacks that extended the glacial climate signal to the mid-latitudes. This wind results from the pressure gradient between the subtropical high and circum-Antarctic low pressure belts with today's strongest circulation occurring between 50-60°S. Dynamics of this wind belt may reflect either changes in the tropics, the mid-high latitudes, or both, and are rapidly transmitted to a range of latitudes in the southern hemisphere. We suggest that during the ACR, the westerly belt shifted north, driven by simultaneous changes in the southern ocean and Antarctic temperatures, and very likely in the subtropical cell, which is tied to the location of the thermal equator.

The onset of the ACR in the south coincided with the Bølling in the north and the consequent northward migration of the thermal equator and tropical rain belt (Wang *et al*., 2004; cf. Severinghaus, 2009; Cheng *et al*., 2009). The contemporaneous southern climate change throughout the ACR could be linked to the events in the North Atlantic. In this interhemispheric atmospheric see-saw model, climate shifts in the north and south occurred near-synchronously but with opposite sign, as recently suggested for Termination I (Anderson *et al*., 2009; Denton *et al*., 2010).

In summary, quasi-synchronous late-glacial climate changes described here for the southern mid-to-high latitude glaciers, Southern Ocean upwelling, Antarctic ice cores and deglacial atmospheric CO_2 imply the existence of direct cryosphere-atmosphere-ocean links, which defined the last glacial-interglacial transition in the southern mid-latitudes.

CHAPTER

5. CONCLUSIONS

- During the last glacial cycle, the Patagonian ice sheet deposited at least seven moraine belts in the Torres del Paine region: RV I, II, and III and TDP I, II, III and IV. The AG moraines likely were deposited coevally with the RV I landforms. These ice-marginal landforms resulted from glacial advances or stillstands triggered by stadial conditions between ≥50,000 and 14,000 years ago.
- Our reconstruction shows that ice was more extensive than generally thought for the last major glacial period, but smaller than proposed in some early works.
- Glacial fluctuations were accompanied by the formation of glacial paleolake Tehuelche that drained into the Atlantic Ocean. At least three main phases describe the history of this lake: Early Phase, represented by two independent lakes at 300 m a.s.l. and 420 m a.s.l., associated with the outer RV and AG moraines, respectively. Middle Phase, represented by a lake at 250-280 m a.s.l., formed during retreat from the RV III and AG moraines; and Late Phase, represented by a lake at 125-155 m a.s.l. that very likely merged with paleolake Consuelo in Última Esperanza at the end of the LGM. Paleolake Tehuelche drained by the early late glacial period.
- The Patagonian ice sheet expanded to the outer moraines in the Torres del Paine region at ~49,000 (RV I moraines), 41,000 (TDP I_{LA}), at or slightly before 16,500 (TDP I_{DT}) and at 14,200 (TDP II, III, IV) years ago during local glacial conditions

of the last ice age. At present, available data precludes defining the overall position, structure and duration of the Last Glacial Maximum (LGM) in the Torres del Paine region. Additional dating on the RV II and RV III and AG moraines should resolve this important problem.

- Data available today show that some aspects of the glaciation and deglaciation in Torres del Paine are significantly different from other sites in Patagonia and the Chilean Lake District. Particularly, the location of the late glacial moraines just proximal to moraines thought to have been deposited during and at the end of the main glacial phase is anomalous. However, this conclusion cannot be evaluated fully until the position of the LGM ice in Torres del Paine has been completely documented.
- The Patagonian ice sheet in the Torres del Paine region reached its maximum extent during MIS 3, possibly associated with the southern westerly wind belt centered close to this latitude.
- The Patagonian ice sheet expanded to the TDP II, III and IV moraines between 14,200 and 12,600 ka. These dates afford direct moraine-based evidence for the duration of the Antarctic Cold Reversal (ACR) in the southern mid-latitudes, as recorded by glaciers.
- During a good portion of the last glacial period, the Patagonian ice sheet snout fluctuated near the same position at Laguna Azul, where the ACR moraines are located just inside the 41 ka moraines.
- Southern mid-latitude glacier expansions during the last glacial cycle occurred irrespective of the insolation phase. Millennial-scale stadial conditions in the

southern hemisphere during MIS 3 and the ACR suggest oceanic and atmospheric reorganizations that prompted near simultaneous hemispheric-wide climate changes. Northern shifts of the Antarctic Frontal Zone, Subtropical Zone and particularly the southern westerly wind belt may have played a key role in expanding the Antarctic glacial climate into the southern middle latitudes and in driving near-simultaneous changes in the southern hemisphere during stadials of the last glacial period.

REFERENCES

Ackert Jr., R.P., Singer, B.S., Guillou, H., Kaplan, M.R, Kurza, M.D., 2003. Long-term cosmogenic 3He production rates from 40Ar/39Ar and K-Ar dated Patagonian lava flows at 47ºS. Earth and Planetary Science Letters 210 119-136

Ackert, Robert P., Becker, R.A., Singer, B.S., Kurz, M.D., Caffee, M.W., Mickelson, D.M., 2008. Patagonian Glacier Response During the Late Glacial-Holocene Transition. Science 321, 392-395.

Adem, J. 1964. On the physical basis for the numerical prediction of monthly and seasonal temperatures in the troposphere-ocean-continent system. Monthly Weather Review, 92, 3, 91-103.

Alley, R.B, Brook, E.J., Anandakrishnan, S., 2002. A northern lead in the orbital band: north–south phasing of Ice-Age events. Quaternary Science Reviews 21, 431–441.

Almond, P.C., Moar, N.T., Lian, O.B., 2001. Reinterpretation of the glacial chronology of South Westland, New Zealand. New Zealand Journal of Geology and Geophysics 44, 1-15.

Anderson, R.F., Ali, S., Bradtmiller, L.I., Nielsen S.H.H., Fleisher, M.Q., Anderson, B.E., Burckle, L.H., 2009. Wind-Driven Upwelling in the Southern Ocean and the Deglacial Rise in Atmospheric CO_2. Science 323, 1443-1448.

Aniya, M. and Wakao, Y., 1997. Glacier variations of Hielo Patagónico Norte, Chile, between 1944/45 and 1995/95. Bulletin of Glacier Research, 15, 11-18.

Aniya, M., Sato, H. , Naruse, R., Skvarca, P., Cassasa, G., 1996. Remote sensing application to inventorying glaciers in a large, remote area-Southern Patagonia Icefield. Photogrammetric Engineering and Remote Sensing, 62, 1361-1369.

Balco, G., Stone, J., Porter, S., Caffee, M., 2002. Cosmogenic-nuclide ages for New England coastal moraines, Martha's Vineyard and Cape Cod, Massachusetts, USA. Quaternary Science Reviews 21, 2127–2135.

Balco, G., Briner, J., Finkel, R., Rayburn, J., Ridge, J., Schaefer, J., 2009. Regional beryllium-10 production rate calibration for late-glacial northeastern North America. Quaternary Geochronology 4, 93-107.

Balco, G., Stone, J.O., Lifton, N.A., Dunai, T.J., 2008. A complete and easily accessible means of calculating surface exposure ages or erosion rates from Be-10 and Al- 26 measurements. Quaternary Geochronology 3, 174–195.

Barker, S., Diz, P., Vautravers M.J., Pike, J., Knorr, G., Hall, I.R., Broecker, W.S., 2009. Interhemispheric Atlantic seesaw response during the last deglaciation. Nature 457, 1097-1103.

Barrows, T.T., Stone, J.O., Fifield, L.K., Cresswell, R.G., 2001. Late Pleistocene Glaciation of the Kosciusko Massif, Snowy Mountains, Australia. Quaternary Research 55, 179-189.

Barrows, T.T., Stone, J.O., Fifield, L.K., Creswell, R.G., 2002. The timing of the Last Glacial maximum in Australia. Quaternary Science Reviews 21, 159-173.

Benn D.I. and Clapperton, C.M., 2000. Pleistocene glacitectonic landforms and sediments around central Magellan Strait, southernmost Chile: evidence for fast outlet glaciers with cold-based margins. Quaternary Science Reviews 19, 591-612.

Bennett, K.D., Haberle, S.G., and Lumley, S.H., 2000. The last glacial–Holocene transition in southern Chile: Science, v. 290, p. 325–328, doi: 10.1126/science.290.5490.325.

Berger, A. and Loutre, M.F. 1991. Insolation values for the climate of the last 10 million years. Quaternary Science Reviews 10: 297-317.

Bianchi, C. and Gersonde, R., 2004. Climate evolution at the last deglaciation: the role of the Southern Ocean. Earth and Planetary Science Letters 228, 407-424.

Blunier, T. and Brook, E. J., 2001.Timing of millennial-scale climate change in Antarctica and Greenland during the last glacial period. Science 291, 109–112.

Boulton G.S and Jones, A.S., 1979. Stability of Temperate ice caps and ice sheets resting on beds of deformable sediment. Journal of Glaciology 24, 29-43.

Brauer, A., Haug, G.H., Dulski, P., Sigman, D.M., Negendank, J.F.W., 2008. An abrupt wind shift in western Europe at the onset of the Younger Dryas cold period. Nature Geoscience 1, 520-523.

Briner, J.P., Miller, G.H., Davis, T.R., Finkel, R., 2005. Cosmogenic exposure dating in arctic glacial landscapes: implications for the glacial history of northeastern Baffin Island, Arctic Canada. Canadian Journal of Earth Sciences 42, 67–84.

Broccoli, A.J. and Manabe, S., 1987. The influence of continental ice, atmospheric CO2, and land albedo on the climate of the last glacial maximum. Climate Dynamics 1, 87-99

Broecker, W., 1978. The cause of glacial to interglacial climate change, in Evolution of Planetary Atmospheres and Climatology of the Earth, pp. 165-190, Centre National d'Etudes Spatiales (France).

Broecker, W. S., and Denton G. H., 1989. The role of ocean atmosphere reorganizations in glacial cycles, Geochim. Cosmochim. Acta, 53, 2465–2501.

Broecker, W., 1998. Paleocean circulation during the last deglaciation: A bipolar seesaw? Paleoceanography, vol.13, 2, 119-121.

Caldenius, C.C., 1932. Las glaciaciones Cuaternarias en la Patagonia y Tierra del Fuego. Geografiska Annaler 14, 1–164.

Carrasco, J. F., Cassasa, G., Rivera, A., Aniya, M., Naruse, R., 2002. Meteorological and climatological aspects of the Southern Patagonia Icefield. In Cassasa, G. and Casassa, G., Sepúlveda, F. V., Sinclair, R. M.(eds.) *The Patagonian Icefields* (Kluwer Academic/Plenum Publishers, New York)

Cassasa, G., Rivera, A., Aniya, M., Naruse, R., 2002. Current knowledge of the Southern Patagonia Icefield. In Cassasa, G. and Casassa, G., Sepúlveda, F. V., Sinclair, R. M.(eds.) *The Patagonian Icefields* (Kluwer Academic/Plenum Publishers, New York).

Cerveny, R,, V, 1998. Present climates of South America. In Hobbs, J. E., Lindesay, J. A and Bridgman H. A., Climates of the southern continents: present, past, and future. (Wiley, Baffins Lane, 1998).

Cheng, H., Edwards, R.L., Broecker, W.S., Denton, W.H., Kong, X., Wang, Y., Zhang, R., Wang, X., 2009. Ice age terminations. Science 326, 248-252.

Clapperton, C.M. 1993. Quaternary Geology and Geomorphology of South America. Elsevier: Amsterdam.

Clapperton, C.M., 2000: Interhemispheric synchroneity of Marine Oxygen Isotope Stage 2 glacier fluctuations along the American cordilleras transect. Journal of Quaternary Science, 13, 435–468.

Clark P., Alley, R.B., Pollard, D., 1999. Northern Hemisphere Ice-Sheet Influences on Global Climate Change. Science 286, 1104-1111.

Clark, P.U., Dyke, A.S., Shakun, J.D., Carlson, A.E., Clark, J., Wohlfarth B., Mitrovica, J.X., Hostetler S.W., McCabe, A.M., 2009. The Last Glacial Maximum. Science, 325, 710-714

Dansgaard, W., White, J.W.C., Johnsen, S.J., 1989. The abrupt termination of the Younger Dryas climate event. Nature 339, 532-534.

Denton, G. and Hughes, T., 1981. The last great ice sheets. Wiley-Interscience. New York.

Denton, G.H., Heusser, C.J., Lowell, T.V., Moreno, P.I. Andersen, B.G., Heusser, L.E., Schlüchter, C. and Marchant, D.R., 1999a. Interhemispheric linkage of paleoclimate during the last glaciation. Geografiska Annaler, 81A 107–153.

Denton, G.H., Lowell, T.V., Heusser, C.J., Schlüchter, C., Andersen, B.G., Heusser, L..E., Moreno, P.I. and Marchant D.R., 1999b: Geomorphology, stratigraphy, and radiocarbon chronology of Llanquihue drift in the area of the southern Lake District, Seno Reloncaví and Isla Grande de Chiloé, Chile. Geografiska Annaler, 81A:167–229.

Denton, G.H., Alley, R.B., Comer, G.C., and Broecker, W.S., 2005. The role of seasonality in abrupt climate change: Quaternary Science Reviews 24, 1159–1182.

Denton, G. H., Anderson, R. F., Toggweiler, J. R., Edwards, R. L., Schaefer, J. M., Putnam, A. E., 2010. The Last Glacial Termination. Science 328, 1652-1656.

Desilets, D. and Zreda, M., 2003. Spatial and temporal distribution of secondary cosmic-ray nucleon intensities and applications to in-situ cosmogenic dating. Earth and Planet. Sci. Lett. 206, 21- 42.

Doughty, A.M., 2008. ^{10}Be cosmogenic exposure ages of late pleistocene moraines near the Maryburn Gap of the Pukaki Basin, New Zealand. Unpublished Thesis (M. S).

Douglass, D.C., Singer, B.S., Kaplan, M.R., Mickelson, D.M., Caffee, M.W., 2006. Cosmogenic nuclide surface exposure dating of boulders on last-glacial and late-glacial moraines, Lago Buenos Aires, Argentina: interpretive strategies and paleoclimate implications. Quat. Geochronol. 1, 43–58.

Douglass, Daniel C., 2005. Glacial chronology, soil development, and paleoclimate reconstructions for mid-latitude South America, 1 Ma to recent. Ph.D. thesis, University of Wisconsin.

Douglass, D.C., Singer, B.S., Kaplan, M.R., Mickelson, D.M., Caffee, M.W., 2006. Cosmogenic nuclide surface exposure dating of boulders on last-glacial and late glacial moraines, Lago Buenos Aires, Argentina: interpretive strategies and paleoclimate implications. Quat. Geochronol. 1, 43–58.

Dunai, T. J., 2001. Influence of secular variation of the magnetic field on production rates of in situ produced cosmogenic nuclides. Earth and Planet. Sci. Lett. 193, 197-212.

EPICA community members, 2004. Eight glacial cycles from an Antarctic ice core. Nature 429, 623–628.

EPICA Community Members, 2006. One-to-one coupling of glacial climate variability in Greenland and Antarctica. Nature 444, 195-198.

Evans, D.J.A., 2003. Glacial Landsystems. Arnold. London. 531 p.

Fairbanks, G. R., Mortlock, A., Chiu, T.C., Cao, L., Kaplan, A., Guilderson, T.P., Fairbanks, T.W., Bloom, A.L., 2005. Marine Radiocarbon Calibration Curve Spanning 0 to 50,000 Years B.P. Based on Paired 230Th/234U/238U and 14C Dates on Pristine Corals. Quaternary Science Reviews 24, 1781-1796.

Faure, G., and Mensing, T.M., 2005. *Isotopes Principles and Applications.* Third Edition. Wiley Editions, USA. 897pp.

Fergusson, T. H., 1961. Rules for rejection of outliers. Revue Inst. Int. de Stat. 3, 29-43.

Fogwill, C. J. and Kubik, P. W., 2005. A glacial stage spanning the Antarctic Cold Reversal in Torres del Paine (51ºS), Chile, based on preliminary cosmogenic exposure dating. Geografiska Annaler, 87A(2), 403-408.

Furbish D.J. and Andrews, J.T., 1984. The use of hypsometry to indicate long term stability and response of valley glaciers to changes in mass transfer. Journal of Glaciology 30, 99–211.

Ganopolski, A., Rahmstorf, S., Petoukhov, V., Claussen, M., 1998. Simulation of modern and glacial climates with a coupled global model of intermediate complexity. Nature 391, 351-356.

Garreaud, R.D., 2007. Precipitation and Circulation Covariability in the Extratropics. Journal of Climate 20, 4789-4797.

Gersonde, R., Abelmann, A., Brathauer, U., Becquey, S., Bianchi, C., Cortese, G., Grobe, H., Kuhn, G., Niebler, H.-S., Segl, M., Sieger, R., Zielinski, U., Futterer, D.K., 2003a. Last glacial sea-surface temperatures and sea-ice extent in the Southern Ocean (Atlantic–Indian sector)—A multiproxy approach. Paleoceanography 18 (3), 1061 doi:1029/2002PA000809.

Glasser, N.F., Jansson, K., Harrison, S., Kleman, J., 2008. The glacial geomorphology and Pleistocene history of southern South America between 38 S and 56 S. Quaternary Science Reviews 27, 365–390.

Glasser, N.F., Harrison S., Jansson. K.N., 2009. Topographic controls on glacier sediment–landform associations around the temperate North Patagonian Icefield. Quaternary Science Reviews 28, 2817-2832.

Grubbs, F. E., 1969 Procedures for detecting outlying observations in samples. Technometrics 11, 1-21.

Guilderson T.P., Hajdas I., Heaton T.J., Hogg A.G., Hughen K.A., Kaiser K.F., Kromer B., McCormac F.G., Manning S.W., Reimer R.W., Richards D.A., Southon J.R., Talamo S., Turney C.S.M., J. van der Plicht, C.E. Weyhenmeyer, (2009). IntCal09 and Marine09 radiocarbon age calibration curves, 0–50,000 years cal BP. Radiocarbon 51(4), 1111–50.

Hall, B.L., Denton, G.H., Fountain, A. G., Hendy, C.H., Hernderson, G.M., 2010. Antarctic lakes suggest millennial reorganizations of Southern Hemisphere atmospheric and ocean circulation. PNAS 107 (50), 21355-21359.

Hall, B., Porter, C., Denton, G., Lowell, T., Bromley, G. Deglaciation of Cordillera Darwin, southern Chile, during the last termination. In prep.

Hauthal, Wilckens, Paulcke, 1905. Die obere Kreide Südpatagoniens und ihre Fauna. Ber. d. Naturf. Ges. zu Freiburg i. Br. 15. p. 91.

Hays J.D and Morley, J.J., 2003. The Sea of Okhotsk: A Window on the Ice Age. Ocean Deep-Sea Research I 50, 1481–1506.

Hays, J., Imbrie, J., Shackleton, N., 1976. Variations in the Earth's orbit: Pacemaker of the ice ages. Science 194, 1121–1132.

Hein, A.S., Hulton, N.R.J., Dunai, T.J., Schnabel, C., Kaplan, M.R., Naylor, M., Xu, S., 2009. Middle Pleistocene glaciation in Patagonia dated by cosmogenic-nuclide measurements on outwash gravels. Earth Planet. Sci. Lett. 286, 184–197.

Hein, A.S., Hulton, N.R.J., Dunai, T.J., Kaplan, M.R., Sugden, D., Xu, S., 2010. The chronology of the Last Glacial Maximum and deglacial events in central Argentine Patagonia. Quaternary Science Reviews, 29, 1212– 1227.

Heusser, C. J. et al., 1989. Southern westerlies during the last glacial maximum. Quaternary Research 31, 423-425.

Heusser, C. J., 1993. Late-glacial of southern South America. Quaternary Science Reviews 12, 345–350.

Heusser, C. J., 1998. Deglacial paleoclimate of the American sector of the Southern Ocean: Late Glacial–Holocene records from the latitude of Canal Beagle (55°S), Argentine Tierra del Fuego. Palaeogeography, Palaeoclimatology, Palaeoecology 141, 277–301.

Heusser, C.J., Heusser, L., Lowell, T.V., Moreira, A., Moreira, S., 2000. Deglacial Palaeoclimate at Puerto del Hambre, subantarctic Patagonia, Chile. Journal of Quaternary Science 15 (2) 101–114.

Heusser, C. J., 2003. Ice Age Southern Andes A Chronicle of Paleoecological Events. (Elsevier, Amsterdam).

Hobbs, J. E., Lindesay, J. A and Bridgman H. A. Climates of the southern continents: present, past, and future. (Wiley, Baffins Lane, 1998).

Horvath, A., 1997. La definición de Límites o el Límite a la Indolencia. Eds. Cruz del Sur de la Trapananda, Coyhaique, pp. 131.

Huybers, P. and Wunsch, C., 2005. Obliquity pacing of the late Pleistocene glacial terminations. Nature, 434, 491-494.

Huybers, P. 2006. Early Pleistocene glacial cycles and the integrated summer insolation forcing. Science 513, 508-511.

Imbrie, J., Boyle, E.A., Clemens, S.C., Duffy, A., Howard, W.R., Kukla, G., Kutzbach, J., Martinson, D.G., McIntyre, A., Mix, A.C., Molfino, B., Morley, J.J., Peterson, L.C., Pisias, N.G., Prell, W.L., Raymo, M.E., Shackleton, N.J., Toggweiler, J.R., 1992. On the structure and origin of major glaciation cycles: 1: Linear responses to Milankovitch forcing. Paleoceanography 7, 701–738.

Imbrie, J., Berger, A., Boyle, E.A., Clemens, S.C., Duffy, A., Howard, W.R., Kukla, G., Kutzbach, J., Martinson, D.G., McIntyre, A., Mix, A.C., Molfino, B., Morley, J.J., Peterson, L.C., Pisias, N.G., Prell, W.L., Raymo, M.E., Shackleton, N.J., Toggweiler, J.R., 1993. On the structure and origin of major glaciation cycles: 2. The 100,000-year cycle. Paleoceanography 8, 699–735.

Ivins, E. R. & James, T. S., 1999. Simple models for late Holocene and present-day Patagonian glacier fluctuations and predictions of a geodetically detectable isostatic response. Geophysics Journal International 138: 601-624.

Jackson, L.E., Phillips, F.M., Little, E.C., 1999. Cosmogenic 36Cl dating of the maximum limit of the Laurentide Ice Sheet in southwestern Alberta. Canadian Journal of Earth Sciences 36 (8), 1347–1356.

Jouzel, J., Masson-Delmotte, V., Cattani, O., Dreyfus, G., Falourd, S., Hoffmann, G., Minster, B., Nouet, J., M. Barnola, J., Chappellaz, J., Fischer, H., Gallet, J.C., Johnsen, S., Leuenberger, M., Loulergue, L., Luethi, D., Oerter, H., Parrenin, F., Raisbeck, G., Raynaud, D., Schilt, A., Schwander J., Selmo, E., Souchez, R., Spahni, R., Stauffer, B., Steffensen, J.P., Stenni, B.T., Stocker, F., Tison, J.L., Werner, M. 11, Wolff, E.W., 2007. Orbital and millennial Antarctic variability over the last 800000 years. Science 317, 793-796.

Johnson, R. G. and McClure, B. T. A, 1976. A model for Northern Hemisphere continental ice sheet variation. Quat. Res. 6, 325–355.

Kaiser, J., Lamy, F., Hebbeln, D., 2005. A 70-kyr sea surface temperature record off southern Chile (Ocean Drilling Program Site 1233). Paleoceanography 20 PA4009, doi:10.1029/2005PA001146.

Kaplan, M.R., Strelin, J., Schaefer, J.M, Denton, G.H., Finkel, R.C, Schwartz, R., Vandergoes, M., Putnam, A.E. The 10Be production rate in southern South America and the coherency of late glacial chronologies. Accepted in Earth and Planetary Science Letters, pending minor revisions.

Kaplan, M. R., Ackert, R. P., Singer, B. S., Douglass, D. C., Kurz, M. D., 2004. Cosmogenic nuclide chronology of millennial-scale glacial advances during O-isotope Stage 2 in Patagonia. Geological Society of America Bulletin 116, 308–321.

Kaplan, M. R., Douglass, D. C., Singer, B. S., Ackert, R. P., Caffee. M. W., 2005. Cosmogenic nuclide chronology of pre-last glacial maximum moraines at Lago Buenos Aires, 46ºS, Argentina. Quaternary Research 63, 301–315.

Kaplan, M.R., Hulton, N.R.J., Coronato, A., Rabassa, J.O., Stone, J.O., Kubik, P.W., Freeman, S., 2007. Cosmogenic nuclide measurements in southernmost South America and implications for landscape change. Geomorphology 87, 284–301.

Kaplan, M. R., Moreno, P. I. and Rojas, M., 2008. Glacial dynamics in southernmost South America during Marine Isotope Stage 5e to the Younger Dryas chron: a brief review with a focus on cosmogenic nuclide measurements. Journal of Quaternary Science 23, 649-658.

Kaplan, M.R., Fogwill, C.J., Sugden, D.E., Hulton, N., Kubik, P.W., Freeman, S., 2008. Southern Patagonian glacial chronology for the Last Glacial period and implications for Southern Ocean climate. Quat. Sci. Rev. 27, 284–294.

Kaplan, M. R., Schaefer, J.M., Denton, G.H., Barrell, D.J.A., Chinn, T.J.H., Putnam, A.E, Andersen, B.G., Finkel, R.C., Schwartz, R., Doughty, A., 2010. Glacier retreat in New Zealand during the Younger Dryas Stadial. Nature 467, 194-197.

Kawamura, K., Parrenin, F., Lisiecki, L., Uemura, R., Vimeux, F., Severinghaus, J.P., Hutterli, M.A., Nakazawa, T., Aoki, S., Jouzel, J., Raymo, M.E., Matsumoto, K., Nakata, H., Motoyama, H., Fujita, S., Goto-Azuma, K., Fujii, Y., Watanabe, O., 2007. Northern Hemisphere forcing of climatic cycles in Antarctica over the past 360,000 years, Nature, 448, 912-916.

Kelly, M.A., Lowell, T.V., Hall, B.L., Schaefer J.M., Finkel , R.C., Goehring, B.M, Alley, R.B., Denton, G.H., 2008. A 10Be chronology of lateglacial and Holocene mountain glaciation in the Scoresby Sund region, east Greenland: implications for seasonality during lateglacial time. Quaternary Science Reviews 27, 2273–2282.

Kelley, S.E., 2009.¹°Be surface-exposure chronology of the left-lateral moraines of the former Pukaki glacier lobe in the Mackenzie Region, South Island, New Zealand. Unpublished Thesis (M.S.).

Kerr, A. and Sugden, D.E., 1994.The sensitivity of the south Chilean snowline to climatic change. Climatic Change 28, 255–272.

Knorr, G. and Lohmann, G., 2003. Southern Ocean origin for the resumption of Atlantic thermohaline circulation during deglaciation. Nature 424, 532-536

Kukla, G. J., 1975. The missing link of Milankovitch and Climate. Nature 253, 600–603.

Lamy, F., Kaiser, J., Ninnemann, U., Hebbeln, D., Arz, H.W., Stoner, J., 2004. Antarctic Timing of Surface Water Changes off Chile and Patagonian Ice Sheet Response. Science 304, 1959-1962.

Lamy, F., Kilian, R., Arz, H.G., Francois, J.P., Kaiser, J., Prange, M., Steinke, T., 2010. Holocene changes in the position and intensity of the southern westerly wind belt. Nature Geoscience 3, 695-699.

Lemieux-Dudon B., Blayo E., Petit J.-R., Waelbroeck C., Svensson A., Ritz C., Barnola J.-M., Narcisi B., Parrenin F., 2010. Consistent dating for Antarctic and Greenland ice cores. Quaternary Science Reviews 29, 8-20.

Licciardi, J. M., 2000. PhD, Alpine glacier and pluvial lake records of late Pleistocene climate variability in the western United States. Oregon State University.

Lifton, N., Smart, D. and Shea, M., 2008. Scaling time-integrated in situ cosmogenic nuclide production rates using a continuous geomagnetic model. Earth and Planet. Sci. Lett. 268, 190-201.

Lisiecki, L. Raymo, M.E., 2005. A Pliocene-Pleistocene stack of 57 globally distributed benthic D18O records. Paleoceanography 20, PA1003.

Long, A., Martin, P.S., 1974. Death of American ground sloths. Science 186, 638–640.

Lowell, T. Waterson, N., Fisher, T., Loope, H., Glover, K., Comer, G., Hajdas, I., Denton. G., Schaefer, J., Rinterknecht, V., Broecker, W., Teller, J., 2005. Testing the Lake Agassiz Meltwater Trigger for the Younger Dryas. Eos Trans. AGU, 86(40), 365

Luebert, F. and Pliscoff, P., 2006: Sinopsis bioclimática y vegetacional de Chile. Editorial Universitaria, Santiago, Chile. 316 p.

Lumley, S. H. & Switsur, R., 1993. Late Quaternary chronology of the Taitao Peninsula, Southern Chile. Journal of Quaternary Science 8, 161–165.

Lüthi, D., Floch, M. Le, Bereiter, B., Blunier, T., Barnola, J.M, Siegenthaler, U., Raynaud, D., Jouzel, J., Fischer, H., Kawamura, K., Stocker, T.F., 2008. High-resolution carbon dioxide concentration record 650,000-800,000 years before present.Nature 453, 379-382.

Mackintosh A, Dugmore A, Hubbard A. 2002. Holocene climatic changes in Iceland: evidence from modelling glacier length fluctuations at Sólheimajökull. Quaternary International 91, 39–52.

Mackintosh, A.N., Barrows, T.T., Colhoun, E.A., Fifield, L.K., 2006. Exposure dating and glacial reconstruction at Mt Field, Tasmania, Australia, identifies MIS 3 and MIS 2 glacial advances and climatic variability. Journal of Quaternary Science 21, 363-376.

Marchitto, T. M., Lehman, S. J., Ortiz, J. D., Flückiger, J., van Geen, A., 2007. Marine Radiocarbon Evidence for the Mechanism of Deglacial Atmospheric CO2 Rise. Science 316, 1456-1459.

Marden, C. J., 1993. Late Quaternary glacial history of the South Patagonia Icefield at Torres del Paine, Chile. Unpublished Ph.D. Thesis, University of Aberdeen, 298 pp.

Marden C. J. & Clapperton, C. M., 1995. Fluctuations of the South Patagonian Icefield during the last glaciation and the Holocene. Journal of Quaternary Science 10, 197-210.

Marden, C. J., 1997. Late-glacial fluctuations of South Patagonian Icefield, Torres del Paine National Park, southern Chile. Quaternary International 38/39, 61-68.

Markgraf, V., 1991. Younger Dryas in southern South America? Boreas, 20, 63–69.

Markgraf, V, 1998. Past climates of South America. In Hobbs, J. E., Lindesay, J. A and Bridgman H. A., Climates of the southern continents: present, past, and future. (Wiley, Baffins Lane).

McCulloch, R.D., Bentley, M.J., Purves, R.S., Hulton, Sugden, D.E., Clapperton, C.M., 2000. Climatic inferences from glacial and palaeoecological evidence at the last glacial termination, southern South America. Journal of Quaternary Science 15, 409–417.

McCulloch, R.D., Davies, S.J., 2001. Late-glacial and Holocene palaeoenvironmental change in the central Strait of Magellan, southern Patagonia. Palaeogeogr. Palaeoclimatol. Palaeoecol. 173, 143–173.

McCulloch, R.D., Bentley, M.J., Tipping, R.M. and Clapperton, C.M. 2005: Evidence for late-glacial ice-dammed lakes in the central Strait of Magellan and Bahía Inútil, southernmost South America. Geografiska Annaler, 87 A (2): 335–362.

McCulloch, R.D., Fogwill, C.J., Sugden, D., Bentley, M.J., Kubik, P.W., 2005 Chronology of the last glaciation in central Strait of Magellan and Bahía Inútil, southernmost South America. Geografiska Annaler, Series A- Physical Geography 87, 289–312.

Meglioli A., 1992. Glacial geology and chronology of Southernmost Patagonia and Tierra del Fuego, Argentina and Chile. Phd Thesis Thesis, Lehigh University, Pennsylvania, 215 pp.

Mercer, J. H., 1976. Glacial history in southernmost South America. Quaternary Research 6, 125-166.

Mercer, J. H., 1984. Simultaneous climatic change in both hemispheres and similar bipolar interglacial warming: evidence and implications. In Ewing, M. (ed.) Climate Processes and Climate Sensitivity, vol. Geophysical Monograph 29, 307–313 (American Geophysical Union, 1984).

Mesolella, K. J., R. K. Matthews, W. S. Broecker, D. L. Thurber, 1969. J. Geol. 77, 250.

Milankovitch, M. (1941), Kanon der Erdbestrahlung und seine Andwendung auf das Eiszeiten-problem, R. Serbian Acad., Belgrade.

Miller, A., 1976. The climate of Chile. In: Schwerdtfeger, W. (Ed.), Climates of Central and SouthAmerica, vol.12. Amsterdam Elsevier, (World Survey of Climatology), pp. 113–145.

Mix, A.C., Bard, E., Schneider, R., 2001. Environmental processes of the ice age: land, ocean, glaciers (EPILOG). Quaternary Science Reviews 20, 627–657.

Monnin, E, Indermühle, A., Dällenbach, A., Flückiger, J., Stauffer, B., Stocker, T.F., Raynaud, D., Barnola, J.M., . 2001. Atmospheric CO2 Concentrations over the Last Glacial Termination. Science 291, 112-114.

Moreno, P.I., Lowell, T.V., Jacobson, G.L., Jr. and Denton, G.H., 1999: Abrupt vegetation and climate changes during the last glacial maximum and last termination in the Chilean Lake District: A case study from Canal de la Puntilla (41ºS). Geografiska Annaler, 81A:285-311.

Moreno, P.I., Jacobson, G.L., Lowell, T.V., and Denton, G.H., 2001, Interhemispheric climate links revealed by a late-glacial cooling episode in southern Chile: Nature, v. 409, p. 804–808

Moreno, P.I, Kaplan, M.R., François, J.P., Villa-Martínez, R. Moy, C.M, Stern, C.R., Kubik, P.W., 2009. Renewed glacial activity during the Antarctic cold reversal and persistence of cold conditions until 11.5 ka in southwestern Patagonia. Geology 37, 375-378.

Nishiizumi, K., Imamura, M., Caffee, M.W., Southon, J.R., Finkel, R.C., McAninch, J., 2007. Absolute calibration of Be-10 AMS standards. Nuclear Instrum. Methods Phys. Res. Sect. B 258, 403–413.

Nordenskjöld, O. 1898. Über die Posttertiären Ablagerungen der Magellansländer etc. Svenska expedition till Magellansländerna, Bd 1, No 2. Stockholm.

North Greenland Ice Core Project members. 2004.High-resolution record of Northern Hemisphere climate extending into the last interglacial period. Nature 431, 147-151.

Oerlemans J. 1989. On the response of valley glaciers to climatic change. In Glacier Fluctuations and Climatic Change, Oerlemans J (ed). Kluwer: Dordrecht; 407–417.

Oerlemans, J., and Fortuin, J.P.F., 1992. Sensitivity of glaciers and small ice caps to greenhouse warming: Science, v. 258, p. 115–117.

Peterson, L. C. et al., 2000. Rapid Changes in the Hydrologic Cycle of the Tropical Atlantic During the Last Glacial. Science 290, 1947-1951.

Pigati, J. S. and Lifton, N. A., 2004. Geomagnetic effects on time-integrated cosmogenic nuclide production with emphasis on in situ 14C and 10Be. Earth and Planet. Sci. Lett. 226, 193-205.

Putnam, A., Schaefer, J., Barrell, D.J.A., Vandergoes, M., Denton, G.H., Kaplan, M., Finkel, R.C., Schwartz, R., Goehring, B.M., Kelley, S., 2010b. In situ cosmogenic ^{10}Be production-rate calibration from the Southern Alps, New Zealand. Quaternary Geochronology 5, 392–409.

Putnam, A.E., Denton, G.H., Schaefer, J.M., Barrell, D.J.A, Andersen, B.G., Finkel, R.C., Schwartz, R., Doughty, A.M., Kaplan, M.R., Schlüchter, C., 2010. Glacier advance in southern middle-latitudes during the Antarctic Cold Reversal. Nature Geoscience 3, 700-704.

Raymo, M. E., 1997. The timing of the major terminations. Paleoceanography 12(4) 577-585.

Raymo M.E. and K. Nisancioglu, 2003. The 41 kyr world: Milankovitch's other unsolved mystery. Paleoceanography, vol 18 (1) 1011.

Reimer, P.J., Baillie, M.G.L., Bard ,E., Bayliss, A., Beck, J.W., Blackwell, P.G., Bronk Ramsey, C., Buck, C.E., Burr, G.S., Edwards, R.L., Friedrich, M., Grootes, P.M., Guilderson, T.P., Hajdas, I., Heaton, T.J., Hogg. A.G., Hughen, K.A., Kaiser, K.F., Kromer, B., McCormac, F.G., Manning, S.W., Reimer, R.W., Richards, D.A., Southon, J.R., Talamo, S., Turney, C.S.M., Van der Plicht, J., Weyhenmeyer , C.E., 2009. IntCal09 and Marine09 radiocarbon age calibration curves, 0–50,000 years cal BP. Radiocarbon 51(4), 1111–1150.

Roe, G. 2006. In defense of Milankovitch, Geophys. Res. Lett., 33, L24703, doi:10.1029/2006GL027817.

Rojas, M., Moreno, P.I., Kageyama, M., Crucifix, M., Hewitt, C., Abe-Ouchi, A., Ohgaito, R., Brady, E.C., Hope, P., 2009. The Southern Westerlies during the last glacial maximum in PMIP2 simulations. Climate Dynamics 32, 525–548.

Röthlisberger, R., R. Mulvaney, E. W. Wolff, M. A. Hutterli, M. Bigler, S. Sommer, and J. Jouzel (2002), Dust and sea-salt variability in central East Antarctica (Dome C) over the last 45 kyrs and its implications for southern high-latitude climate, Geophys. Res. Lett., 29(20), 1963, doi:10.1029/2002GL015186.

Sagredo, E. A., Moreno, P. I., Villa-Martinez R., Kaplan, M. R., Kubik, P. W., Stern, C. R., 2011. Fluctuations of the Ultima Esperanza ice lobe (52ºS), Chilean Patagonia, during the last glacial maximum and termination 1. Geomorphology, 125, 92-108.

Saxon, E. 1976 La prehistoria de Fuego-Patagonia: colonización de un hábitat marginal. Anales del Instituto de la Patagonia 7: 63-73.

Schaefer, J.M., Denton, G.H., Barrell, D.J.A., Ivy-Ochs, S., Kubik, P.W., Andersen, B.G.,Phillips, F.M., Lowell, T.V., Schlüchter, C., 2006. Near-synchronous interhemispheric termination of the Last Glacial maximum in mid-latitudes. Science 312, 1510-1513.

Schaefer, J. M. Denton, G.H., Kaplan, M.R., Putnam, A., Finkel, R.C., Barrell, J.A., Andersen, B.G., Schwartz, R., Mackintosh, A., Chinn, T., Schlüchter, C., 2009. High-frequency Holocene glacier fluctuations in New Zealand differ from the northern signature. Science 324, 622–625.

Severinghaus, J.P., Sowers, T., Brook, E.J., Alley, R.B., Bender, M.L., 1998. Timing of abrupt climate change at the end of the Younger Dryas interval from thermally fractionated gases in polar ice. Nature 391, 141–146.

Severinghaus, J. P., 2009. Monsoons and Meltdowns. Science 326, 240-241.

Shaw and Donn, 1968. Milanckovitch radiation variations: A quantitative Evaluation. Science, 162, 1270-1272.

Shulmeister, J., Thackray, G.D., Rieser, U., Hyatt, O.M., Rother, H., Smart C.C., Evans, D.J.A., 2010. The stratigraphy, timing and climatic implications of glaciolacustrine deposits in the middle Rakaia Valley, South Island, New Zealand. Quaternary Science Reviews 29, 2362-2381.

Sigman, D. and Boyle, E., 2001. Palaeoceanography: Antarctic stratification and glacial CO2. Nature 412, 606.

Singer, B.S., Ackert. R.P. Jr., Guillou, H., 2004. 40Ar/39Ar and K-Ar chronology of Pleistocene glaciations in Patagonia. GSA Bulletin 116, 434-450.

Solari M.A., Calderon M., Airo A., Le Roux J.P. and Hervé F. Holocene and last Glacial variability of the Great Tehuelche Paleolake in the Torres del Paine National Park. Accepted in Andean Geology.

Solari, M., 2010. Paleotermometría y evolucion del sistema hidrologico del parque nacional Torres del Paine, Patagonia. Unpublsihed Ph.D.

Sowers, T. and Bender, M., 1995: Climate records covering the last deglaciation. Science, 269:210-214.

Steig, E.J., Brook, E.J., White, W.C., Suchter, C.M., Berder, M.L., Lehman, S.J., Morse, D.L., Waddington, E.D., Clow, G.D., 1998. Synchronous Climate Changes in Antarctica and the North Atlantic Science, 282, 92-95.

Stern C.R., Moreno P.I., Villa-Martínez R.P., Sagredo E.A., Prieto A., Labarca, R., in press. Evolution of ice-dammed proglacial lakes in Última Esperanza, Chile: implicatuons from the late-glacial R1 eruption of Reclús volcano, Andean Austral Volcanic Zone. Andean Geology 38.

Stern, C.R., 2011. Fluctuations of the Última Esperanza ice lobe (52°S), Chilean Patagonia, during the last glacial maximum and termination 1. Geomorphology 125, 92-108.

Stine, S. and Stine, M., 1990. A record from Lake Cardiel of climate change in southern South America. Nature 345, 705-708.

Stone, J. O., 2000. Air pressure and cosmogenic isotope production. J. Geophys. Res. 105, 23753- 23759.

Strelin, J. and Denton, G. H., 2005. The Puerto Bandera Moraines. In Proceedings of the XVI Congreso Geológico Argentino 6.

Stuiver, M. and Grootes, P. M., 2000. GISP2 Oxygen Isotope Ratios. Quaternary Research 53, 277-284.

Suarez, M. J. & Held, I. M., 1976. Modelling climatic response to orbital parameter variations. Nature 263, 46–47.

Sugden D.E., Bentley M.J., Fogwill C.J., Hulton N.R.J., McCulloch R.D., Purves R.S., 2005. Late-glacial glacier events in southernmost South America: a blend of 'northern' and 'southern' hemispheric climatic signals? Geografiska Annnaler 87A, 273–288.

Teller, J.T., et al., 2002. Freshwater outbursts to the oceans from glacial Lake Agassiz and their roll in climate change during the last deglaciation. Quaternary Science Reviews 21, 879–887.

Toggweiler, J. R., Russell, J. L., and Carson S. R., 2006. Midlatitude westerlies, atmospheric CO2, and climate change during the ice ages. Paleoceanography 21, PA2005 Doi:10.1029/2005PA001154.

Wang, Y. J., Cheng, H. Edwards, R. L., An, Z. S., Wu, J. Y., Shen, C.-C., Dorale, J.A., 2001. A High-Resolution Absolute-Dated Late Pleistocene Monsoon Record from Hulu Cave, China. Science 294, 2345-2348.

Wang, X., Auler, A.S., Edwards, R.L., Cheng, H., Cristalli, P.S., Smart, P.L., Richards, D.A., Shen, C-C., 2004. Wet periods in northestern Brazil over the past 210 kyr linked to distant climate anomalies. Nature 432, 740-743.

Weertman, J. 1976. Milankovitch solar radiation variations and ice age ice sheet sizes. Nature 261, 17–20.

Williams, P.W., 1996. A 230 ka record of glacial and interglacial events from Aurora Cave, Fiordland, New Zealand. New Zealand Journal of Geology and Geophysics 39, 225-241.

Winn, R. D. Jr. & Dott, R. H. Jr., 1977. Large-scale traction structures in deep-water fan channel conglomerates in southern Chile. Sedimentology, 26, 203-228.

Winograd, I.J., Coplen T.B., Landwehr, J.M., Riggs, A.C., Ludwig, K.R., Szabo, B.J., Kolesar, P.T., and Revesz, K.M., 1992. Continuous 500,000-Year Climate Record from Vein Calcite in Devils Hole, Nevada. Science 258, 255-260.

Wunsch, C., 2004. Quantitative estimate of the Milankovitch-forced contribution to observed Quaternary climate change. Quaternary Science Reviews 23, 1001–1012.

APPENDIX A: SUPPLEMENTARY INFORMATION

1. Supplementary Note:

Physiography of the Laguna Azul-Lago Sarmiento Area

The Torres del Paine region occurs on the only continental landmass at these southern latitudes (51ºS), in the subantarctic climatic zone governed by the southern westerly wind belt. This wind system transports cyclones northward that originate in the Antarctica Frontal Zone (AFZ), and is associated with elevated precipitation levels (Garreaud, 2007). For comparison, during the Last Glacial Maximum (LGM) the southern westerly wind belt is thought to have shifted as far north as ~40ºS (Moreno *et al*., 1999; Lamy *et al*., 2004), affecting climate and glacier dynamics all along the southern Andes in response to its direct effect on the Patagonian ice sheet mass balance. The present ice fields in Patagonia (Northern and Southern Patagonian Ice Fields) extend 17,200 km^2 (Aniya *et al*., 1996; Cassasa *et al*., 2002) along the southern Andes. Torres del Paine National Park occurs on the lee of the Andes adjacent to the southeastern tip of the Southern Patagonian Ice Field. The equilibrium line altitude (ELA) throughout this ice field varies from about 900-1400 m a.s.l. (Cassasa *et al*., 2002), which demonstrates the significant geographical and glaciological variability among outlets draining the ice field.

During late-glacial time, outlet glaciers draining the Patagonian ice sheet and the alpine Cordillera Paine ice cap in the Torres del Paine region coalesced to form three main piedmont lobes: Laguna Azul, Lago Sarmiento and Lago del Toro ice lobes. At this

time, low surface gradient glacier ice extended about 45 km beyond the present ice terminus at the Southern Patagonian Ice Field and shaped the Torres del Paine landscape.

The overall landscape in Torres del Paine shows a classical glacially scoured morphology, interrupted by deep elongated west-east troughs occupied by lakes (Fig. A1). These lakes are settled within a dramatic high-relief topography and fringed at their eastern margins by thick glacial deposits, including the distinctive four TDP moraine belts (TDP I-IV) and associated outwash plains. The TDP II, III, and IV moraines are morphologically distinct and mostly continuous between lake basins. Each of the TDP II and TDP III moraines comprise 5-10 sharp, well-defined ridges (Plate 2, pocket). TDP IV moraines are less prominent and usually occur as two parallel well-defined moraine ridges. TDP I moraine is a wider, smooth, much more prominent landform when compared with the TDP II, III, and IV moraines (Marden and Clapperton, 1995; Marden, 1997).

Laguna Azul (220 m a.s.l.) and Lago Sarmiento (75 m a.s.l.) occupy the bottom of two independent basins, separated by ~12 km of open, low-relief, bedrock-controlled topography (~500-250 m a.s.l., Fig. A1). The surface here is mantled with a relatively thin glacial drift, sprinkled with small dry lake bodies and crossed by north-south moraine ridges. Some of the outer moraines are virtually uninterrupted between L. Azul and L. Sarmiento and it is possible to track them for more than 10 km. Between these two lakes, the glacial drift limit, in parts marked by boulder lines, is exceptionally well-defined (Marden, 1993; Plate 2, pocket). South of L. Azul, glacier ice buttressed against eastern relief, locally cut by channel conduits. The Cañadon del Macho is a prominent meltwater channel that interrupts the continuity of TDP II, III, and IV moraines. At least

two terrace levels are present in this channel and glaciofluvial sediments are up to boulder size. Vega Capón/Baguales is another meltwater channel occurring to the north of the study area (Figure A1, Plate 2, pocket) that during TDP II, III, and IV advances carried meltwater into the paleo Río de las Chinas.

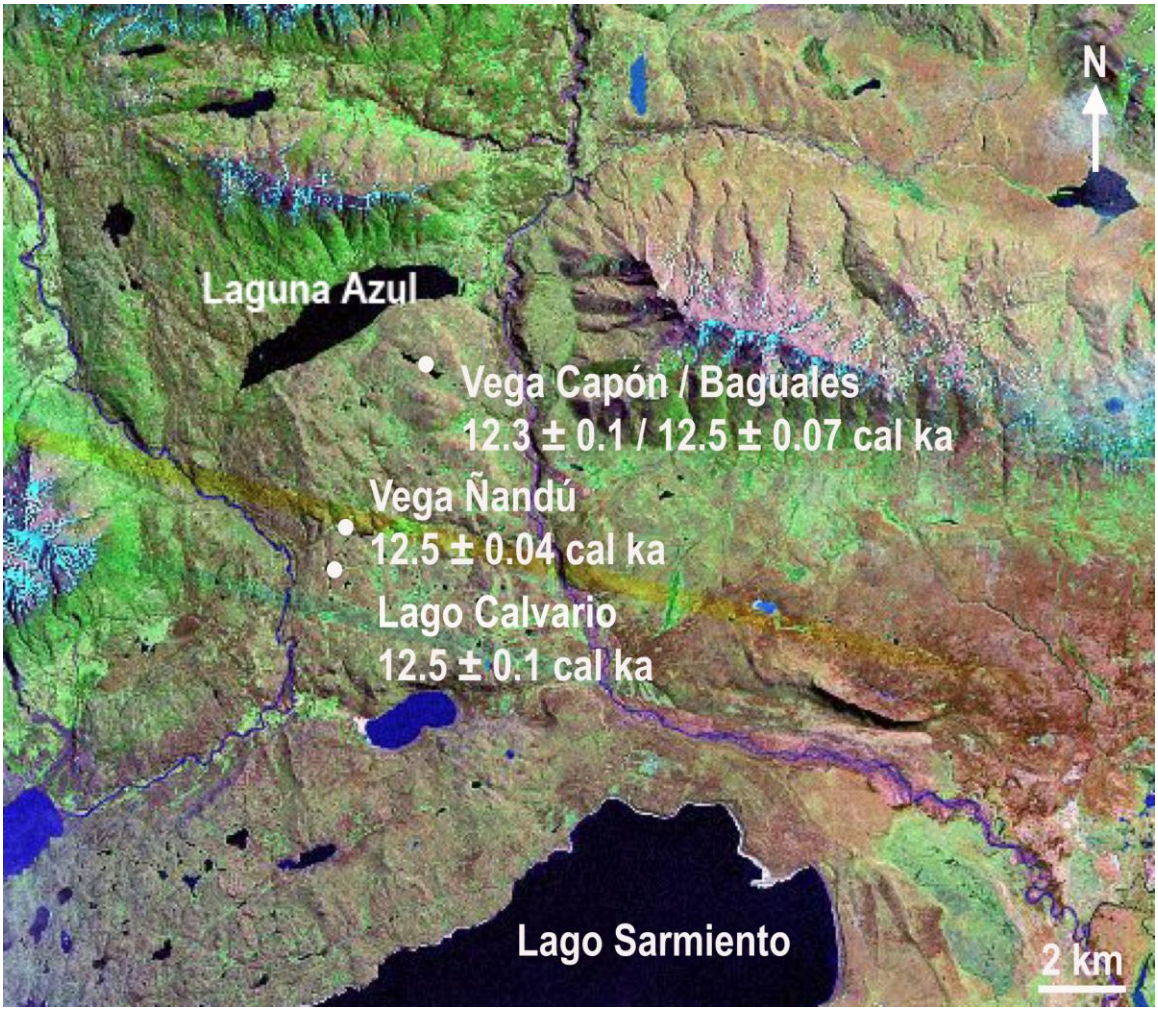

Figure A.1. Satellite image showing physiographical attributes of the Laguna Azul-Lago Sarmiento Area and surrounding terrain. Vega Baguales meltwater channel ^{14}C calibrated age of 12.5±0.07 cal ka BP (this study) is a basal- minimum age for deglaciation from TDP IV moraines and closely-agrees with the deglacial ages published in Moreno *et al*. (2009) (e.g., Vega Ñandú, Lago Calvario and Vega Capón shown in figure; see also Plate 2, pocket). A deglacial age of 12.5 cal ka B.P. agrees with the ACR age for the TDP II-IV moraines (i.e., 14.2 ka).

2. Supplementary Note:

Radiocarbon ages

In this study we dated a gastropod shell layer (laboratory sample OS-74487; Sample ID LC_03) close to the base of a core extruded at Vega Baguales (Figure A1; Plate 2, pocket). We obtained a ^{14}C age of 10,550 ± 55 years before present ($\delta^{13}C$ -4.12‰). For calibration of radiocarbon ages, we used the IntCal09 curve by Reimer *et al*. (2009). The calibrated 1σ ranges for sample OS-74487 are 12,424 cal BP: 12,492 cal BP (relative area 0.53448) and 12,516 cal BP: 12,572 cal BP (relative area 0.46552).

- Vega Baguales. Sample LC_03 ($\delta^{13}C$ -4.12‰): 10,550 ± 55 ^{14}C years B.P.

  Calibrated age (1σ range):

  12,424 - 12,492 cal B.P. (0.53448)

  12,516 - 12,572 cal B.P. (0.46552)

Mean: 12,544 ± 40 cal yrs B.P.

- Maximum age of the Puerto Bandera moraines (Ref. S25). Mean: 11,170 ± 98 ^{14}C years B.P.

  Calibrated age (1σ range):

  12,923 - 13,175 cal B.P. (1)

Mean: 13,049 ± 178 cal yrs B.P.

Calibration of radiocarbon close-minimum ages published by Ref. 14:

- Vega Ñandu. Sample PS0304A T4_398-400: 10,555 ± 40 ^{14}C years B.P.

  Calibrated age (1σ range):

  12428 - 12476 cal B.P. (0.458398)

  12521 - 12575 cal B.P. (0.541602)

  Mean: 12,548 ± 40 cal yrs B.P.

- Lago Calvario. Weighted mean: 10,492 ± 45 ^{4}C years B.P.

  Calibrated age (1σ range):

  12406 – 12542 cal B.P. (1)

  Mean: 12,474 ± 96 cal yrs B.P.

- Vega Capón. Weighted mean: 10,418 ± 49 ^{4}C years B.P.

  Calibrated age (1σ range):

  12,149 – 12,191 cal B.P. (0.166451)

  12,211 – 12357 cal B.P. (0.634385)

  12368 - 12413 cal B.P. (0.199163)

  Mean: 12,284 ± 103 cal yrs B.P.

3. Supplementary Methods

3.1 Sampling Protocol and assumptions

We sampled boulders with quartz-bearing lithologies (mostly granite, greywacke and dacite types) embedded in or resting on stable moraine tops. We tried to avoid boulders located close to erosional and unstable surfaces and steeply dipping slopes. Sampled boulder surfaces (usually upper 2 cm) were mostly horizontal (≤10°) and very well preserved. We tried to avoid weathered surfaces and top sections with clear erosional signs, such as deep cracks and fractured tops, rainwater corrosion or exfoliation. Minimum height of boulders was ≥65 cm and mostly between 100 and 200 cm. Some samples were from striated boulder surfaces, which afforded evidence for minimal erosion.

There is limited information of the spatial and temporal variability in erosion rates in Patagonia (Kaplan *et al*., 2004; Kaplan *et al*., 2005). At Lago Buenos Aires, preliminary maximum estimates based on a few samples varied between 1.0 to 2.3 mm per 1000 years, with an average of 1.4 mm per 1000 years, over long exposure times (10^5 years). In addition, other work (Douglass, 2006) at the same site, with additional data, found erosion rates on average of <1 mm per 1000 years. Regardless, these values should be taken as provisional, because they come from few boulders at a single site in northeast Patagonia and are maximum rates. Patagonia is a vast region with a variety of geographical and climatological settings. If we apply an erosion rate of 1.4 mm per 1000 years to Laguna Azul and Lago Sarmiento, TDP exposure ages would increase ages by ~1.5%, which does not affect our conclusions. Given the lack of data on erosion rates in

Torres del Paine, evidence for excellent preservation of moraines and boulders, and low preliminary estimates elsewhere in Patagonia, we assume no erosion effect in our age calculations. The fact the sample exposure time corresponds to the last ~14 ka years, mostly under a warmer and drier interglacial climate (Moreno *et al*., 2009), may have favored local landscape stability.

Snow shielding may affect the production rate of cosmogenic nuclides when the seasonal snowpack is thick (e.g., greater than one meter) and lingers for a number on months on top of rock surfaces (Jackson *et al*., 1999). Average winter temperature in Torres del Paine is >0°C (Carrasco *et al*., 2002) close to where the moraine belts are located, which makes thick snow accumulation for long periods unlikely. The regional climatology is under the pervasive influence of temperate maritime air masses advected by the westerly winds. These humid air masses bring precipitation in the form of rain or snow, depending on elevation. The Southern Andes relief enhances regional orographic precipitation and produces a sharp precipitation gradient between west and east across the Andes, with the eastern sides receiving only 5% of the precipitation recorded at the western coast (Carrasco *et al*., 2002). Rock samples for cosmogenic-exposure dating were obtained from areas below 400 m a.s.l., distant from the mountain front (~45 km from present ice margins), and in locations exposed to the wind which would inhibit snow accumulation on rock surfaces. Therefore, snow build up on moraine crests is minimized due to low snow accumulation and windy conditions for much of the year.

The semiarid condition in the Torres del Paine region produces the well-known steppe plains of eastern Patagonia, with the last forest remains present at the foothills of the Andes. Although pollen records show forest being more generally distributed in

Torres del Paine during the mid-Holocene (Moreno *et al.*, 2009), the eastern area of the park has remained at the forest-steppe ecotone. There is no soil evidence for thick forests that would have shielded our boulders and affected significantly ^{10}Be cosmogenic nuclide history.

3.2 Sample Preparation and Analysis

Sample preparation and beryllium extraction was developed in the laboratory facilities of the Earth Sciences Department and Climate Change Institute at the University of Maine (UMAINE), and in the Cosmogenic Nuclide Laboratory at Lamont-Doherty Earth Observatory (LDEO). We followed laboratory protocols of the Cosmogenic Isotope Laboratory at the University of Washington (http://washington_cosmolab/chem.) and an updated version of Licciardi (2000) (http://LDEO_Cosmogenic_Nuclide_Lab/Chemistry.). In the UMAINE facilities we separated and obtained clean quartz samples (between 4 and 15 grams). ^{10}Be extraction and isotope dilution procedure was carried out at LDEO. We use a low background ^{9}Be carrier that leads to a low-ratio process blank. This led to measurement of ^{10}Be/^{9}Be ratios as low as 10^{-14}-10^{-15} and significant improvement in the precision of our ages compared to prior studies in the area (see technical details in Schaefer *et al.*, 2009).

Accelerator mass spectrometer (AMS) ^{10}Be/^{9}Be analysis was carried out at the Lawrence Livermore National Laboratory (LLNL), which resulted in accurate ^{10}Be/^{9}Be ratios and low analytical errors (<4%). All samples and blanks were measured relative to the 07KNSTD standard (Nishiizumi *et al.*, 2007). Table 4.1 (Chapter 4) shows the

analytical data from our samples in Torres del Paine. The technological advances utilized in this study (Nishiizumi *et al*., 2007), plus a careful sampling protocol reduced uncertainties and led to detailed exposure-age chronology for the region.

*3.3 ^{10}Be Production Rate (PR***)**

Because of the lack of a calibration site in Torres del Paine to account accurately for the local ^{10}Be PR, we used PRs measured at sites from outside our study area. Those available today produce cosmogenic-exposure ages discrepancies of >10% (Kaplan *et al*., 2008; Balco *et al*., 2009). Under this scenario, the ideal condition is to use a ^{10}Be PR calculated from a calibration site similar in magnetic latitude, elevation, and geographical and climatological conditions. Cross-checking ages with complementary ^{14}C chronologies allows validation of the PR used.

We used two ^{10}Be PRs to calculate the exposure age of our samples: one measured at New Zealand's Macaulay site (43ºS) (Putnam *et al*., 2010; cf, Kaplan *et al.*, in review), and the second from the "global calibration data set" (Balco *et al*., 2008). Table 4.2 (Chapter 4) shows ^{10}Be ages obtained using both referred PRs. The average difference between the ^{10}Be ages is 14.2%, with the ages being ~1,000-3000 years younger when using the "global calibration data set".

Radiocarbon dating at the Vega Baguales meltwater channel in Torres del Paine (50º53'47''S; 72º44'35''W, 455 m a.s.l. Figs. A1, A2; Plate 2, pocket), which served as a main conduit for meltwater escaping the ice front when it was at TDP II, III, and IV moraines, represents an opportunity to test the local validity of both PRs used in our

study. A piston core extruded from the distal part of the channel exhibits at the base glaciolacustrine rhythmites made up of fine sand and muddy layers, overlain first by coarser sand containing very well preserved gastropods shells and subsequently by organic silt and fiber-rich sediment. A calibrated age of 12.5 ± 0.07 (1σ) kcal yr B.P. obtained from a gastropod shell close to the base of the core (272 cm depth) defines a close-minimum age for abandonment of this conduit after ice retreat from the TDP IV position. This minimum-limiting deglacial age is statistically indistinguishable from that obtained in previous work (Moreno *et al*., 2009) from Vega Capón, a site located less than one kilometer in the up-ice direction along the same channel. The date is also similar to those from other sites in Torres del Paine (Moreno *et al*., 2009) (Plate 2, pocket). The implications of these radiocarbon ages are important. They suggest that by 12.5 ka there was no ice occupying the proximal part of Vega Capón (Moreno *et al*., 2009) and therefore ice had retreated from the late-glacial moraines. Moreover, evidence from the distal core in Vega Baguales shows that the meltwater conduit was abandoned by this time and organic remains had begun to accumulate.

This scenario and the radiocarbon ages for ice recession are in conflict with most of the ^{10}Be ages produced by the "global calibration data set" (Balco *et al*., 2008). On the other hand, the New Zealand's PR (Putnam *et al*., 2010) produces ^{14}C and ^{10}Be ages in better agreement. New Zealand Macaulay Site PR is the only ^{10}Be calibration site for the Southern Hemisphere outside the tropics and is located in the Southern mid-latitudes, as is Torres del Paine. In addition, both the age of the landslide used at New Zealand's Macaulay Site and ^{10}Be ages in Torres del Paine are relatively similar (i.e., both occur close to the Pleistocene-Holocene boundary), and therefore both sites have been affected

similarly by the external factors controlling ^{10}Be production rates, such as variations in the geomagnetic field. Moreover, the New Zealand's PR has been confirmed recently at Lago Argentino, ~100 km north of Torres del Paine (Kaplan *et al*., accepted). For the above reasons, we think that the Torres del Paine ^{10}Be ages obtained using New Zealand's PR are more accurate than those obtained from the 'global calibration' dataset. The chronology presented here also agrees with previous work in the region (Moreno *et al*., 2009; Fogwill and Kubik, 2005).

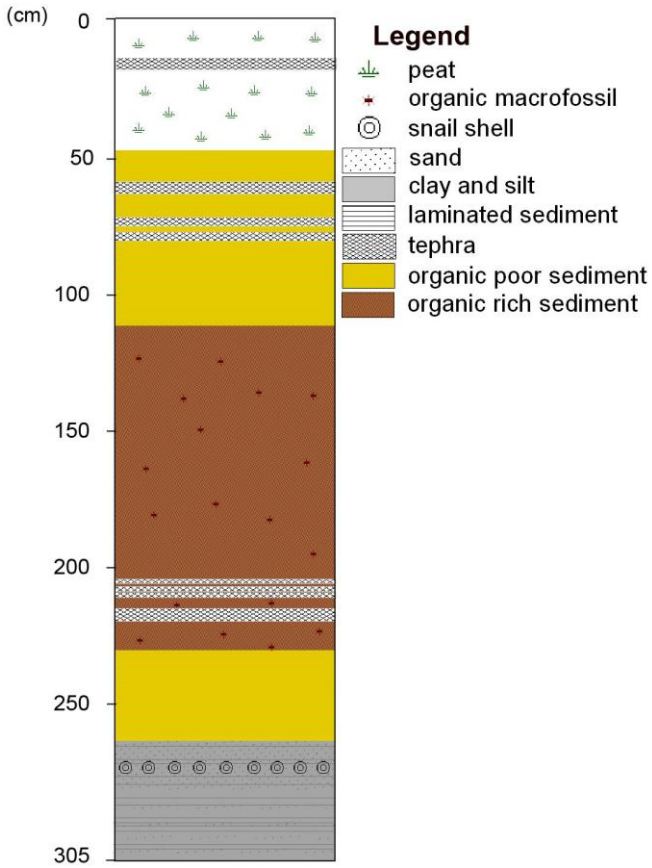

Figure A.2. Vega Baguales (50º53'47''S; 72º44'35''W, 455 m a.s.l.) stratigraphic column. A ^{14}C sample was obtained from a gastropod layer at 272 cm and yielded a calibrated age of 12.5 ± 0.07 kcal yr BP (radiocarbon age of 10550 ± 55years). See text for details.

3.4 Outliers detection and rejection

In order to detect and reject outliers, we applied the Grubbs test (Fergusson, 1961; Grubbs, 1969) to the age population of each of the three moraines in Torres del Paine: TDP II, TDP III, and TDP IV. We also treated sample ages that were more than 2σ from the arithmetic mean as outliers. Fig. A3 and Fig. 4.3 (Chaper 4) illustrate moraines age distributions in probability plots before and after outlier rejection, respectively. For TDP IV we included and recalculated CAMS ^{10}Be ages obtained in previous work (Moreno *et al*., 2009). The Grubbs test detected (with 99% confidence level) three outliers in TDPII moraine age population: samples LA0714, LA0716 and LA0732. In the same moraine belt, SAR0719 and SAR0702 are >2σ from the arithmetic mean and also are considered outliers. Although LA0701 and LA0906 ages from TDP III moraine data set are early-Holocene in age, the statistical test didn't treat them as outliers. Nevertheless, these two ages are 3σ different from the mean age of TDP III moraine, and therefore we consider them as outliers. After eliminating LA0701 and LA0906, the Grubbs test detected two more outliers (99% confidence level): LA0512 and LA0724 in the TDP III data set. SAR0722 in TDP IV is >2σ from the arithmetic mean moraine age and therefore was also treated as an outlier.

Figure A.3. Relative probability plots of ^{10}Be exposure-age distribution for each moraine belt. Probability plots with outliers are presented for each moraine belt. The thin curves represent individual sample ages ± 1σ. The thick curve is the normalized probability distribution of the moraine age population. Central vertical lines in plots denote the arithmetic mean ±1σ (yellow rectangle), 2σ (red vertical line) and 3σ (green vertical line). Values used in the text are arithmetic means and associated uncertainties obtained after rejecting outliers. **a** – TDP II moraine; **b** – TDP III moraine; **c** – TDPIV moraine. TDP IV includes two CAMS recalculated dates from Moreno *et al.* (2009).

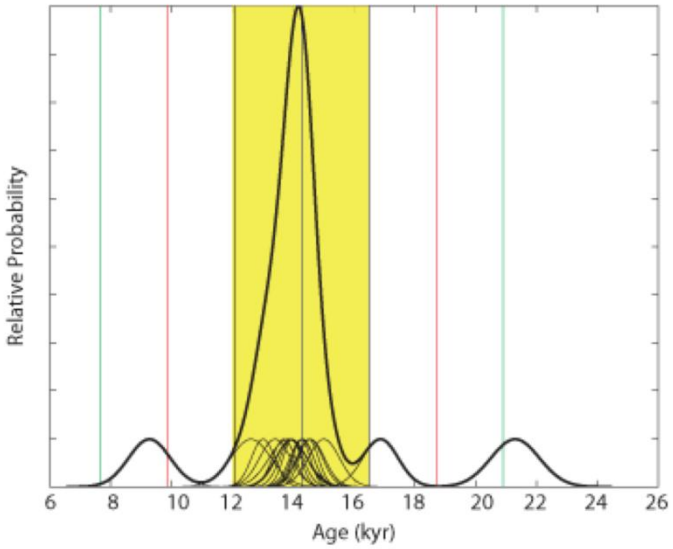

a) TDP II moraine belt (n=19):
LA0714, 15, 16, 20, 32, 03, 07, 0901
RP0815, 17, 20
SAR0702, 03, 05, 13, 18, 19, 25, 0907

Statistics
Arithmetic mean/1 sigma uncertainty: 14,300±2210 yrs
Including production rate uncertainty: 14,300±2220 yrs
Weighted mean/weighted uncertainty: 14,200±100 yrs
Peak age: 14,200 yrs
Median/Interquartile Range: 14,000±820 yrs
Reduced χ^2: 10.1

Figure A.3. Continued.

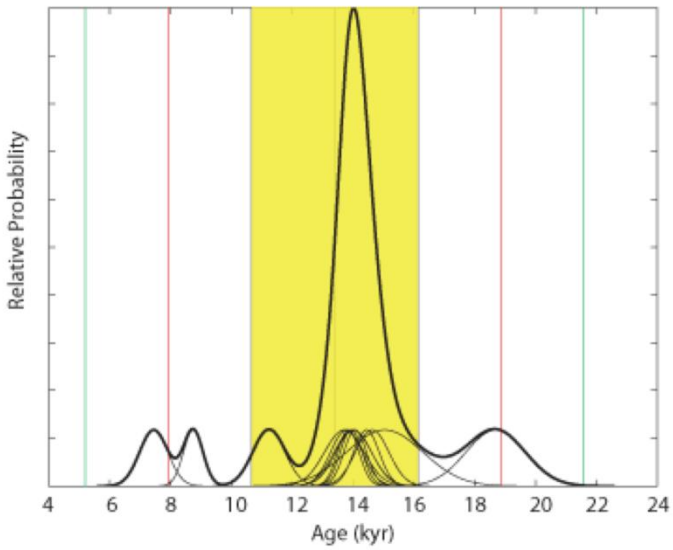

b) TDP III moraine belt (n=14):
LA0512, 22, 0704, 27, 28
RP0705, 0903, 04, 05, 06
SAR0701, 24, 0906, 08

Statistics
Arithmetic mean/1 sigma uncertainty: 13,400±2730 yrs
Including production rate uncertainty: 13,400±2750 yrs
Weighted mean/weighted uncertainty: 12,680±130 yrs
Peak age: 14,000 yrs
Median/Interquartile Range: 14,000±730 yrs
Reduced χ^2: 34.0

Figure A.3. Continued.

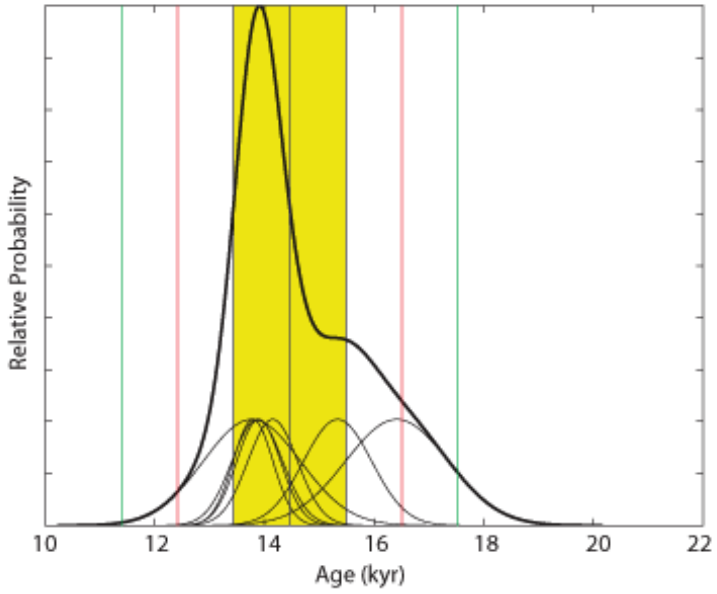

c) TDP IV moraine belt, with recalculated ages (samples VN0525, 26) from Moreno *et al*. (2009). Samples (n=7):
RP0701, 03
SAR0721, 22, 23
VN0525, 26

Statistics
Arithmetic mean/1 sigma uncertainty: 14,500±1020 yrs
Including production rate uncertainty: 14,500±1080 yrs
Weighted mean/weighted uncertainty: 14,100±190 yrs
Peak age: 13,900 yrs
Median/Interquartile Range: 13,900±1230 yrs
Reduced χ^2: 2.4

Outlier ages may be due mainly to post-depositional geomorphic processes. A group of outliers includes anomously young ages (samples LA0512, LA0714, SAR0714, SAR0906) that date to the Early Holocene and most likely indicate post-depositional landform adjustments. However, 8% of the ^{10}Be ages date to the Last Glacial Maximum

and beginning of the Termination (Samples LA0716, LA0732, SAR0722, SAR0724), and thus form a group of older-age outliers. These boulders may reflect reworked samples; the ice margin may have incorporated boulders from older glacial deposits into younger moraines. Therefore, most of the detected outliers occur distant from the mean age of the respective moraine, and define two opposite extremes. Only two samples were considered outliers because they occurred just outside 2 sigma from the mean (samples SAR0719 and SAR0702).

4. Supplementary Note:

Interhemispheric teleconnections/westerly wind belt/Late-glacial climate

Both relatively low temperatures, particularly during the summer ablation season, and perhaps an increased amount of snow precipitation were needed to produce glacier readvance in Torres del Paine at 14,200 ± 560 years ago. During the last termination, the Heinrich 1 Stadial event in the North Atlantic, with extreme cold winters and sea ice (Denton *et al.*, 2005), likely produced a southern latitudinal shift of the thermal equator and wind belts, affecting global climate by both direct and indirect means (e.g., Wang, *et al.*, 2001; Peterson *et al.*, 2000). In the southern hemisphere, this poleward migration also displaced the westerly wind belt and drove an intensive Southern Ocean circulation, a prerequisite for enhanced upwelling in the region and ventilation of deep waters (Anderson *et al.*, 2009; Toggweiler *et al.*, 2006). CO_2 released by this mechanism may have propagated the deglacial warming trend globally (Anderson *et al.*, 2009; Denton *et al.*, 2010). At this time, glacier recession took place in most of southern South America

(McCulloch *et al*., 2005; Hein *et al*., 2010; Denton *et al*., 1999b) and the southern westerly wind belt migrated >10° of latitude from the Chilean Lake District (Moreno *et al*., 1999; Lamy *et al*., 2004) (40ºS) over the Southern Ocean (50-60ºS).

If this interhemispheric sequence of events is correct, then as soon as the Heinrich Stadial 1 came into an end and the rate of wind-driven opal-flux and upwelling in the Southern Ocean decreased, the southern westerly wind belt must have shifted north from its Southern Ocean position. Therefore, two main controllers acted on shifting the southern westerlies northward during the ACR: decrease in sea-surface temperatures and the termination of the Heinrich Stadial 1 in the North Atlantic. Based on our moraine-based chronology in Torres del Paine, we hypothesize the ACR position of the southern westerly belt in Southern South America was at ~51ºS as early as 14.2 ka.

The location of the westerly belt close to 51ºS in South America during the early late glacial is consistent with glacial readvance in Torres del Paine at this time. In the same manner, the location of the Antarctic Frontal Zone as far north as 53ºS in the region during the ACR is consistent with palynological records from southernmost South America (e.g., Tierra del Fuego and Beagle Channel), which suggest cold and dry conditions during the late-glacial (Heusser 1993; Heusser, 1998; Heusser, 2003; Moreno *et al*, 2009). We show that south Patagonian glaciers retreated after the end of the ACR, coincident with southward shift of the westerly winds, likely driven this time by warmer sea-surface temperatures and the North Atlantic Younger Dryas Stadial (Fig. 4.1, Chapter 4), at the end of which, the region experienced a distinct wetter period (Lamy *et al*., 2010). Our data suggest that the latitudinal migration of the westerly winds tied to major environmental changes in the North Atlantic basin was important during the full late

glacial interval and raises the question if this variability also occurred during the whole glacial period.

5. Supplementary References

Anderson, R.F., Ali, S., Bradtmiller, L.I., Nielsen S.H.H., Fleisher, M.Q., Anderson, B.E., Burckle, L.H., 2009. Wind-Driven Upwelling in the Southern Ocean and the Deglacial Rise in Atmospheric CO2. Science 323, 1443-1448.

Aniya, M., Sato, H. , Naruse, R., Skvarca, P., Cassasa, G., 1996. Remote sensing application to inventorying glaciers in a large, remote area-Southern Patagonia Icefield. Photogrammetric Engineering and Remote Sensing, 62, 1361-1369.

Aniya, M. and Wakao, Y., 1997. Glacier variations of Hielo Patagónico Norte, Chile, between 1944/45 and 1995/95. Bulletin of Glacier Research, 15, 11-18.

Ariztegui, D., Bianchi, M.M., Massaferro, J., Lafargue, E., Niessen, F., 1997. Interhemispheric synchrony of Late-glacial climatic instability as recorded in proglacial Lake Mascardi, Argentina. Journal of Quaternary Science 12, 333-338.

Balco, G., Stone, J.O., Lifton, N.A., Dunai, T.J., 2008. A complete and easily accessible means of calculating surface exposure ages or erosion rates from Be-10 and Al- 26 measurements. Quaternary Geochronology 3, 174–195.

Balco, G., Briner, J., Finkel, R., Rayburn, J., Ridge, J., Schaefer, J., 2009. Regional beryllium-10 production rate calibration for late-glacial northeastern North America. Quaternary Geochronology 4, 93-107.

Carrasco, J. F., Cassasa, G., Rivera, A., Aniya, M., Naruse, R., 2002. Meteorological and climatological aspects of the Southern Patagonia Icefield. In Cassasa, G. and Casassa, G., Sepúlveda, F. V., Sinclair, R. M.(eds.) *The Patagonian Icefields* (Kluwer Academic/Plenum Publishers, New York)

Cassasa, G., Rivera, A., Aniya, M., Naruse, R., 2002. Current knowledge of the southern Patagonia Icefield. In *The Patagonian Icefields* (Kluwer Academic/Plenum Publishers, New York).

Denton, G.H., Lowell, T.V., Heusser, C.J., Schlüchter, C., Andersen, B.G., Heusser, L..E., Moreno, P.I. and Marchant D.R., 1999: Geomorphology, stratigraphy, and radiocarbon chronology of Llanquihue drift in the area of the southern Lake District, Seno Reloncaví and Isla Grande de Chiloé, Chile. Geografiska Annaler, 81A:167–229.

Denton, G.H., Alley, R.B., Comer, G.C., and Broecker, W.S., 2005. The role of seasonality in abrupt climate change: Quaternary Science Reviews 24, 1159–1182.

Denton, G. H., Anderson, R. F., Toggweiler, J. R., Edwards, R. L., Schaefer, J. M., Putnam, A. E., 2010. The Last Glacial Termination. Science 328, 1652-1656.

Desilets, D. and Zreda, M., 2003. Spatial and temporal distribution of secondary cosmic-ray nucleon intensities and applications to in-situ cosmogenic dating. Earth and Planet. Sci. Lett. 206, 21- 42.

Douglass, Daniel C., 2005. Glacial chronology, soil development, and paleoclimate reconstructions for mid-latitude South America, 1 Ma to recent. Ph.D. thesis, University of Wisconsin.

Dunai, T. J., 2001. Influence of secular variation of the magnetic field on production rates of in situ produced cosmogenic nuclides. Earth and Planet. Sci. Lett. 193, 197-212.

Fergusson, T. H., 1961. Rules for rejection of outliers. Revue Inst. Int. de Stat. 3, 29-43.

Fogwill, C. J. and Kubik, P. W., 2005. A glacial stage spanning the Antarctic Cold Reversal in Torres del Paine (51ºS), Chile, based on preliminary cosmogenic exposure dating. Geografiska Annaler, 87A(2), 403-408.

Garreaud, R.D., 2007. Precipitation and Circulation Covariability in the Extratropics. Journal of Climate 20, 4789-4797.

Grubbs, F. E., 1969 Procedures for detecting outlying observations in samples. Technometrics 11, 1-21.

Hein, A.S., Hulton, N.R.J., Dunai, T.J., Kaplan, M.R., Sugden, D., Xu, S., 2010. The chronology of the Last Glacial Maximum and deglacial events in central Argentine Patagonia. Quaternary Science Reviews, 29, 1212– 1227.

Heusser, C. J., 1993. Late-glacial of southern South America. Quaternary Science Reviews 12, 345–350.

Heusser, C. J., 1998. Deglacial paleoclimate of the American sector of the Southern Ocean: Late Glacial–Holocene records from the latitude of Canal Beagle (55°S), Argentine Tierra del Fuego. Palaeogeography, Palaeoclimatology, Palaeoecology 141, 277–301.

Heusser, C. J., 2003. Ice Age Southern Andes A Chronicle of Paleoecological Events. (Elsevier, Amsterdam).

Jackson, L.E., Phillips, F.M., Little, E.C., 1999. Cosmogenic 36Cl dating of the maximum limit of the Laurentide Ice Sheet in southwestern Alberta. Canadian Journal of Earth Sciences 36, 1347–1356.

Kaplan, M. R., Ackert, R. P., Singer, B. S., Douglass, D. C., Kurz, M. D., 2004. Cosmogenic nuclide chronology of millennial-scale glacial advances during O-isotope Stage 2 in Patagonia. Geological Society of America Bulletin 116, 308–321.

Kaplan, M. R., Douglass, D. C., Singer, B. S., Ackert, R. P., Caffee. M. W., 2005. Cosmogenic nuclide chronology of pre-last glacial maximum moraines at Lago Buenos Aires, 46ºS, Argentina. Quaternary Research 63, 301–315.

Kaplan, M.R., Hulton, N.R.J., Coronato, A., Rabassa, J.O., Stone, J.O., Kubik, P.W., Freeman, S., 2007. Cosmogenic nuclide measurements in southernmost South America and implications for landscape change. Geomorphology 87, 284–301.

Kaplan, M. R., Moreno, P. I. and Rojas, M., 2008. Glacial dynamics in southernmost South America during Marine Isotope Stage 5e to the Younger Dryas chron: a brief review with a focus on cosmogenic nuclide measurements. Journal of Quaternary Science 23, 649-658.

Kaplan, M. et al. Coherent late glacial and LGM glacier fluctuations in southern mid-latitudes based on an updated 10Be production rate for southern South America. Accepted, pending minor revisions.

Lamy, F., Kaiser, J., Ninnemann, U., Hebbeln, D., Arz, H.W., Stoner, J., 2004. Antarctic Timing of Surface Water Changes off Chile and Patagonian Ice Sheet Response. Science 304, 1959-1962.

Lamy, F., Kilian, R., Arz, H.G., Francois, J.P., Kaiser, J., Prange, M., Steinke, T., 2010. Holocene changes in the position and intensity of the southern westerly wind belt. Nature Geoscience 3, 695-699.

Licciardi, J. M., 2000. PhD, Alpine glacier and pluvial lake records of late Pleistocene climate variability in the western United States. Oregon State University.

Lifton, N., Smart, D. and Shea, M., 2008. Scaling time-integrated in situ cosmogenic nuclide production rates using a continuous geomagnetic model. Earth and Planet. Sci. Lett. 268, 190-201.

Marden C. J. and Clapperton, C. M., 1995. Fluctuations of the South Patagonia Icefield during the last glaciation and the Holocene. Journal of Quaternary Science 10, 197-210.

Marden, C. J., 1997. Late-glacial fluctuations of South Patagonian Icefield, Torres del Paine National Park, southern Chile: Quaternary International 38-39, 61–68.

McCulloch, R.D., Fogwill, C.J., Sugden, D., Bentley, M.J., Kubik, P.W., 2005 Chronology of the last glaciation in central Strait of Magellan and Bahía Inútil, southernmost South America. Geografiska Annaler, Series A- Physical Geography 87, 289–312.

Moreno, P.I., Lowell, T.V., Jacobson, G.L., Jr. and Denton, G.H., 1999: Abrupt vegetation and climate changes during the last glacial maximum and last termination in the Chilean Lake District: A case study from Canal de la Puntilla (41ºS). Geografiska Annaler, 81A:285-311.

Moreno, P.I., Jacobson, G.L., Lowell, T.V., and Denton, G.H., 2001, Interhemispheric climate links revealed by a late-glacial cooling episode in southern Chile. Nature 409, 804–808.

Moreno, P. I., Kaplan M. R., François J.P., Villa-Martínez R., Moy, C.M., Stern, C.R., Kubik, P.W., 2009. Renewed glacial activity during the Antarctic cold reversal and persistence of cold conditions until 11.5 ka in southwestern Patagonia. Geology 37, 375-378.

Nishiizumi, K., Imamura, M., Caffee, M.W., Southon, J.R., Finkel, R.C., McAninch, J., 2007. Absolute calibration of Be-10 AMS standards. Nuclear Instrum. Methods Phys. Res. Sect. B 258, 403–413.

Peterson, L. C. et al., 2000. Rapid Changes in the Hydrologic Cycle of the Tropical Atlantic During the Last Glacial. Science 290, 1947-1951.

Pigati, J. S. and Lifton, N. A., 2004. Geomagnetic effects on time-integrated cosmogenic nuclide production with emphasis on in situ 14C and 10Be. Earth and Planet. Sci. Lett. 226, 193-205.

Putnam, A., Schaefer, J., Barrell, D.J.A., Vandergoes, M., Denton, G.H., Kaplan, M., Finkel, R.C., Schwartz, R., Goehring, B.M., Kelley, S., 2010. In situ cosmogenic ^{10}Be production-rate calibration from the Southern Alps, New Zealand. Quaternary Geochronology 5, 392–409.

Reimer, P.J., Baillie M.G.L., Bard E., Bayliss A., Beck J.W., Blackwell P.G., Bronk Ramsey, C., Buck, C.E., Burr, G.S., Edwards, R.L., Friedrich, M., Grootes, P.M., Guilderson, T.P., Hajdas, I., Heaton, T.J., Hogg. A.G., Hughen, K.A., Kaiser, K.F., Kromer, B., McCormac, F.G., Manning, S.W., Reimer, R.W., Richards, D.A., Southon, J.R., Talamo, S., Turney, C.S.M., Van der Plicht, J., Weyhenmeyer , C.E., 2009. IntCal09 and Marine09 radiocarbon age calibration curves, 0–50,000 years cal BP. Radiocarbon 51(4), 1111–50.

Schaefer, J. M. Denton, G.H., Kaplan, M.R., Putnam, A., Finkel, R.C., Barrell, J.A., Andersen, B.G., Schwartz, R., Mackintosh, A., Chinn, T., Schlüchter, C., 2009. High-frequency Holocene glacier fluctuations in New Zealand differ from the northern signature. Science 324, 622–625.

Stone, J. O., 2000. Air pressure and cosmogenic isotope production. J. Geophys. Res. 105, 23753- 23759.

Strelin, J. and Denton, G. H., 2005. The Puerto Bandera Moraines. In Proceedings of the XVI Congreso Geológico Argentino 6.

Toggweiler, J. R., Russell, J. L., and Carson S. R., 2006. Midlatitude westerlies, atmospheric CO2, and climate change during the ice ages. Paleoceanography 21, PA2005 Doi:10.1029/2005PA001154.

Wang, Y. J., Cheng, H. Edwards, R. L., An, Z. S., Wu, J. Y., Shen, C.-C., Dorale, J.A., 2001. A High-Resolution Absolute-Dated Late Pleistocene Monsoon Record from Hulu Cave, China. Science 294, 2345-2348.

APPENDIX B: SAMPLED BOULDERS

RV I moraines

Sample ID: IIPG0801
Lat S-Long W: 51.1057-71.8733
Elevation (m a.s.l.): 330
Height (cm): 37
Age (± 1σ): 49600 ± 1270 yrs

Sample ID: IIPG0802
Lat S-Long W: 51.0993-71.8686
Elevation (m a.s.l.): 312
Height (cm): 122
Age (± 1σ): 48400 ± 960 yrs

TDP I_{LA} moraines
Laguna Azul

Sample ID: LA0505 (sampled by M. Kaplan)
Lat S-Long W: 50.8946-72.7432
Elevation (m a.s.l.): 466
Height (cm): 101
Age (± 1σ): 42500 ± 1010 yrs

Sample ID: LA05029 (sampled by M. Kaplan)
Lat S-Long W: 50.8995-72.7316
Elevation (m a.s.l.): 455
Height (cm): 166
Age (± 1σ): 40700 ± 1060 yrs

Sample ID: LA0530 (sampled by M. Kaplan)
Lat S-Long W: 50.8991-72.8980
Elevation (m a.s.l.): 409
Height (cm): 88
Age (± 1σ): 40900 ± 1380 yrs

Sample ID: LA0531 (sampled by M. Kaplan)
Lat S-Long W: 50.9004-72.7235
Elevation (m a.s.l.): 366
Height (cm): 129
Age (± 1σ): 41100 ± 1290 yrs

Sample ID: LA0702
Lat S-Long W: 50.8936-72.7331
Elevation (m a.s.l.): 417
Height (cm): 223
Age (± 1σ): 48800 ± 1080 yrs

Sample ID: LA0801
Lat S-Long W: 50.8991-72.7380
Elevation (m a.s.l.): 434
Height (cm): 78
Age (± 1σ): 40400 ± 1120 yrs

TDP I_{DT} moraines
Lago del Toro

Sample ID: TOR1001
Lat S-Long W: 51.1484-72.5267
Elevation (m a.s.l.): 102
Height (cm): 105
Age (± 1σ): 16600 ± 710 yrs

Sample ID: TOR1002
Lat S-Long W: 51.1495-72.5323
Elevation (m a.s.l.): 91
Height (cm): 175
Age (± 1σ): 17100 ± 1140 yrs

Sample ID: TOR1004
Lat S-Long W: 51.1332-72.5159
Elevation (m a.s.l.): 73
Height (cm): 67
Age (± 1σ): 16300 ± 1290 yrs

Sample ID: TOR1005
Lat S-Long W: 51.1322-72.5150
Elevation (m a.s.l.): 78
Height (cm): 112
Age (± 1σ): 16300 ± 530 yrs

Sample ID: TOR1007
Lat S-Long W: 51.1242-72.5113
Elevation (m a.s.l.): 103
Height (cm): 98
Age (± 1σ): 16000 ± 540 yrs

Sample ID: TOR1008
Lat S-Long W: 51.1336-72.5194
Elevation (m a.s.l.): 66
Height (cm): 97
Age (± 1σ): 11300 ± 670 yrs

TDP II moraines
Laguna Azul
Sample ID: LA0703
Lat S-Long W: 50.8867-72.7378
Elevation (m a.s.l.): 386
Height (cm): 178
Age (± 1σ): 14600 ± 410 yrs

Sample ID: LA0707
Lat S/Long W: 50.8892-72.7286
Elevation (m a.s.l.): 353
Height (cm): 284
Age (± 1σ): 14500 ± 320 yrs

Sample ID: LA0901
Lat S/Long W: 50.8891-72.7272
Elevation (m a.s.l.): 350
Height (cm): 89
Age (± 1σ): 14000 ± 300 yrs

Sample ID: LA0714
Lat S/Long W: 50.9064-72.7486
Elevation (m a.s.l.): 442
Height (cm): 361
Age (± 1σ): 9300 ± 680 yrs

Sample ID: LA0715
Lat S/Long W: 50.9067-72.7483
Elevation (m a.s.l.): 435
Height (cm): 238
Age (± 1σ): 13900 ± 490 yrs

Sample ID: LA0716
Lat S/Long W: 50.9106-72.7478
Elevation (m a.s.l.): 379
Height (cm): 338
Age (± 1σ): 16900 ± 580 yrs

Sample ID: LA0720
Lat S/Long W: 50.9119-72.7481
Elevation (m a.s.l.): 376
Height (cm): 155
Age (± 1σ): 13800 ± 610 yrs

Sample ID: LA0732
Lat S/Long W: 50.9303-72.7283
Elevation (m a.s.l.): 266
Height (cm): 245
Age (± 1σ): 21300 ± 800 yrs

Lago Sarmiento

Sample ID: SAR0702
Lat S/Long W: 50.9903-72.7070
Elevation (m a.s.l.): 261
Height (cm): 135
Age (± 1σ): 13000 ± 380 yrs

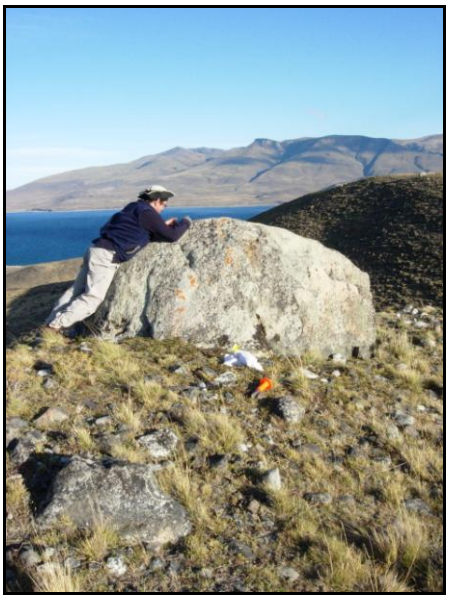

Sample ID: SAR0703
Lat S/Long W: 50.9900-72.7062
Elevation (m a.s.l.): 257
Height (cm): 253
Age (± 1σ): 14300 ± 390 yrs

Sample ID: SAR0705
Lat S/Long W: 50.9781-72.6861
Elevation (m a.s.l.): 188
Height (cm): 284
Age (± 1σ): 13700 ± 380 yrs

Sample ID: SAR0713
Lat S/Long W: 50.9861-72.7342
Elevation (m a.s.l.): 296
Height (cm): 188
Age (± 1σ): 14300 ± 360 yrs

Sample ID: SAR0718
Lat S/Long W: 50.9869-72.6919
Elevation (m a.s.l.): 146
Height (cm): 176
Age (± 1σ): 13900 ± 520 yrs

Sample ID: SAR0719
Lat S/Long W: 50.9764-72.6550
Elevation (m a.s.l.): 146
Height (cm): 114
Age (± 1σ): 12600 ± 660 yrs

Sample ID: SAR0725
Lat S/Long W: 50.9919-72.7322
Elevation (m a.s.l.): 312
Height (cm): 163
Age (± 1σ): 13900 ± 380 yrs

Sample ID: SAR0907
Lat S/Long W: 50.9948-72.7123
Elevation (m a.s.l.): 299
Height (cm): 70
Age (± 1σ): 14300 ± 290 yrs

Río Paine *east* *(referring to the area between C. del Macho and L. Amarga)*

Sample ID: RP0815
Lat S/Long W: 50.9344-72.7281
Elevation (m a.s.l.): 227
Height (cm): 145
Age (± 1σ): 14600 ± 460 yrs

Sample ID: RP0817
Lat S/Long W: 50.9483-72.7321
Elevation (m a.s.l.): 286
Height (cm): 203
Age (± 1σ): 15000 ± 520 yrs

Sample ID: RP0820
Lat S/Long W: 50.9520-72.7360
Elevation (m a.s.l.): 304
Height (cm): 190
Age (± 1σ): 13400 ± 510 yrs

TDP III moraines
Laguna Azul

Sample ID: LA0512 (sampled by M. Kaplan)
Lat S-Long W: 50.8968-72.7620
Elevation (m a.s.l.): 423
Height (cm): 83
Age (± 1σ): 15000 ± 1260 yrs

Sample ID: LA0522 (sampled by M. Kaplan)
Lat S-Long W: 50.8896-72.7563
Elevation (m a.s.l.): 465
Height (cm): 147
Age (± 1σ): 11200 ± 530 yrs

Sample ID: LA0704
Lat S-Long W: 50.8867-72.7378
Elevation (m a.s.l.): 358
Height (cm): 199
Age (± 1σ): 13800 ± 350 yrs

Sample ID: LA0727
Lat S-Long W: 50.9058-72.7644
Elevation (m a.s.l.): 350
Height (cm): 146
Age (± 1σ): 14600 ± 550 yrs

Sample ID: LA0728
Lat S-Long W: 50.9033-72.7592
Elevation (m a.s.l.): 364
Height (cm): 279
Age (± 1σ): 13800 ± 520 yrs

Lago Sarmiento

Sample ID: SAR0701
Lat S-Long W: 50.9906-72.6971
Elevation (m a.s.l.): 192
Height (cm): 89
Age (± 1σ): 8700 ± 320 yrs

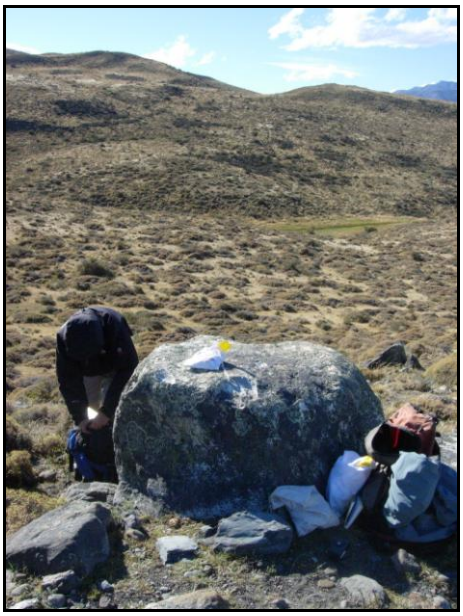

Sample ID: SAR0724
Lat S-Long W: 51.0011-72.7481
Elevation (m a.s.l.): 311
Height (cm): 149
Age (± 1σ): 18700 ± 980 yrs

Sample ID: SAR0906
Lat S-Long W: 50.9929-72.7016
Elevation (m a.s.l.): 207
Height (cm): 106
Age (± 1σ): 7400 ± 470 yrs

Sample ID: SAR0908
Lat S-Long W: 50.9975- 72.7273
Elevation (m a.s.l.): 307
Height (cm): 99
Age (± 1σ): 14000 ± 580 yrs

Río Paine east (Here referring to the area between C. del Macho and L. Amarga, except for RP0705)

Sample ID: RP0705
Lat S-Long W: 50.9203- 72.7853
Elevation (m a.s.l.): 441
Height (cm): 161
Age (± 1σ): 14400 ± 420 yrs

Sample ID: RP0903
Lat S-Long W: 50.9436- 72.7516
Elevation (m a.s.l.): 234
Height (cm): 157
Age (± 1σ): 13900 ± 360 yrs

Sample ID: RP0904
Lat S-Long W: 50.9469- 72.7566
Elevation (m a.s.l.): 245
Height (cm): 95
Age (± 1σ): 14000 ± 610 yrs

Sample ID: RP0905
Lat S-Long W: 50.9482- 72.7575
Elevation (m a.s.l.): 245
Height (cm): 83
Age (± 1σ): 13700 ± 650 yrs

Sample ID: RP0906
Lat S-Long W: 50.9536- 72.7633
Elevation (m a.s.l.): 266
Height (cm): 84
Age (± 1σ): 14100 ± 370 yrs

TDP IV moraines
Lago Sarmiento

Sample ID: SAR0721
Lat S-Long W: 50.9097- 72.7311
Elevation (m a.s.l.): 242
Height (cm): 142
Age (± 1σ): 15300 ± 620 yrs

Sample ID: SAR0722
Lat S-Long W: 51.0036- 72.7353
Elevation (m a.s.l.): 251
Height (cm): 249
Age (± 1σ): 16400 ± 940 yrs

Sample ID: SAR0723
Lat S-Long W: 51.0022-72.7547
Elevation (m a.s.l.): 318
Height (cm): 158
Age (± 1σ): 13800 ± 890 yrs

Río Paine

Sample ID: RP0701
Lat S-Long W: 50.9097- 72.7998
Elevation (m a.s.l.): 375
Height (cm): 165
Age (± 1σ): 13800 ± 360 yrs

Sample ID: RP0703
Lat S-Long W: 50.9225- 72.7878
Elevation (m a.s.l.): 404
Height (cm): 180
Age (± 1σ): 13900 ± 460 yrs

Sample ID: VN-05-25 (sampled by M. Kaplan)
Lat S-Long W: 50.9470- 72.7863
Elevation (m a.s.l.): 218
Height (cm): 135
Age (± 1σ): 14100 ± 450 yrs

Sample ID: VN-05-26 (sampled by M. Kaplan)
Lat S-Long W: 50.9489- 72.7879
Elevation (m a.s.l.): 204
Height (cm): 92
Age (± 1σ): 13900 ± 400 yrs

BIOGRAPHY OF THE AUTHOR

Juan Luis García was born in Santiago, Chile on July 3rd, 1976. He graduated from the Pontificia Universidad Católica de Chile with a Bachelor Degree in Geography in July 2000. In 2004, he moved to the city of Valdivia in the Chilean Lake District to begin graduate studies at the Universidad Austral de Chile, completing a Master in Earth Sciences in September 2007. His Master's thesis was titled: *The Llanquihue Glaciation at the Archipelago de Chiloé, Southern Chile*. Juan Luis is a candidate for the Doctor of Philosophy degree in Earth Sciences from the University of Maine in May 2011.

Plate I. Torres del Paine region

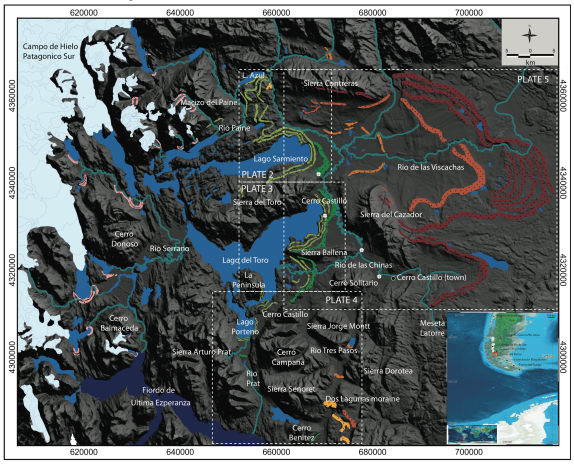

Plate 2. Laguna Azul - Lago Sarmiento area

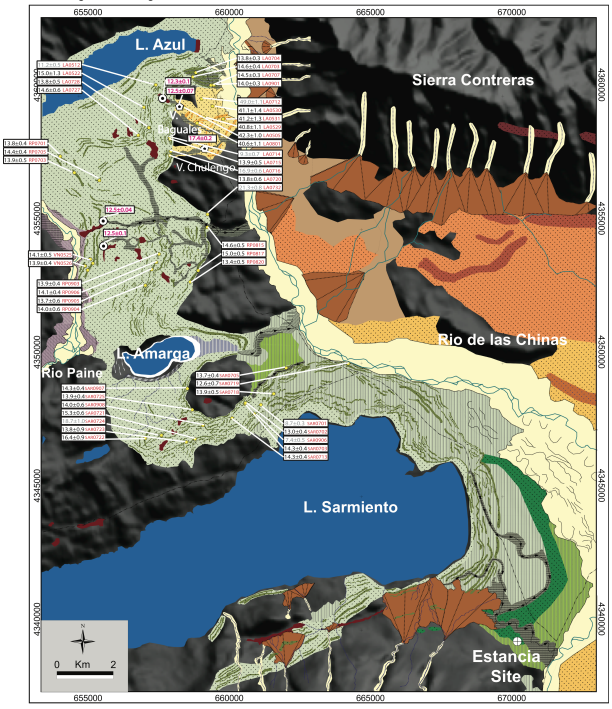

Plate 4. Lago del Toro area (sur)

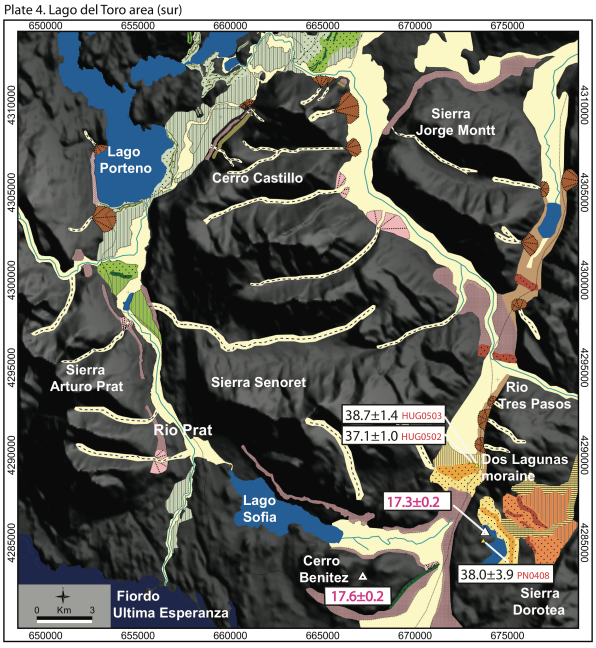

Plate 3. Lago del Toro area (norte)

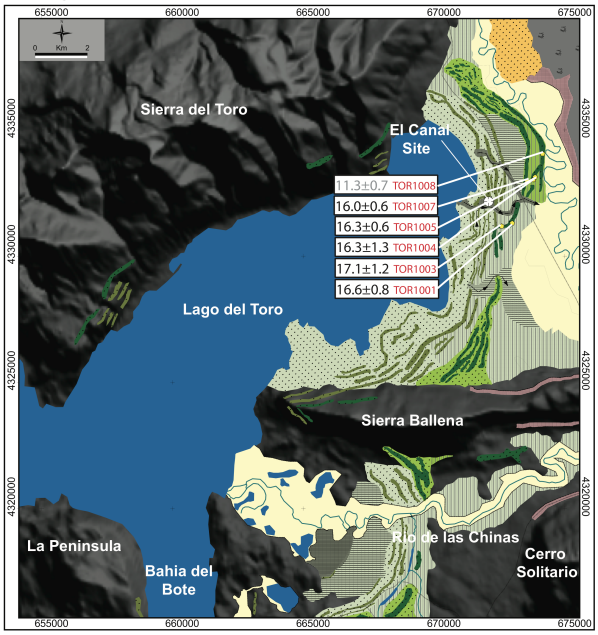

Legend

Plate 5. Rio de las Viscachas area